UCLA
UCLA Electronic Theses and Dissertations

Title

The Nature of meta-Tyrosine Toxicity to Phenylalanyl-tRNA Synthetase Editing-Defective
Escherichia coli

Permalink

https://escholarship.org/uc/item/1sk0294h

Author

Howitz, Nathaniel Shimon

Publication Date

2016

Peer reviewed|Thesis/dissertation

UNIVERSITY OF CALIFORNIA

Los Angeles

The Nature of *meta*-Tyrosine Toxicity to Phenylalanyl-tRNA Synthetase Editing-

Defective *Escherichia coli*

A dissertation submitted in partial satisfaction of the requirements

for the degree Doctor of Philosophy in

Microbiology, Immunology, and Molecular Genetics

by

Nathaniel Shimon Howitz

2016

ABSTRACT OF THE DISSERTATION

The Nature of *meta*-Tyrosine Toxicity to Phenylalanyl-tRNA Synthetase Editing-

Defective *Escherichia coli*

by

Nathaniel Shimon Howitz

Doctor of Philosophy in Microbiology, Immunology, and Molecular Genetics

University of California, Los Angeles, 2016

Professor Beth Lazazzera, Chair

Faithful translation of the genetic code into amino acid sequences is important for the

viability of organisms. One source of error in translation is the mischarging of tRNAs with the

incorrect amino acid due to structural similarities between the cognate and non-cognate amino

acids. If gone unchecked, these mischarged tRNAs would provide an amino acid to the

ribosome that does not match its codon, thereby causing mistranslation of the mRNA sequence.

The proteins that are responsible for charging tRNAs with the correct amino acids are called

aminoacyl-tRNA synthetases (aaRS). Some of these aaRSs have evolved an editing mechanism

that allows them to cleave off a non-cognate amino acid from the mischarged tRNA, which is broadly conserved across all domains of life. This editing activity seems like it would be essential for life, however there are many examples of organisms who have lost their editing function to no ill effect. Moreover, there are examples of organisms that have conserved their editing function, but do not show a growth defect when it is eliminated, such as *E. coli* and its phenylalanine aaRS (PheRS).

We chose to study *E. coli*'s PheRS to understand why its editing function is evolutionarily conserved. We discovered that the non-protein amino acid *meta*-Tyrosine (*m*-Tyr) is toxic to PheRS editing-defective (PheRS edit⁻) *E. coli*. We then sought to understand why *m*-Tyr is so toxic to PheRS edit⁻ cells. We used chemical mutagenesis to find *m*-Tyr resistant mutants and then performed whole genome sequencing to find mutated genes that could contribute to the resistance. We found that mutations in uptake and efflux transport could provide resistance by keeping or getting *m*-Tyr out of the cell. We also identified a resistance mutation that likely elevated Phe production, which provided resistance by most likely increasing competitive inhibition of the *m*-Tyr. We also observed PheRS edit⁻ *E. coli* after *m*-Tyr exposure directly via light and electron microscopy. We observed large protein aggregates forming in the cells, which indicated that the *m*-Tyr destabilized a large fraction of the proteome. We also performed transcriptomic analysis of PheRS edit⁻ *E. coli* after *m*-Tyr exposure to see what stress responses they used to deal with *m*-Tyr toxicity. We found a strong induction of the unfolded protein stress response, as well as oxidative stress, DNA damage stress, and indications of lost ion homeostasis. Based on these findings, we proposed a model of *m*-Tyr toxicity that involves a cascading and self-reinforcing chain reaction of cellular stresses that ultimately leads to cell death.

The dissertation of Nathaniel Shimon Howitz is approved.

Robert Gunsalus

James Gober

Wenyuan Shi

Beth Lazazzera, Committee Chair

University of California, Los Angeles

2016

DEDICATION

This thesis is dedicated to my parents Konrad and Victoria Howitz, and to my wonderful wife

Emily Melzer. Without any of them, this thesis would not be possible.

TABLE OF CONTENTS

List of Figures and Tables

ACKNOWLEDGEMENTS

VITA

2010	B.S., Microbiology and Economics
	University of Pittsburgh
	Pittsburgh, Pennsylvania
2010	Graduate Student
	University of California, Los Angeles
	Los Angeles, California

PUBLICATIONS AND PRESENTATIONS

Bullwinkle, Tammy J., et al. "Oxidation of cellular amino acid pools leads to cytotoxic mistranslation of the genetic code." *Elife* 3 (2014): e02501.

Nathaniel Howitz and Beth Lazazzera "The Selective Pressures Maintaining Phenylalanine-tRNA Synthetase Editing Function in *E. coli*." Poster presentation. Molecular Genetics of Bacteria and Phage Meeting. (2015)

Goodrich, Katherine, et al. "Reduced herbivory of spicebush growing in association with black walnut." *Submitted for publication*

Howitz, Nathaniel, et al. "Mechanism of *m*-Tyrosine toxicity to PheRS editing-defective *E. coli*." *Manuscript in preparation*

Chapter 1:

Introduction

Quality Control in Translation is Important for Life

A keystone of the way life works is its ability to faithfully translate information into action. The most obvious example of this is how a DNA sequence is transcribed to an RNA sequence, which is then translated into a protein. Errors that occur in these steps could potentially threaten the viability of an organism. This is why organisms have quality control (QC) mechanisms to help limit the number of errors that occur. One type of error that can occur is a mistake in transcription, which could lead to an incorrectly translated protein. Organisms prevent this by having a proofreading function in the RNA polymerase[1]. Another type of error that can occur is the adding of an incorrect amino acid to a nascent polypeptide chain because the amino acid was charged onto a non-cognate tRNA. In this case, the ribosome can detect the mistake and abort the polypeptide synthesis[2]. Additionally, there are two QC mechanisms that guard against mischarged tRNAs before they reach the ribosome. One of them is carried out by Elongation Factor-Tu (EF-Tu). EF-Tu brings aminoacyl-tRNAs (aa-tRNA) to the ribosome so that the charged amino acid can be added to the polypeptide chain. They can also recognize tRNAs that have a non-cognate amino acid charged onto it and reject the aa-tRNA, thereby preventing mistranslation[3]. The second QC mechanism that deals with mischarged tRNAs is performed by amino-acyl-tRNA synthetases.

Aminoacyl-tRNA Synthetases Possess an Important Quality Control Mechanism

The proteins that are responsible for charging specific tRNAs with the correct amino acids are called aminoacyl-tRNA synthetases (aaRS). They catalyze two reactions in the process of completing this function. First, they activate an amino acid by hydrolyzing an adenosine triphosphate (ATP) to covalently link the adenosine monophosphate (AMP) and the amino acid.

They then transfer the amino acid to the tRNA in a process that releases the AMP[4]. This process allows for three opportunities for QC measures (Fig. 1-1). The first is simply the binding specificity of an aaRS for its cognate amino acid. This layer of QC is adequate for 11/20 of the aaRSs as they lack any further QC mechanisms[4]. The second and third QC layers are different types of editing activity. Editing refers to the enzymatic hydrolysis and release of a non-cognate amino acid either pre-transfer or post-transfer to the tRNA. During pre-transfer editing, the AMP is hydrolyzed off of the non-cognate amino acid while they are still in the activation site. During post-transfer editing the non-cognate amino acid is hydrolyzed off of the tRNA by that tRNA's aaRS. This post-transfer editing function is usually carried out by a separate domain of the aaRSs from the aminoacylation domain, which is referred to as *cis* editing[5]. However, in some cases standalone proteins provide this editing function, which is known as *trans* editing[6-9].

What makes editing function in some aaRSs necessary is the structural similarities between the cognate and non-cognate amino acids that allow the non-cognate amino acids to slip through the first QC filter of the aaRSs (Table 1-1). The presence of these editing domains can greatly decrease the rate of mischarging tRNAs. For example, the isoleucine (Ile) aaRS (IleRS) only charges Ile ~200 times more often than valine (Val)[10]. However, the error rate for Val replacing Ile in final protein products has been shown to be much lower ($\sim3\times10^{-4}$)[11].

Non-Protein Amino Acids (NPAs) Make Editing Even More Necessary

In addition to canonical non-cognate amino acids, non-protein amino acids (NPAs) pose a broader and more diverse challenge to aaRSs' ability to charge a tRNA with its cognate amino acid (Table 1-2). A large source of NPAs is amino acid precursors and metabolites that occur naturally inside the cell during the course of normal cellular function. For example, α-

aminobutyrate, also known as homoalanine, is an alpha amino acid that serves as an intermediate in the biosynthesis of opthalmate[12]. In mammalian cells, homoalanine has been shown to be
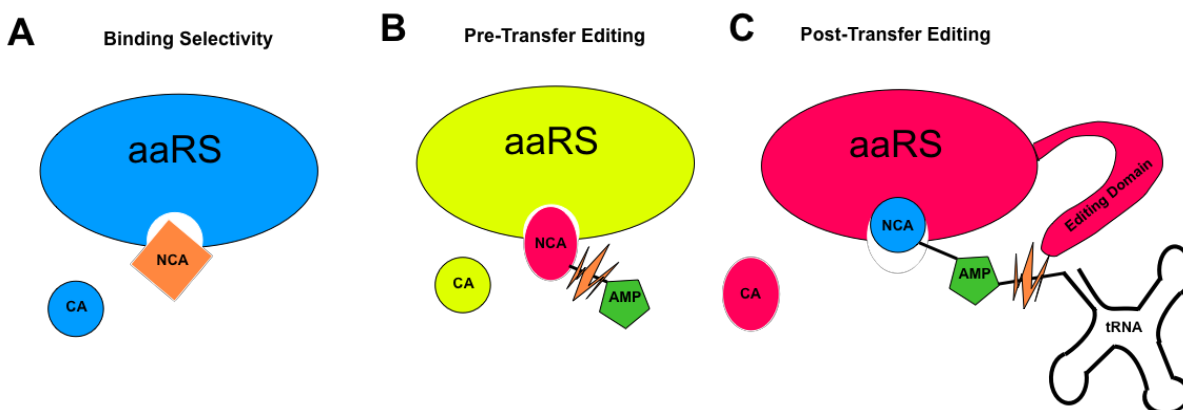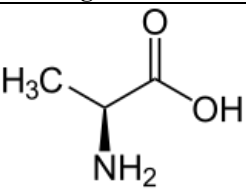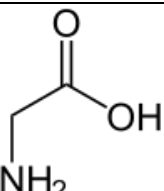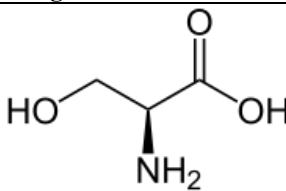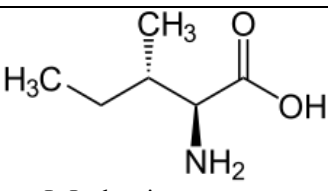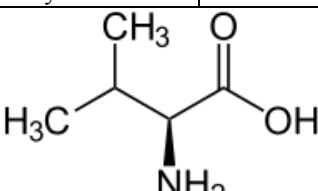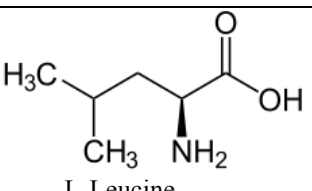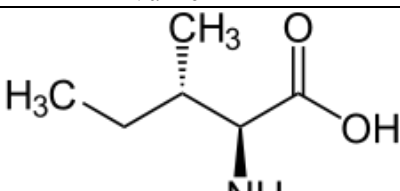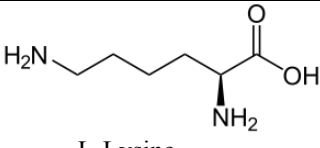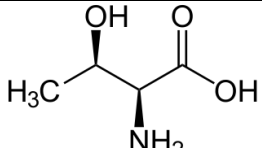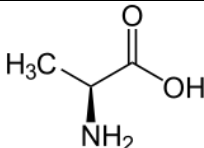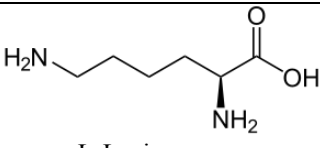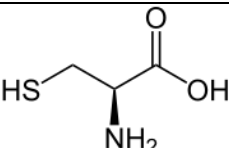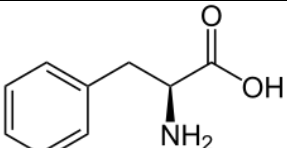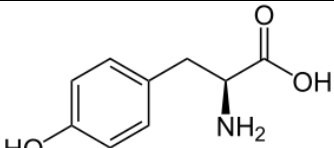
Figure 1-1. aaRSs have three QC mechanisms available to them. Binding specificity (A) prevents a non-cognate amino acid (NCA) from even entering the catalytic pocket instead of the cognate amino acid (CA). Pre-transfer editing (B) cleaves off the AMP from a NCA before it can be attached to the incorrect tRNA. Post-transfer editing (C) is performed by a separate domain of the aaRS that cleaves the tRNA-amino acid bond.

1.5 fold more prone to mischarging by the Val aaRS (ValRS) than other off target canonical amino acids such as threonine (Thr) [13,14]. In mice fibroblast cells with an editing-deficient ValRS, homoalanine was shown to be more disruptive to translational fidelity, and more deadly as measured by amounts of cell lysis and amount of caspase-3 induction, than other non-cognate amino acids[13].

aaRSs activate many amino acid biosynthesis precursors that then need to be edited pre-transfer. L-Homocysteine (Hcy) is an intermediate in the methionine (Met) biosynthetic pathway that only differs from Met by a single methyl group, making it very difficult to discriminate between the two[15-17]. In both *S. cerevisiae* and *E. coli*, Hcy is misactivated and edited by the Met aaRS (MetRS). In *E. coli* Hcy is also edited by IleRS, ValRS, leucine (Leu) aaRS (LeuRS), and lysine (Lys) aaRS (LysRS)[18,19]. L-Homoserine is a precursor amino acid in the biosynthesis of methionine, threonine, and isoleucine[17,20,21]. It has been shown that ValRS, IleRS, and LysRS edit homoserine[22]. L-Ornithine is a product of the urea cycle and an

intermediate in the production of putrescine[23,24]. LysRS has been shown to activate L-ornithine

and then to hydrolyze it via pre-transfer editing[25].

Table 1-1. The structures of the cognate amino acids of aminoacyl-tRNA synthetases and of some of the canonical non-cognate amino acids edited by the aminoacyl-tRNA synthetases.

aaRS	Ref.	Cognate Amino Acid	Canonical Non-Cognate Amino Acids	
AlaRS	26	L-Alanine	Glycine	L-Serine
IleRS	27	L-Isoleucine	L-Valine	
LeuRS	28	L-Leucine	L-Isoleucine	
LysRS	29	L-Lysine	L-Threonine	L-Alanine
LysRS	29	L-Lysine	L-Cysteine	
PheRS	30	L-Phenylalanine	L-Tyrosine	

5
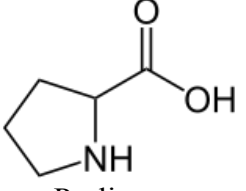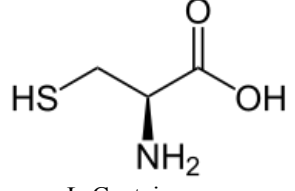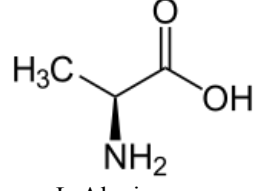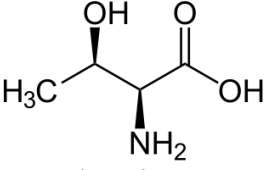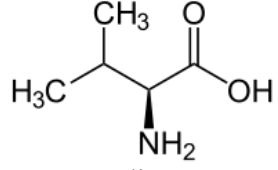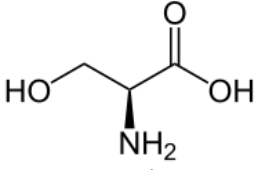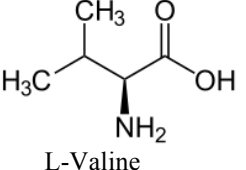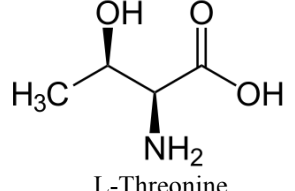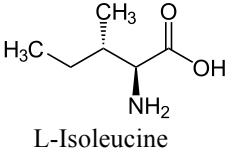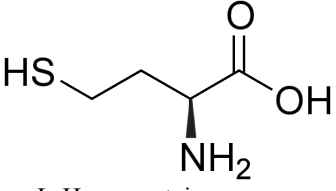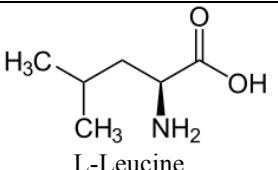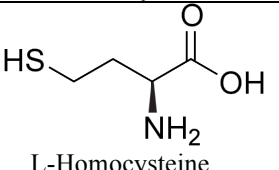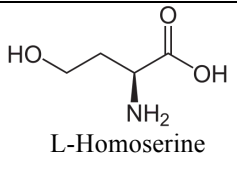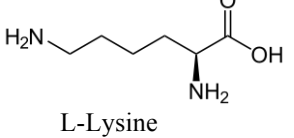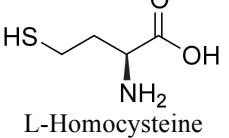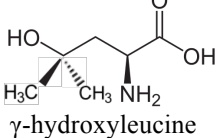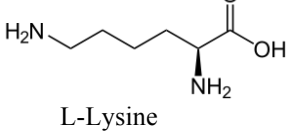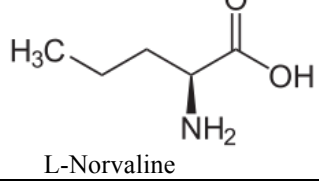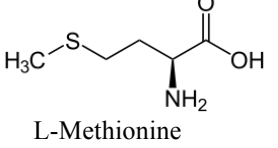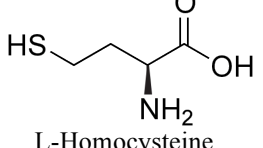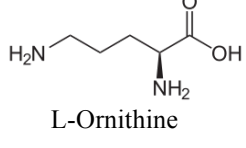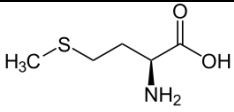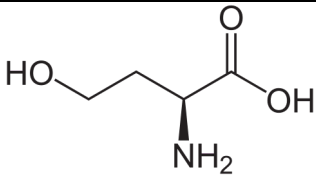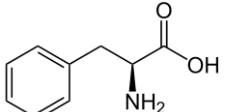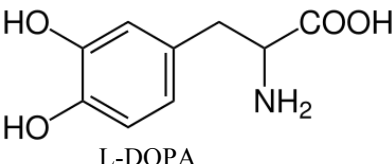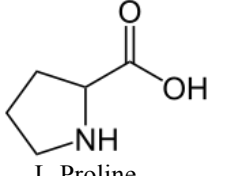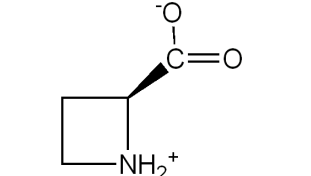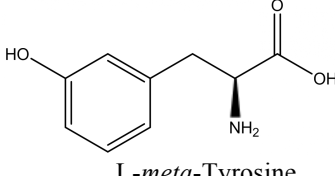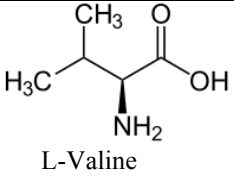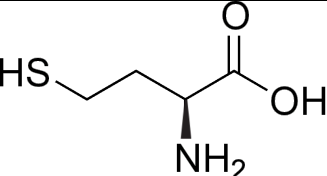
aaRS	Ref.			
ProRS	31,32	Proline	L-Cysteine	L-Alanine
ThrRS	33	L-Threonine	L-Valine	L-Serine
ValRS	34	L-Valine	L-Threonine	

Table 1-2. The structures of the cognate amino acids of aminoacyl-tRNA synthetases and of some of the non-protein amino acids edited by the aminoacyl-tRNA synthetases.

aaRS	Ref.	Cognate Amino Acid	Non-Protein Amino Acids	
IleRS	19	L-Isoleucine	L-Homocysteine	
LeuRS	19,28	L-Leucine	L-Homocysteine	L-Homoserine
LysRS	19,25,35	L-Lysine	L-Homocysteine	γ-hydroxyleucine
LysRS	19,25,35	L-Lysine	L-Norvaline	
MetRS	18	L-Methionine	L-Homocysteine	L-Ornithine

MetRS	18	L-Methionine	L-Homoserine	
PheRS	35-37	L-Phenylalanine	L-DOPA	
ProRS	38	L-Proline	Azetidine-2-carboxylic acid	L-*meta*-Tyrosine
ValRS	19,39	L-Valine	L-Homocysteine	

Oxidative damage from reactive oxygen species (ROS) can also create NPAs that pose serious problems for aaRS activation and charging fidelity. This can occur either by oxidative damage to a free-floating amino acid, or to an amino acid already in a protein that is then subsequently degraded[40,41]. A hydroxyl radical attacking the *meta* position on a tyrosine ring produces 3,4 dihydroxyphenylalanine (L-DOPA). L-DOPA is an intermediate in the dopamine biosynthetic pathway. It has been shown that the Tyr aaRS (TyrRS) in mammalian and bacterial cells, which lacks an editing domain, charges L-DOPA onto the tRNA[Tyr] and L-DOPA is incorporated into proteins at Tyr positions[35,42,43]. L-DOPA has also been shown to be edited by PheRS *in vitro*[37]. Other hydroxylated amino acids such as various leucine hydroxides and valine hydroxides have been shown to be incorporated into proteins in mammalian cells[35].

Plants use many different NPAs as weapons against competitors and herbivores[44,45].

meta-Tyrosine (*m*-Tyr), another NPA produced via oxidative damage as well as through

biosynthetic pathways, is used by fescue grasses as an allelochemical against other competing

plants[46,47]. They exude high concentrations of *m*-Tyr (as high as 6 mM) out of their roots into

the surrounding soil that inhibits root growth of other plants[46]. The phytotoxicity of *m*-Tyr is

broad spectrum, working on a wide range of monocots and dicots[46]. Root growth in *Arabidopsis*

thaliana, when treated with *m*-Tyr, could be partially rescued by the addition of canonical amino

acids[46]. The most effective of these included Phe and Tyr, which indicated that *m*-Tyr toxicity

might stem from misincorporation into proteins in place of those amino acids[46]. Further work

uncovered a *m*-Tyr resistant (*m*-Tyr[R]) *A. thaliana* mutant that over-accumulated Phe[48]. Because

of its broad phytotoxicity, *m*-Tyr is being investigated as a possible herbicide[49]. A patent has

been filed for creating genetically modified plants that would utilize a transgenic bacterial PheRS

in the chloroplasts and mitochondria, thereby providing resistance to a *m*-Tyr-like herbicide[50].

This bacterial post-transfer editing competent PheRS would provide a missing QC mechanism to

the plant organelles to deal with *m*-Tyr. Other studies have revealed that *m*-Tyr is also toxic to

mammalian cells, and that the human mitochondrial PheRS charges *m*-Tyr onto tRNA[Phe] and is

incapable of post-transfer editing of the resulting mischarged tRNA[Phe][35,36].

Other NPAs that plants use as defensive chemicals include L-canavanine and azetidine-2-

carboxylic acid. L-canavanine is mischarged onto tRNA[Arg] by the arginine (Arg) aaRS (ArgRS)

of some insects and animals[51,52]. Some insects have evolved various strategies for tolerating L-

canavanine including metabolic processing to homoserine (*Heliothis virscens*) and a more

selective ArgRS that does not charge L-canavine efficiently (*Caryedes brasiliensis*) [53,54].

Azetidine-2-carboxylic acid is mistaken for proline (Pro) by the Pro aaRS (ProRS) in sensitive

animals, plants, and bacteria and is charged onto their tRNA[Pro]. These organisms' ProRSs are incapable of post-transfer editing of azetidine-2-carboxylic acid[38].

There are still questions to be answered about NPAs. For example, how many can be commonly found in the environment or inside a cell. Are the majority of NPAs just biproducts and intermediates of biosynthetic pathways, or are they more commonly used as weapons against competing organisms like *m*-Tyr is used by fescue grass? What makes a NPA more or less disruptive to the proteins they are incorporated into?

Significance of aaRS Editing for Human Health

A better understanding of aaRS editing could provide insights into disease mechanisms and lead to improved treatments. Work has been done to develop a new class of antibiotics that targets the bacterial PheRS, but does not affect human cytoplasmic and mitochondrial PheRSs, mainly through binding pocket inhibition that cannot be cleared by the PheRS editing domain[55]. There has also been extensive research into developing anti-fungal drugs that specifically target the LeuRS editing domain[56-60].

There is an expanding body of research showing negative health consequences of aaRS editing defects in mammals. There have also been studies that link editing defects in tRNA synthetases to mutagenesis in aging organisms[61,62]. Mice with an editing defective alanine (Ala) aaRS (AlaRS) have been shown to be prone to neurodegeneration. Protein aggregates, presumably formed due to mistranslation of Ala codons, were observed in neurons of the mutant mice[62]. In mouse cells with an editing-defective ValRS, mistranslation and a caspase-3-mediated apoptotic response was observed[13]. In humans, an encephalomyopathy-causing mutations in mitochondrial ThrRS has been shown to decrease post-transfer editing[63]. It has even been

9

proposed that atherosclerosis could be linked to MetRS editing of Hcy, because the byproduct of this editing reaction is toxic and elevated Hcy levels have been correlated with the disease [64].

Questions still remain about the ways the aaRS editing function can affect human health. For example, it appears that the most common negative health effect from a loss of aaRS editing in mammals is neurodegeneration[62,63]. It is still not clear why only neuronal cells are affected by a lack of aaRS editing. Additionally, the full therapeutic potential of targeting the aaRS editing function of pathogens has not been fully explored. The question of which human aaRSs are sufficiently divergent from those of pathogens to allow for inhibitors to be used without damaging patients has yet to be answered.

Microbial Cells Experience Negative Effects from losing aaRS Editing Function

There is research that has shown both a damaging and a neutral effect on cellular function when an aaRS editing function is eliminated. *E. coli* lacking an IleRS editing function had temperature sensitive cell growth and an increased sensitivity to norvaline[65]. It has also been shown that the same *E. coli* strain experiences an elevated mutation rate as the cells age[61]. *E. coli* expressing an editing defective ValRS were able to grow without defect on minimal media plates. However, when the strain was exposed to either elevated concentrations of Thr or homoalanine, the cells displayed a strong growth defect[39]. On the other hand, an editing defective yeast mitochondrial LeuRS did not cause a growth defect in the yeast strain, even when grown with high amounts of Ile[66]. Later, it was shown that the yeast mitochondrial LeuRS had diverged from other LeuRSs and lost its editing function in favor of gaining RNA splicing function[67]. These reports raise the question: why and how is it ok for microbes to sometimes lose their aaRS editing activity?

Aminoacyl-tRNA Synthetase Editing Functions are Not Universally Conserved

Given the plethora of environmental insults to translational fidelity and the dramatic

negative effects of lost editing function in some organisms, one might expect aaRS editing

functions to be universally conserved and widespread. However, there are many examples of

organisms that have evolved to lack editing functions in aaRSs. For example, the human

mitochondrial LeuRS has lost post-transfer editing activity, but has compensated by increasing

the discrimination ratio between Leu and non-cognate amino acids[68]. Many *Mycoplasma*

parasite species have evolved deletions and point mutations in the editing domains of several

different aaRSs[69]. Researchers have hypothesized that the purpose of this is to allow for antigen

variation to evade a host's immune system[69]. *E. coli* has given mixed results when different

aaRSs were mutated to ablate editing function. LeuRS editing defective mutants had diminished

cell viability when grown in media supplemented with Ile[66]. Contrastingly, *E. coli* PheRS

editing defective mutants showed no significant growth defects when grown under standard

laboratory growth conditions or with Tyr[70,71]. These observations raise the question: what are

the selective pressures that maintain editing function in tRNA synthetases like PheRS that do not

show a phenotype when their editing function is ablated?

E. coli Phenylalanyl-tRNA Synthetase Editing as a Model

E. coli PheRS is an ideal system with which to explore the importance of aaRS editing

function. As mentioned above, *E. coli* shows no growth defect under standard laboratory growth

conditions when using an editing-defective PheRS[70]. Phe is structurally very similar to Tyr, only

differing by one hydroxyl group. Because of this, Tyr is sometimes mischarged onto tRNA[Phe].

However, PheRS is often able to correct the mistake with its editing function[72]. *E. coli*'s PheRS is a tetramer made up of two α and two β subunits[73]. The editing domain lies in the β subunit encoded by the gene *pheT*. A G318W substitution in the β-subunit has been shown to have a 78-fold decrease in editing function compared to WT, while still maintaining WT levels of Phe-tRNA^{Phe} charging[74]. Using this editing-defective PheRS mutant strain, we sought to identify the circumstances in which PheRS editing function is important to *E. coli*.

References

1. Shaevitz, J. W., Abbondanzieri, E. A., Landick, R. & Block, S. M. Backtracking by single RNA polymerase molecules observed at near-base-pair resolution. *Nature* **426,** 684–687 (2003).

2. Zaher, H. S. & Green, R. Quality control by the ribosome following peptide bond formation. *Nature* **457,** 161–166 (2009).

3. Becker, H. D. & Kern, D. Thermus thermophilus: a link in evolution of the tRNA-dependent amino acid amidation pathways. *Proceedings of the National Academy of Sciences of the United States of America* **95,** 12832–12837 (1998).

4. Pang, Y. L. J., Poruri, K. & Martinis, S. A. tRNA synthetase: tRNA aminoacylation and beyond. *WIREs RNA* **5,** 461–480 (2014).

5. Mascarenhas, A. P., An, S., Rosen, A. E. & Martinis, S. A. Fidelity mechanisms of the aminoacyl-tRNA synthetases. *Protein …* (2009).

6. Wong, F. C., Beuning, P. J., Silvers, C. & Musier-Forsyth, K. An Isolated Class II Aminoacyl-tRNA Synthetase Insertion Domain Is Functional in Amino Acid Editing. *J Biol Chem* **278,** 52857–52864 (2003).

7. An, S. & Musier-Forsyth, K. Trans-editing of Cys-tRNAPro by Haemophilus influenzae YbaK Protein. *J Biol Chem* **279,** 42359–42362 (2004).

8. Ahel, I., Korencic, D. & Ibba, M. Trans-editing of mischarged tRNAs. in (2003).

9. Chong, Y. E., Yang, X.-L. & Schimmel, P. Natural homolog of tRNA synthetase editing domain rescues conditional lethality caused by mistranslation. *J Biol Chem* **283,** 30073–30078 (2008).

10. Reynolds, N. M., Lazazzera, B. A. & Ibba, M. Cellular mechanisms that control mistranslation. *Nature Publishing Group* **8,** 849–856 (2010).

11. Loftfield, R. B. & Vanderjagt, D. The frequency of errors in protein biosynthesis. *Biochem. J.* **128,** 1353–1356 (1972).

12. Orlowski, M. & Wilk, S. Synthesis of ophthalmic acid in liver and kidney in vivo. *Biochem. J.* **170,** 415–419 (1978).

13. Nangle, L. A., Motta, C. M. & Schimmel, P. Global effects of mistranslation from an editing defect in mammalian cells. *Chem. Biol.* **13,** 1091–1100 (2006).

14. Bullwinkle, T., Lazazzera, B. & Ibba, M. Quality Control and Infiltration of Translation by Amino Acids Outside of the Genetic Code. *Annual review of genetics* **48,** 149–166

(2014).

15. Perła-Kaján, J., Twardowski, T. & Jakubowski, H. Mechanisms of homocysteine toxicity in humans. *Amino Acids* **32,** 561–572 (2007).

16. Guest, J. R., Friedman, S., Foster, M. A., Tejerina, G. & Woods, D. D. Transfer of the methyl group from N5-methyltetrahydrofolates to homocysteine in Escherichia coli. *Biochem. J.* **92,** 497–504 (1964).

17. Flavin, M. Methionine biosynthesis. *Metabolism of sulfur compounds. Metabolic pathways* **7,** 457–503 (1975).

18. Jakubowski, H. Proofreading in vivo: editing of homocysteine by methionyl-tRNA synthetase in the yeast Saccharomyces cerevisiae. *The EMBO Journal* **10,** 593–598 (1991).

19. Jakubowski, H. Proofreading in vivo. Editing of homocysteine by aminoacyl-tRNA synthetases in Escherichia coli. *J Biol Chem* **270,** 17672–17673 (1995).

20. WATANABE, Y., KONISHI, S. & SHIMURA, K. BIOSYNTHESIS OF THREONINE FROM HOMOSERINE. *The Journal of Biochemistry* **44,** 299–307 (1957).

21. Strassman, M., Thomas, A. J., Locke, L. A. & Weinhouse, S. INTRAMOLECULAR MIGRATION AND ISOLEUCINE BIOSYNTHESIS1. *J. Am. Chem. Soc.* **76,** 4241–4242 (1954).

22. Jakubowski, H. Quality control in tRNA charging -- editing of homocysteine. *Acta Biochim. Pol.* **58,** 149–163 (2011).

23. Srb, A. & Horowitz, N. H. The ornithine cycle in Neurospora and its genetic control. *J Biol Chem* **154,** 129–139 (1944).

24. Gale, E. F. The production of amines by bacteria: The production of putrescine from l (+)-arginine by Bacterium coli in symbiosis with Streptococcus faecalis. *Biochem. J.* **34,** 853 (1940).

25. Jakubowski, H. Misacylation of tRNALys with noncognate amino acids by lysyl-tRNA synthetase. *Biochemistry* **38,** 8088–8093 (1999).

26. Guo, M. *et al.* Paradox of mistranslation of serine for alanine caused by AlaRS recognition dilemma. *Nature* **462,** 808–812 (2009).

27. Fukunaga, R. & Yokoyama, S. Structural Basis for Substrate Recognition by the Editing Domain of Isoleucyl-tRNA Synthetase. *Journal of Molecular Biology* **359,** 901–912 (2006).

28. Cvetesic, N., Palencia, A., Halasz, I., Cusack, S. & Gruic-Sovulj, I. The physiological

target for LeuRS translational quality control is norvaline. *The EMBO Journal* **33,** 1639–1653 (2014).

29.   Jakubowski, H. Misacylation of tRNA Lyswith Noncognate Amino Acids by Lysyl-tRNA Synthetase †. *Biochemistry* **38,** 8088–8093 (1999).

30.   Ling, J., Yadavalli, S. S. & Ibba, M. Phenylalanyl-tRNA synthetase editing defects result in efficient mistranslation of phenylalanine codons as tyrosine. *RNA* **13,** 1881–1886 (2007).

31.   Ahel, I. *et al.* Cysteine activation is an inherent in vitro property of prolyl-tRNA synthetases. *J Biol Chem* **277,** 34743–34748 (2002).

32.   Beuning, P. J. & Musier-Forsyth, K. Hydrolytic editing by a class II aminoacyl-tRNA synthetase. *Proceedings of the National Academy of Sciences of the United States of America* **97,** 8916–8920 (2000).

33.   Dock-Bregeon, A.-C. *et al.* Transfer RNA–mediated editing in threonyl-tRNA synthetase: the class II solution to the double discrimination problem. *Cell* **103,** 877–884 (2000).

34.   Fukunaga, R. & Yokoyama, S. Structural Basis for Non-cognate Amino Acid Discrimination by the Valyl-tRNA Synthetase Editing Domain. *J Biol Chem* **280,** 29937–29945 (2005).

35.   Rodgers, K. J., Wang, H., Fu, S. & Dean, R. T. Biosynthetic incorporation of oxidized amino acids into proteins and their cellular proteolysis. *Free Radic. Biol. Med.* **32,** 766–775 (2002).

36.   Klipcan, L., Moor, N., Kessler, N. & Safro, M. G. Eukaryotic cytosolic and mitochondrial phenylalanyl-tRNA synthetases catalyze the charging of tRNA with the meta-tyrosine. *Proceedings of the National Academy of Sciences* **106,** 11045–11048 (2009).

37.   Moor, N., Klipcan, L. & Safro, M. G. Bacterial and Eukaryotic Phenylalanyl-tRNA Synthetases Catalyze Misaminoacylation of tRNA Phe with 3, 4-Dihydroxy-L-Phenylalanine. *Chem. Biol.* **18,** 1221–1229 (2011).

38.   Rubenstein, E. Biologic effects of and clinical disorders caused by nonprotein amino acids. *Medicine* **79,** 80–89 (2000).

39.   Nangle, L. A., de Crécy-Lagard, V., Döring, V. & Schimmel, P. Genetic Code Ambiguity CELL VIABILITY RELATED TO SEVERITY OF EDITING DEFECTS IN MUTANT tRNA SYNTHETASES. *J Biol Chem* **277,** 45729–45733 (2002).

40.   Gurer-Orhan, H. *et al.* Misincorporation of free m-tyrosine into cellular proteins: a potential cytotoxic mechanism for oxidized amino acids. *Biochem. J.* **395,** 277–284 (2006).

41.   Cabiscol, E., Tamarit, J. & Ros, J. Oxidative stress in bacteria and protein damage by reactive oxygen species. *International Microbiology* **3,** 3–8 (2010).

42.   Ozawa, K. *et al.* Translational incorporation of L-3, 4-dihydroxyphenylalanine into proteins. *Febs Journal* **272,** 3162–3171 (2005).

43.   Calendar, R. & Berg, P. The Catalytic Properties of Tyrosyl Ribonucleic Acid Synthetases from Escherichia coli and Bacillus subtilis*. *Biochemistry* (1966).

44.   Huang, T., Jander, G. & de Vos, M. Non-protein amino acids in plant defense against insect herbivores: representative cases and opportunities for further functional analysis. *Phytochemistry* **72,** 1531–1537 (2011).

45.   Vranova, V., Rejsek, K., Skene, K. R. & Formanek, P. Non-protein amino acids: plant, soil and ecosystem interactions. *Plant and Soil* **342,** 31–48 (2011).

46.   Bertin, C. *et al.* Grass roots chemistry: meta-tyrosine, an herbicidal nonprotein amino acid. *Proceedings of the National Academy of Sciences of the United States of America* **104,** 16964–16969 (2007).

47.   Huang, T., Rehak, L. & Jander, G. meta-Tyrosine in Festuca rubra ssp. commutata (Chewings fescue) is synthesized by hydroxylation of phenylalanine. *Phytochemistry* **75,** 60–66 (2012).

48.   Huang, T., Tohge, T., Lytovchenko, A., Fernie, A. R. & Jander, G. Pleiotropic physiological consequences of feedback-insensitive phenylalanine biosynthesis in Arabidopsis thaliana. *The Plant Journal* **63,** 823–835 (2010).

49.   Movellan, J. *et al.* Synthesis and evaluation as biodegradable herbicides of halogenated analogs of L-meta-tyrosine. *Environmental Science and Pollution Research* **21,** 4861–4870 (2014).

50.   Safro, M., Klipcan, L., Maymon, I. & Finarov, I. Transgenic Plants Resistant To Non-Protein Amino Acids. (2014).

51.   ALLENDE, C. C. & ALLENDE, J. E. PURIFICATION AND SUBSTRATE SPECIFICITY OF ARGINYL-RIBONUCLEIC ACID SYNTHETASE FROM RAT LIVER. *J Biol Chem* **239,** 1102–1106 (1964).

52.   Rosenthal, G. A. L-Canavanine: a higher plant insecticidal allelochemical. *Amino Acids* **21,** 319–330 (2001).

53.   Melangeli, C., Rosenthal, G. A. & Dalman, D. L. The biochemical basis for L-canavanine tolerance by the tobacco budworm Heliothis virescens (Noctuidae). *Proceedings of the National Academy of Sciences of the United States of America* **94,** 2255–2260 (1997).

54. Igloi, G. L. & Schiefermayr, E. Amino acid discrimination by arginyl-tRNA synthetases as revealed by an examination of natural specificity variants. *Febs Journal* **276,** 1307–1318 (2009).

55. Pohlmann, J. & Brotz-Oesterhelt, H. New aminoacyl-tRNA synthetase inhibitors as antibacterial agents. *Curr Drug Targets Infect Disord* **4,** 261–272 (2004).

56. Baker, S. J. *et al.* Therapeutic potential of boron-containing compounds. *Future Medicinal Chemistry* **1,** 1275–1288 (2009).

57. Baker, S. J., Tomsho, J. W. & Benkovic, S. J. Boron-containing inhibitors of synthetases. *Chem. Soc. Rev.* **40,** 4279–8 (2011).

58. Yaremchuk, A., Lincecum, T. L., Jr & Tukalo, M. *Structural and Mechanistic Basis of Pre-and Posttransfer Editing by Leucyl-tRNA Synthetase.* (Molecular cell, 2003).

59. Alley, M. R., Baker, S. J., Beutner, K. R. & Plattner, J. Recent progress on the topical therapy of onychomycosis. *Expert Opinion on Investigational Drugs* **16,** 157–167 (2007).

60. Seiradake, E. *et al.* Crystal Structures of the Human and Fungal Cytosolic Leucyl-tRNA Synthetase Editing Domains: A Structural Basis for the Rational Design of Antifungal Benzoxaboroles. *Journal of Molecular Biology* **390,** 196–207 (2009).

61. Bacher, J. M. & Schimmel, P. An editing-defective aminoacyl-tRNA synthetase is mutagenic in aging bacteria via the SOS response. *Proceedings of the National Academy of Sciences of the United States of America* **104,** 1907–1912 (2007).

62. Lee, J. W. *et al.* Editing-defective tRNA synthetase causes protein misfolding and neurodegeneration. *Nature* **443,** 50–55 (2006).

63. Wang, Y. *et al.* A Human Disease-causing Point Mutation in Mitochondrial Threonyl-tRNA Synthetase Induces Both Structural and Functional Defects. *J Biol Chem* **291,** 6507–6520 (2016).

64. Jakubowski, H. Translational accuracy of aminoacyl-tRNA synthetases: implications for atherosclerosis. *The Journal of nutrition* (2001).

65. Bacher, J. M., de Crécy-Lagard, V. & Schimmel, P. R. Inhibited cell growth and protein functional changes from an editing-defective tRNA synthetase. *Proceedings of the National Academy of Sciences of the United States of America* **102,** 1697–1701 (2005).

66. Karkhanis, V. A., Boniecki, M. T., Poruri, K. & Martinis, S. A. A viable amino acid editing activity in the leucyl-tRNA synthetase CP1-splicing domain is not required in the yeast mitochondria. *J Biol Chem* **281,** 33217–33225 (2006).

67. Sarkar, J., Poruri, K., Boniecki, M. T., McTavish, K. K. & Martinis, S. A. The yeast

mitochondrial leucyl-tRNA synthetase CP1 domain has functionally diverged to accommodate RNA splicing at the expense of hydrolytic editing. *Journal of Biological Chemistry* (2012). doi:10.1074/jbc.M111.322412

68.   Lue, S. W. & Kelley, S. O. An aminoacyl-tRNA synthetase with a defunct editing site. *Biochemistry* **44,** 3010–3016 (2005).

69.   Li, L. *et al.* Naturally occurring aminoacyl-tRNA synthetases editing-domain mutations that cause mistranslation in Mycoplasma parasites. *Proceedings of the National Academy of Sciences* **108,** 9378–9383 (2011).

70.   Reynolds, N. M. *et al.* Cell-specific differences in the requirements for translation quality control. **107,** 4063–4068 (2010).

71.   Bullwinkle, T. J. *et al.* Oxidation of cellular amino acid pools leads to cytotoxic mistranslation of the genetic code. *Elife* **3,** (2014).

72.   Ibba, M., Kast, P. & Hennecke, H. Substrate specificity is determined by amino acid binding pocket size in Escherichia coli phenylalanyl-tRNA synthetase. *Biochemistry* **33,** 7107–7112 (1994).

73.   Fayat, G., Blanquet, S., Dessen, P., Batelier, G. & Waller, J.-P. The molecular weight and subunit composition of phenylalanyl-tRNA synthetase from Escherichia coli K-12. *Biochimie* **56,** 35–41 (1974).

74.   Ling, J., Roy, H. & Ibba, M. Mechanism of tRNA-dependent editing in translational quality control. *Proceedings of the National Academy of Sciences of the United States of America* **104,** 72–77 (2007).

Chapter 2:

The non-protein amino acid *meta*-Tyrosine is toxic to PheRS editing-defective *E. coli*

An essential step for the maintenance of translation fidelity in all organisms is the charging of a tRNA with its cognate amino acid. The proteins that are responsible for charging specific tRNAs with the correct amino acids are called aminoacyl-tRNA synthetases (aaRS). Errors can occur during this charging step due to structural similarities between amino acids (e.g. valine vs. isoleucine), leading to a tRNA charged with a non-cognate amino acid. To reduce this type of error some aaRSs have an editing domain that can hydrolyze off non-cognate amino acids from a tRNA. The presence of these editing domains can greatly decrease the rate of mischarging tRNAs. The charging reaction of isoleucine (Ile) aaRS (IleRS) mistakenly charges tRNA^{Ile} with a Val about one out of 200 times (5×10^{-3})[1]. However, the overall error rate for Val replacing Ile in final protein products has been shown to be much lower ($\sim 3 \times 10^{-4}$)[2].

aaRS editing domains are widespread, but are not universally conserved. Many *Mycoplasma* parasite species have evolved deletions and point mutations in the editing domains of several different aaRSs, possibly due to the selective advantage of increased antigen variation and consequent evasion of the host's immune system[11]. There are also examples of mitochondrial aaRSs which have lost editing domains, for which the loss of translational fidelity is partially offset by increased binding specificity[3].

However, there are instances in which the advantage of a conserved editing function is relatively clear. Loss of the editing function can often cause an organism to have increased sensitivity to unbalanced amino acid pools or to non-protein amino acids (NPAs). For example, *E. coli* LeuRS editing defective mutants had diminished cell viability when grown in media supplemented with Ile[3]. Surprisingly, *E. coli* phenylalanyl (Phe) aaRS (PheRS) editing defective mutants showed no significant growth defects when grown under standard laboratory growth

20

conditions[4]. This lack of an obvious growth defect in an *E. coli* PheRS editing defective mutant raises the question: why is the PheRS editing function in *E. coli* conserved?

To answer this question, we constructed an editing-defective PheRS mutant and a control strains in a WT K-12 MG1655 *E. coli* strain background. We used the λ-red recombineering system to introduce the *pheT(G318W)* mutation, which has been shown to ablate the editing function of PheRS while still maintaining WT levels of amino acylation[5-7]. Competent cells of an MG1655 derivative containing pSIM6, a plasmid that carries the λ-red system, were prepared as previously described[8,9]. These cells were transformed with a 70-mer ssDNA oligonucleotide (Table 2-1) that has several wobble mutations (underlined) on either side of the *pheT(G318W)* mutation (bolded). The wobble mutations serve to overwhelm the mismatch repair system[10]. Positive clones were identified by colony PCR, with a primer that recognized the mutated sequence and a reverse primer 500-bp distant (Table 2-1), and subsequent DNA sequencing. One clone was chosen to serve as the intermediate strain and was subjected to a second round of recombineering with an oligo (Table 2-1) to remove the wobble mutations and leave solely the *pheT(G318W)* mutation (strain *BAL 4073*). The intermediate strain was also transformed with an oligo (Table 2-1) that would revert the strain back to the wild type *pheT* sequence. This revertant strain (strain *BAL 4074*) served as the wild type control strain in studies with the *pheT(G318W)* derivative of *E. coli* MG1655. Again, positive clones were screened by colony PCR and DNA sequencing.

As an initial assessment of the growth phenotypes of the *pheT(G318W)* and WT *pheT* strains, we measured their growth curves in rich Luria-Broth media (LB). Twenty-five ml cultures in 250 ml Erlenmeyer flasks were inoculated to an initial OD_{600} of 0.01 from starter LB cultures in mid-log phase and set shaking at 37°C. OD_{600} measurements were taken every hour

for 8 hours. As can be seen in Fig. 2-1, the growth rate and growth yield of the two strains were not different.

It has been previously shown that other *E. coli* PheRS editing mutants (*pheT(H265A, A356W, and E334A)*) mischarge tRNA^{Phe} with tyrosine (*p*-Tyr)[7]. We might then expect that the
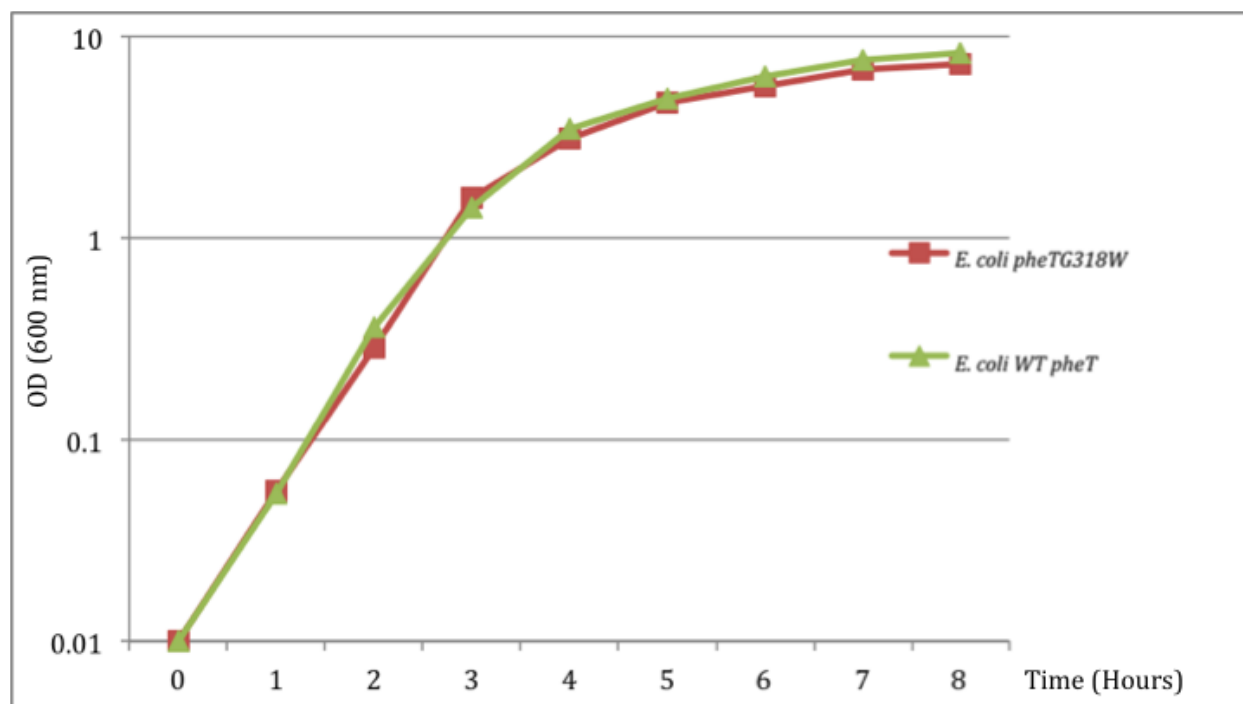
Figure 2-1. Representative LB liquid culture growth curve of *E. coli* MG1655 with *pheT(G318W)* and WT *pheT* in three independent replicates.

pheT(G318W) mutant would have a different growth phenotype than the WT *pheT* strain when grown in the presence of excess *p*-Tyr. To test this, single colonies of *E. coli*, wild type *pheT* or *pheT(G318W)*, were picked from LB plates, resuspended in sterile water and used to inoculate liquid culture at an initial OD$_{600}$ of 0.04. Cultures were grown in M9 media supplemented with glucose (2 g/l), thiamine (1 mg/l), MgSO$_4$ (1 mM), CaCl$_2$ (0.1 mM), and varying amounts of amino acids[11]. For ease of titrating several amino acid concentrations, cultures were grown in 250 μl volumes using 96-well plates, at 37°C. Phe was kept constant at 0.003 mM and *p*-Tyr was

varied from 0.003 mM to 3 mM). The OD$_{600}$ were read using an xMark™ Microplate

Absorbance Spectrophotometer (Bio-Rad Laboratories, Hercules, California) after 12-18 hours

of growth. Surprisingly, even the highest concentration of *p*-Tyr did not appear to affect the

growth of the *pheT(G318W)* strain (Figure 2-2). It is possible that the rate of *p*-Tyr

misincorporation into proteins in the *pheT(G318W)* strain was not high enough to cause

detectable problems for the mutant strain.
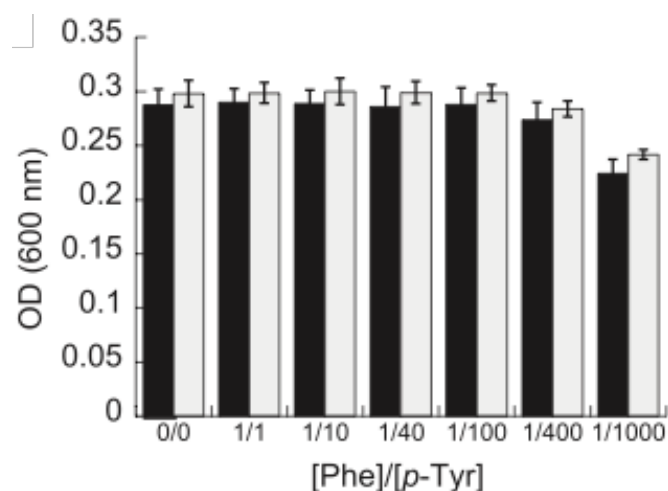
Figure 2-2. Growth of *E. coli pheT*(G318W) strain (grey bars) relative to wild type (black bars) under increasing concentrations of L-*p*-Tyr. A ratio of 1:1 corresponds to 3 μM of each amino acid. The bars are the mean of three independent trials, and the error bars are standard deviation. L-*p*-Tyr had no discernable effect on growth at any tested concentration[5].

Another possible harmful growth condition for editing-defective *pheT(G318W) E. coli*

could be the presence of NPAs. *In vitro* amino acylation assays performed by our collaborators

showed that the NPA *meta*-Tyrosine (*m*-Tyr) was charged onto tRNA^{Phe} at the highest rate of all

the non-cognate amino acids tested by the *pheT(G318W)* mutant PheRS[5]. Phe, however, was

still charged more efficiently than any of the other amino acids tested. Based on these results we

decided to test the growth of the *pheT(G318W)* and WT *pheT* strains in the presence of *m*-Tyr.

The test cultures were prepared in the same manner as the *p*-Tyr cultures were. When grown in

M9 minimal media supplemented with a fixed amount of Phe (3 µM) and an increasing amount

of *m*-Tyr (up to 3 mM), the *pheT(G318W)* strain's growth was inhibited while the WT strain was

unaffected (Fig. 2-3).
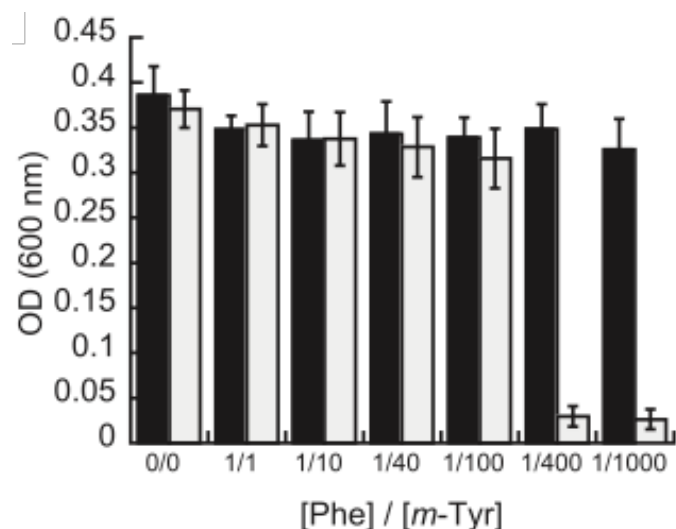
Figure 2-3. Growth of *E. coli pheT(G318W)* strain (grey bars) relative to wild type (black bars) under increasing concentrations of D,L-*m*-Tyr. A ratio of 1:1 corresponds to 3 µM of each amino acid. The bars are the mean of three independent trials, and the error bars are standard deviation. D,L-*m*-Tyr was lethal to *pheT(G318W)* cells at the higher concentrations tested, whereas the growth of wild type was unaffected[5].

There are reasons to suspect that *m*-Tyr may be a key reason for the conservation of the

PheRS editing function in *E. coli*. *m*-Tyr is a NPA that is produced naturally *in vivo* via reactive

oxygen species (ROS) attack on the third carbon in the Phe ring[12]. Our collaborators *in vitro*

aminoacylation results showed that the G318W PheRS mischarged *m*-Tyr at a similar rate as Phe,

while several other NPAs, including L-DOPA and *ortho*-Tyrosine, as well as *p*-Tyr, were

charged much less effectively[5]. Combined with our experimental growth results, this indicates

that, with the exception of *m*-Tyr, the binding specificity of PheRS is enough to prevent these

non-cognate amino acids from causing *E. coli* any significant problems. The available evidence

then, including the fact that *m*-Tyr is readily mistaken for Phe by *E. coli* PheRS, would suggest

that the potential for mis-incorporation of *m*-Tyr into proteins is the selective pressure driving the

conservation of the PheRS editing function.

There are many possible sources of exposure to *m*-Tyr for *E. coli*. The ROS hydrogen

peroxide (H_2O_2) splits into two hydroxyl radicals ($^{\bullet}OH$) and can attack the third carbon on the

Phe ring producing *m*-Tyr. During aerobic growth *E. coli* produces H_2O_2 mostly from

monovalent reductions of O_2 from the electron transport chain[13]. Commensal bacteria in the

mammalian gut can induce epithelial cells to produce ROS including H_2O_2, which can then cross

the cell membrane and travel the equivalent of several cell lengths to epithelial-associated

bacteria including *E. coli*[14]. *E. coli* have also been shown to live in temperate soil environments

long term[15,16]. *m*-Tyr is used as an allelochemical that is released into the soil at high

concentrations by fescue grasses to inhibit root growth of competing plants[17]. Thus there is no

lack of circumstances, in native environments, in which *E. coli* can be exposed to *m*-Tyr. This,

along with PheRS's poor *m*-Tyr vs. Phe binding selectivity, is consistent with the idea that such

exposures may be the driving force behind the conservation of PheRS editing activity.

Table 2-1. List of ssDNA oligonucleotides used for λ-red transformation, and the primers used for diagnostic PCR.[a]

Name	Purpose	Sequence
G318W wobbles oligo	Introduce *G318W* mutation	CACAACAAGGCGCTGGCGATGGG<u>A</u>GG<u>A</u>ATATTT**TGG**GGAG AG<u>C</u>ATT<u>C</u>AGGCGTGAATGACGAAACACAAA
G318W no wobbles oligo	Remove wobbles while leaving *G318W* in place	CACAACAAGGCGCTGGCGATGGGCGGCATCTTC**TGG**GGCG AACACTCTGGCGTGAATGACGAAACACAAA
WT oligo	Revert strain back to WT sequence	CACAACAAGGCGCTGGCGATGGGCGGCATCTTCGGTGGCG AACACTCTGGCGTGAATGACGAAACACAAA
WT FW	Diagnostic PCR for WT sequence	CGGCATCTTC**GGT**GGCGAACACTCT
G318W wobbles	Diagnostic PCR for *G318W* with wobbles	<u>A</u>GG<u>A</u>AT<u>A</u>TTT**TGG**GG<u>A</u>G<u>A</u>GC<u>A</u>TTC<u>A</u>
G318W no wobbles	Diagnostic PCR for the removal of the wobbles	CGGCATCTTC**TGG**GGCGAACACTCT
Reverse	Diagnostic PCR	CCGATCAGGCGATCCAGTTTG

[a] Wobble mutations are underlined. The 318th codon that is the desired mutation site is bolded.

References

1.   Reynolds, N. M., Lazazzera, B. A. & Ibba, M. Cellular mechanisms that control mistranslation. *Nature Publishing Group* **8,** 849–856 (2010).

2.   Loftfield, R. B. & Vanderjagt, D. The frequency of errors in protein biosynthesis. *Biochem. J.* **128,** 1353–1356 (1972).

3.   Karkhanis, V. A., Boniecki, M. T., Poruri, K. & Martinis, S. A. A viable amino acid editing activity in the leucyl-tRNA synthetase CP1-splicing domain is not required in the yeast mitochondria. *J Biol Chem* **281,** 33217–33225 (2006).

4.   Reynolds, N. M. *et al.* Cell-specific differences in the requirements for translation quality control. **107,** 4063–4068 (2010).

5.   Bullwinkle, T. J. *et al.* Oxidation of cellular amino acid pools leads to cytotoxic mistranslation of the genetic code. *Elife* **3,** (2014).

6.   Roy, H., Ling, J., Irnov, M. & Ibba, M. Post–transfer editing in vitro and in vivo by the β subunit of phenylalanyl–tRNA synthetase. *The EMBO Journal* (2004).

7.   Ling, J., Yadavalli, S. S. & Ibba, M. Phenylalanyl-tRNA synthetase editing defects result in efficient mistranslation of phenylalanine codons as tyrosine. *RNA* **13,** 1881–1886 (2007).

8.   Yu, D. *et al.* An efficient recombination system for chromosome engineering in Escherichia coli. *Proceedings of the National Academy of Sciences of the United States of America* **97,** 5978–5983 (2000).

9.   Datta, S., Costantino, N. & Court, D. L. A set of recombineering plasmids for gram-negative bacteria. *Gene* **379,** 109–115 (2006).

10.   Costantino, N. & Court, D. L. Enhanced levels of lambda Red-mediated recombinants in mismatch repair mutants. *Proceedings of the National Academy of Sciences of the United States of America* **100,** 15748–15753 (2003).

11.   Miller, J. H. Experiments in molecular genetics. (1972).

12.   Berlett, B. S. & Stadtman, E. R. Protein oxidation in aging, disease, and oxidative stress. *Journal of Biological Chemistry* (1997).

13.   González-Flecha, B. & Demple, B. Metabolic sources of hydrogen peroxide in aerobically growing Escherichia coli. *J Biol Chem* **270,** 13681–13687 (1995).

14.   Jones, R. M., Mercante, J. W. & Neish, A. S. Reactive oxygen production induced by the gut microbiota: pharmacotherapeutic implications. *Curr. Med. Chem.* **19,** 1519–1529

(2012).

15.   Ishii, S., Ksoll, W. B., Hicks, R. E. & Sadowsky, M. J. Presence and Growth of Naturalized Escherichia coli in Temperate Soils from Lake Superior Watersheds. *Applied and Environmental Microbiology* **72,** 612–621 (2006).

16.   Byappanahalli, M. N., Whitman, R. L., Shively, D. A., Sadowsky, M. J. & Ishii, S. Population structure, persistence, and seasonality of autochthonous Escherichia coli in temperate, coastal forest soil from a Great Lakes watershed. *Environmental Microbiology* **8,** 504–513 (2006).

17.   Bertin, C. *et al.* Grass roots chemistry: meta-tyrosine, an herbicidal nonprotein amino acid. *Proceedings of the National Academy of Sciences of the United States of America* **104,** 16964–16969 (2007).

Chapter 3:

Mechanism of *m*-Tyrosine toxicity to PheRS editing-defective *E. coli*

Abstract

Faithful translation of the genetic code into amino acid sequences is important for the viability of organisms. To ensure faithful translation, some aminoacyl-tRNA synthetases (aaRS) have evolved an editing mechanism that allows them to cleave off similarly shaped non-cognate amino acids (NCAs) from a mischarged tRNA. A large source of mischarged NCAs are non-protein amino acids (NPAs). Some of these NPAs have been shown to be toxic to organisms lacking an editing function in aaRSs that would need to edit them off of the aaRSs' cognate tRNAs. One of these NPAs, *meta*-Tyrosine (*m*-Tyr), has been shown to be toxic to *E. coli* that have been engineered to lack an editing function in its phenylalanyl aaRS (PheRS).

Here, we sought to understand why *m*-Tyr is toxic to PheRS editing-defective (PheRS edit⁻) *E. coli*. We used chemical mutagenesis to find *m*-Tyr resistant mutants and then performed whole genome sequencing to find the mutations that contributed to the resistance. We found that mutations affecting uptake and efflux transport could provide resistance by keeping or getting *m*-Tyr out of the cell. We also identified a mutation that likely elevated Phe production that could also provide resistance by most likely increasing competitive inhibition of the *m*-Tyr. We also observed PheRS edit⁻ *E. coli* after *m*-Tyr exposure directly via light and electron microscopy. We observed large protein aggregates forming in the cells, which indicated that the *m*-Tyr destabilized a large fraction of the proteome. We then performed transcriptomic analysis of PheRS edit⁻ *E. coli* after *m*-Tyr exposure to see what stress responses were used to deal with *m*-Tyr toxicity. We found a strong induction of the unfolded protein stress response, as well as oxidative stress, DNA damage stress, and indications of lost ion homeostasis. Based on these findings, we propose a model of *m*-Tyr toxicity that involves a cascading and self-reinforcing chain reaction of cellular stresses that ultimately leads to cell death.

Introduction

       Faithful translation of the genetic code into amino acid sequences is important for the viability of organisms. Various quality control (QC) mechanisms have evolved throughout the translation process to ensure faithful translation takes place. One source of error in translation is the mischarging of tRNAs with the incorrect amino acid due to structural similarities between the cognate and non-cognate amino acids. If gone unchecked, these mischarged tRNAs would provide an amino acid to the ribosome that does not match its codon, thereby causing mistranslation of the mRNA sequence.

       The proteins that are responsible for charging tRNAs with the correct amino acids are called aminoacyl-tRNA synthetases (aaRS). Some of these aaRSs (9 out of 20) have evolved a QC mechanism to deal with mischarged tRNAs called post-transfer editing. Post-transfer editing refers to the hydrolyzing of a non-cognate amino acid off of a tRNA either by a dedicated editing domain attached to the aaRS (*cis* editing) or a standalone protein (*trans* editing)[1-5]. The presence of these editing domains can greatly decrease the rate of mischarging tRNAs. For example, the isoleucine (Ile) aaRS (IleRS) charges Ile only ~200 times more often than valine (Val)[6]. However, the error rate for Val replacing Ile in final protein products has been shown to be much lower (~3×10^{-4})[7]. Since the aaRS post-transfer editing function is one of the last QC mechanisms before the incorrect amino acid is added to a polypeptide, one can infer that the aaRS editing function is largely responsible for this disparity.

       A better understanding of aaRS editing could provide insights into disease mechanisms and lead to improved treatments. There has been extensive research into developing anti-fungal drugs that specifically target the Leucine (Leu) aaRS (LeuRS) editing domain[8-12]. Work has been done to develop a new class of antibiotics that targets the bacterial PheRS, but does not

affect human cytoplasmic and mitochondrial PheRSs, mainly through binding pocket inhibition that cannot be cleared by the PheRS editing domain[13]. There have also been studies that link editing defects in aaRSs to mutagenesis in aging organisms[14,15]. Mice with an editing defective alanine (Ala) aaRS (AlaRS) have been shown to be prone to neurodegeneration. Protein aggregates, presumably formed due to mistranslation of Ala codons, were observed in neurons of the mutant mice[15]. In mouse cells with an editing-defective Val aaRS (ValRS), mistranslation and a caspase-3-mediated apoptotic response was observed[16]. In humans, disease causing mutations in mitochondrial threonine (Thr) aaRS (ThrRS) have been shown to decrease post-transfer editing[17]. It has also been proposed that atherosclerosis could be linked to methionine (Met) aaRS (MetRS) editing of the non-canonical amino acid homocysteine (Hcy), because the byproduct of this editing reaction is toxic and elevated Hcy levels have been correlated with the disease[18].

Non-protein amino acids (NPAs) are a significant source of substrates for tRNA mischarging. One source of these NPAs is biosynthetic intermediates and metabolites. For example, Hcy, ornithine, and homoserine can all be mistaken for lysine (Lys) by the Lys aaRS (LysRS)[19,20]. Another source of NPAs is oxidatively damaged amino acids and proteins[21]. Reactive oxygen species (ROS) such as a hydroxyl radical can attack the *meta* position on a tyrosine (Tyr) ring producing 3,4 dihydroxyphenylalanine (L-DOPA). Another NPA produced by ROS attack is *meta*-tyrosine (*m*-Tyr), produced from a hydroxyl radical attacking the *meta* position on a Phe ring[22].

m-Tyr is charged onto tRNA[Phe] by many species' PheRSs[22-25]. This mischarging requires PheRS to edit *m*-Tyr, if it can, or else the *m*-Tyr will be incorporated into proteins in the place of Phe. We have previously shown that *m*-Tyr is lethal to *E. coli* bearing a mutation that eliminates

its PheRS editing function, while being apparently benign to WT *E. coli*[25]. Our collaborators also showed that *m*-Tyr was the most efficient tested NPA at being charged onto tRNA^{Phe}, although it was still a less efficient substrate than Phe. They also estimated the rates of *m*-Tyr misincorporation, for *E. coli* grown on a sub-lethal concentration of *m*-Tyr, as ~2.5% for the PheRS editing-defective strain and ~1.5% for the WT strain[25]. These observations raise the question: why is a difference of misincorporation of only ~1% so lethal to the PheRS editing-defective mutant?

Here, we attempt to answer that question with a multifaceted investigation of *m*-Tyr toxicity to the *E. coli* PheRS editing-defective mutant. We show that the PheRS editing-defective mutant is more heat-sensitive than WT when grown on a sub-lethal concentration of *m*-Tyr. We isolated *m*-Tyr resistant (*m*-Tyr^R) mutants from a chemical mutagenesis screen and identified three different types of mutations driving their resistance. We observed the WT and PheRS editing-defective mutant directly via Differential Interference Contrast (DIC) and Transmission Electron (TEM) microscopy subsequent to *m*-Tyr treatment. We observed large protein aggregates localized to the poles of the cells in the editing-defective mutant, indicating that *m*-Tyr causes a large-scale proteome unfolding in *E. coli* lacking PheRS editing function. Lastly, we analyzed transcriptional changes in the PheRS editing-defective mutant after exposure to *m*-Tyr and observed various stress responses including an unfolded protein response, signs of oxidative stress, and lost ion homeostasis.

Materials and Methods

Media and Growth Conditions

For standard lambda-red transformations, LB media was used with half the normal concentration of NaCl. For transformations removing the *cat-sacB* cassette, LB media with added 5% sucrose and lacking NaCl was used. Where indicated, cells were grown in M9 minimal media containing 0.2% glucose and M63 minimal media plates with 8 mM *m*-Tyr[26]. Ampicillin (amp) was used at a concentration of 100 μg/ml and chloramphenicol was used at a concentration of (10 μg/ml). Liquid media cultures were inoculated to an OD_{600} of 0.01 and either placed in a roller drum (large test tube) or shaking (250 or 500 ml Erlenmeyer flask) at 37°C, unless otherwise noted. Overnight growth lasted 16-18 hours at 37°C or 24 hours at 28°C, unless otherwise noted.

Strain Construction and *m*-Tyr^R Mutant Isolation

Chemical mutagenesis was performed using ethyl methanesulfonate (EMS) on the *pheT(G318W)* PheRS editing-defective *E. coli* (BAL 4073). 2 ml of an overnight LB culture were spun down and resuspended in the same volume of M9 minimal media. EMS was added to the cells to a concentration of 2%. The cells were incubated for 40 minutes in a roller drum at 37°C. The cells were then washed 5 times with fresh M9, diluted 1:10 in either LB or M9, and allowed to outgrow with shaking at 37°C for 16 hours. The outgrowth cultures were used to inoculate 5 ml M9 + 0.5 mM *m*-Tyr (sub-lethal concentration) cultures to enrich for resistant mutants. The enrichment cultures grew 16 hours shaking at 37°C. In order to select for resistant colonies, the enrichment cultures were plated on M63 + 8 mM *m*-Tyr plates and incubated at 37°C for 16 hours. Colonies were streak purified on M63 + 8 mM *m*-Tyr plates. This chemical

33

mutagenesis protocol was repeated seven times. With the exception of resistant strains Rmt1 and

Rmt2, all identified resistant strains were isolated from different protocol replicates to ensure

each strain was genetically unique and arose independently.

In order to test candidate m-Tyr^R mutations, mutated genes were replaced with their WT

versions in m-Tyr^R strain backgrounds. The WT versions of these genes were also replaced with

candidate mutations in a clean *pheT(G318W)* background. This was done using the λ-red

recombineering system on the pSIM6 plasmid. The selectable and counter-selectable markers in

the *cat-sacB* cassette were used to perform these allele replacements. Linear dsDNA products

containing the *cat-sacB* cassette flanked by homology to the target loci were produced by PCR.

The primers were designed with 30-40 bp of homology to the chromosomal loci of the candidate

m-Tyr^R genes added to the 5' end (Table 3-1). These primers produced *cat-sacB* products that

would recombine on the chromosome and replace the target native sequence flanked by the

homologous sequences added to the *cat-sacB* cassettes. The λ-red recombineering competent

cells were prepared as previously described[27]. At least 100 ng of PCR product was mixed with

50 μl of competent cells before electroporation. The cells were allowed to recover after

electroporation in 1 ml of LB shaking at 28°C for 1 hour. They were then plated on LB + Cm

plates and incubated at 28°C for 24 hours.

Table 3-1. List of primers used to construct *cat-sacB* cassettes with added homology to gene loci recombination targets and PCR products to remove the *cat-sacB* cassettes.

Target Gene	Primer Name	Sequence
aroP[a]	BL1622	CACTGCGTAGATCAAAAAAACAACCACCGCACGAGGTTTCaa aatgagacgttgatcggcacg
aroP[a]	BL1623	ACGGGTGAGGGCGTAGAGAGAatcaaagggaaaactgtcca
aroP[a]	BL1624	ATTATTGCCCTCACCCTGTACGGGTGAGGGCGTAGAGAGAat caaagggaaaactgtcca
rhtC	BL1633	GATTCGTGCGCATGTTGATGGCGATGACGAAGAGTAGTCAGt gtaggctggagctgcttcgaa

(including promoter) [a]		
rhtC (both) [a]	BL1634	TAAACGCCTTATCCGACTTACTCTGAAGACGCGTCTGGCAca tatgaatatcctccttagttcctagtgcttgg
rhtC (excluding promoter) [a]	BL1635	GTATGAAGACTCCGTAAACGTTTCCCCCGCGAGTCAAATGTt gtaggctggagctgcttcgaa
gpp [a]	BL1636	GAATGCAGCCAACACAGAGACAGATTGAAGGATGAAGAGTtg taggctggagctgcttcgaa
gpp [a]	BL1637	ATCTGAAAGCGATGATGGCGGCAAAACGAGGGAAATAATCca tatgaatatcctccttagttcctagtgcttgg
tyrA [a]	BL1638	GAACGGGCAGCTGACGGCTCGCGTGGCTTAAGAGGTTTATTt gtaggctggagctgcttcgaa
tyrA [a]	BL1639	ACTGGATTAttaCTGGCGATTGTCATTCGCCTGACGCAATca tatgaatatcctccttagttcctagtgcttgg
yodD [a]	BL1640	ACTGGCGGCAACAACAGAGTAACGGTTGCGAGGAAAGATGtg taggctggagctgcttcgaa
yodD [a]	BL1641	CACATCAGATTTCCTGGTGTAACGAATTTTTTAAGTGCTTca tatgaatatcctccttagttcctagtgcttgg
aroP [b]	BL1626	CCGAATTGAACCGATTCACTTACCA
aroP [b]	BL1627	GGTCATGGTGAGAAAGCGTTA
rhtC [b]	BL1648	ACTGTTCGCCAAATTACGCA
rhtC [b]	BL1649	TTCGGCTCGTTGTTTATGCT
gpp [b]	BL1642	TCCCGATGAGCTTACTGTAG
gpp [b]	BL1643	GCAGGATGATCTGATTTGGG
tyrA [b]	BL1646	CACGAGGGCAATCAGTCTTC
tyrA [b]	BL1647	TCAGGCCAATCTTGAATCAGC
yodD [b]	BL1644	GCAGGATGATCTGATTTGGG
yodD [b]	BL1645	TCGCGCAGTACTCCTCTTAC

[a]*cat-sacB* insertion cassette primers: Capitalized sequences represent added target homology. Lower case sequences are designed to anneal to the *cat-sacB* cassette.

[b]*cat-sacB* removal primers

In order to remove the *cat-sacB* cassette and replace it with the desired allele, a dsDNA product of the allele was produced by colony PCR using primers homologous to at least 40 bp outside of the *cat-sacB* insertion site (Table 3-1). This produced a PCR product of the desired allele that had enough flanking homology for the recombination to occur, allowing for replacement of *cat-sacB*. The λ-red recombineering competent cells were prepared as previously described[28]. At least 100 ng of PCR product was mixed with 50 μl of competent cells before electroporation. The cells were allowed to recover for 5 hours in 10 ml of LB (No NaCl) shaking at 28°C to allow for complete loss of the *cat-sacB* cassette before the counter-selection. They

were then plated on LB + 5% sucrose plates and incubated at 28°C for 24 hours.

Transformations were confirmed by colony PCR. The pSIM6 plasmid was cured from the

transformed strains by successive streak purification on LB plates grown at 37°C. Colonies were

tested for the loss of the plasmid by patching on LB and LB ampicillin (LB + amp) plates.

Assay for *m*-Tyr Resistance

In order to assess the level of resistance to *m*-Tyr in a strain, 3 cultures from individual

colonies of the strain were grown in LB overnight. These cultures were washed and resuspended

in 0.9% NaCl. Each cell suspension was then used to inoculate three 1 ml M9 + 2 mM *m*-Tyr

culture to an OD_{600} of 0.01 in small test tubes. The cultures were then allowed to grow with

shaking at 37°C for 24 hours. The growth of the cultures as measured by their final OD_{600} was

used as a proxy for a strain's level of *m*-Tyr resistance.

Genome Sequencing of *m*-Tyr^R Strains

Genomic DNA samples were prepared from LB overnight cultures started from single

colonies of the *m*-Tyr^R strains (BAL 4107, 4114, 4672, 4673, 4680, 4681, 4682, and 4683) and

the clean *pheT(G318W)* background strain. The MasterPure™ DNA Purification kit from

Illumina® was used, following the provided protocol. Sample DNA was digested enzymatically

and labeled via barcode ligation onto the ends of DNA fragments using the Illumina® TruSeq®

DNA PCR-Free Library Prep kit[29]. The samples were then sequenced using the Illumina®

NextSeq™ with 75 bp long, pair end reads at the USC Epigenome Center. The sequences were

sorted to their correct strain automatically using a custom python script written by Fabian

Seidel[29]. The sequences were then aligned to the *E. coli* MG1655 reference genome

(NC_000913) using Burrow-Wheeler Aligner and SAMtools[30,31]. SNPs were identified with a minimum requirement of 5x coverage of a given base and 80% agreement on the mutation.

Assay for Thermosensitivity

In order to test if growing in the presence of *m*-Tyr increased the *pheT(G318W)* strain's sensitivity to heat as compared to the WT control, the two strains were assayed for their rate of cell death at a non-permissive temperature. Overnight cultures were washed and resuspended with 0.9% NaCl and used to inoculate 5 ml M9 + 0.5 mM *m*-Tyr cultures to an OD_{600} of 0.01. These cultures were grown for 16 hours with shaking at 37°C, after which cells from the cultures were washed and resuspended in 0.9% NaCl to an OD_{600} of 1.0. Five 100 μl aliquots of serial dilutions 10^{0}-10^{-6} in 0.9% NaCl were aliquoted into PCR tubes. The tubes were incubated in a thermocycler, which ramped from room temperature to hold at 60°C. When the heating block reached 60°C (t=0), the first time-point tubes were removed and placed on ice. Tubes were removed and placed on ice after ever minute for 4 minutes. Each tube was plated on LB plates, including a tube that did not go in the thermocycler, and the CFU/ml at each time point was assessed.

RNA-seq of *pheT(G318W) E. coli* Exposed to *m*-Tyr

A 5 ml LB culture was inoculated from a single colony of the *pheT(G318W)* strain and grown until it reached mid-log phase (OD_{600} 0.4-0.6). A 1 ml sample of the cells were then washed in 0.9% NaCl and used to inoculate a 100 ml, M9 minimal media culture in a 500 ml flask to an OD_{600} of 0.001. The M9 culture was allowed to grow with shaking at 37°C until it

reached an OD_{600} of 0.5. A sample of cells was taken at this time (t=0) for RNA purification and plating on LB plates. A *m*-Tyr solution was then added to the culture to 0.5 mM. The culture was then allowed to continue growing at 37°C with shaking. Additional sampling for RNA purification and LB plating was done at 30, 60, and 120 minutes after *m*-Tyr addition. This protocol was repeated for a total of three biological replicates.

RNA purification was performed using the Qiagen® (Germantown, Maryland, USA) RNeasy® Mini Kit. 1 ml of culture was removed for each time point and mixed with 2 ml of RNAprotect® Bacterial Reagent. The Qiagen® protocols for "Enzymatic Lysis of Bacteria" and "Purification of Total RNA from Bacterial Lysate Using the RNeasy® Mini Kit" in the RNAprotect® manual was used to purify the samples' RNA. RNA quality was then assessed using the Agilent (Santa Clara, CA, USA) 2100 Bioanalyzer. Any residual genomic DNA in the RNA samples was then digested using the Ambion® (Waltham, MA, USA) DNA-*free*® kit. Ribosomal RNA was removed from the RNA samples using the Thermo Fisher Scientific (Waltham, MA, USA) RiboMinus™ Transcriptome Isolation Kit for bacteria. The resulting rRNA-depleted samples were then concentrated using the Qiagen® RNeasy® columns using the "RNA Clean Up" protocol found in the RNeasy® manual. cDNA libraries were then created using New England Biolabs' (Ipswich, MA, USA) NEBNext® Ultra™ Directional RNA Library Prep Kit for Illumina® and the NEBNext® Multiplex Oligos for Illumina (Primer Set 1). The quality of the cDNA libraries was assessed using the Agilent 2100 Bioanalyzer. Sequencing of the 12 cDNA libraries was performed using the Illumina MiSeq Personal Sequencer System with paired end 150 bp reads.

Sequence results were aligned to *E. coli* str. K-12 substr. MG1655 ASM584v2.32 genome sequence using TopHat[32]. Transcript read counts were determined using HTSeq version

0.6.1p1[33]. Normalization of read counts and differential gene expression analysis were performed using R package DESeq2[34]. Results were analyzed by pairwise comparison of two different time-points at a time. The time-points t=30, 60, and 120 were all compared to t=0. Also, the comparisons of t=30 vs. t=60 and t=60 vs. t=120 were used to assess the statistical significance of changes in gene expression over the time course. Identification of pathway regulation patterns was accomplished by using the BioCyc pathway tools to overlay differential expression results onto metabolic and biosynthetic pathway maps[35].

DIC Microscopy

In order to see if *m*-Tyr induced a visible distinguishing phenotype in the *pheT(G318W)* strain, we observed the cells directly using Differential Interference Contrast microscopy as a function of their time of exposure to *m*-Tyr. A 5 ml LB culture was inoculated with a single colony of either the WT or *pheT(G318W)* strain and grown until it reached mid-log phase (OD_{600} 0.4-0.6). Cells were then washed in 0.9% NaCl and inoculated a 100 ml, M9 minimal media culture in a 500 ml flask to an OD_{600} of 0.001. The M9 culture was allowed to grow shaking at 37°C until it reached an OD_{600} of 0.5. A sample of cells was taken at this time (t=0) for imaging. A *m*-Tyr solution was then added to a final concentration of 0.1 or 0.5 mM. The control cultures received the same volume of sterile ddH_2O. Additional samples for imaging were taken 30, 60, 120, and 300 minutes after the addition of *m*-Tyr.

Samples were spun down and concentrated 10 fold in the M9 media. 3 μl of the concentrated sample was then pipetted onto a 1% agarose pad, which contained the same concentration of salts as the M9 growth media, and covered with a coverslip. The cells were imaged with a Zeiss (Jena, Germany) Axioskop 2 DIC microscope, and the images were saved in

ZVI format. For each image, the cell length and the number of visible dark spots of 50 cells with clearly distinguishable borders were quantified using ImageJ with the Fiji plugin[36,37].

Transmission Electron Microscopy

A 100 ml M9 + 0.5 mM *m*-Tyr culture of the *pheT(G318W)* strain was prepared as described above in the DIC and RNA-seq methods. Two hours after the *m*-Tyr was added to the culture, 2 ml of culture was spun down and resuspended in 200 μl Phosphate Buffered Saline (PBS)[26]. Glutaraldehyde was added to the cell suspension to a 2% final concentration for chemical fixation. Droseran, LLC (Pasadena, CA, USA) prepared and imaged the fixed samples. 50 μl aliquots were spun down at 3,000 RPM for 2 minutes (all centrifugation steps used identical settings) and washed twice in ddH$_2$O. Osmium tetroxide was added to the sample to a 1% concentration and allowed to incubate for 30 minutes. The pellet was then washed twice with ddH$_2$O and spun down. Uranyl acetate was then added to the sample to a final concentration of 0.5% and incubated for 30 minutes. The sample was then washed twice with ddH$_2$O. The sample was then incubated in increasing concentrations of ethanol (25%, 50%, 75%, 90%, and twice with 100%) for 10 minutes each. The sample was then incubated in 25% Epon uncatalyzed overnight. The next day the sample was incubated in 75% Epon for 3 hours, then in 100% Epon. The sample was then polymerized at 60°C for 24 hours. The sample was sectioned, and then imaged using an FEI Morgagni 268 at 80kV acceleration voltage.

Results

Isolation of Mutants of the *pheT(G318W)* Strain that Resist *m*-Tyr Toxicity

In order to reveal the mechanism(s) of *m*-Tyr toxicity to *pheT(G318W) E. coli* cells, we

isolated mutants that are *m*-Tyr^R. Cells of this strain were subjected to chemical mutagenesis

with 2% ethyl methanesulfonate (EMS) and were then outgrown in either M9 minimal media or

LB in the absence of *m*-Tyr. The mutagenized cells were then transferred to M9 minimal media

with a sub-lethal concentration of *m*-Tyr (0.5 mM) to allow for enrichment of *m*-Tyr^R mutants.

The enriched cultures were then plated onto minimal media plates with a lethal *m*-Tyr

concentration (8 mM), and resistant colonies were streak purified. We performed 7 independent

mutagenesis assays and isolated 8 unique *m*-Tyr^R strains (Table 3-2.). Strains were designated

Rmt(1-8) for "Resistant to *m*-Tyr" and the order they were isolated.

To quantify the resistance levels of the newly isolated *m*-Tyr^R mutants, they were

inoculated into minimal media with a lethal *m*-Tyr concentration (2 mM) and allowed to grow at

37°C shaking for 24 hours (Fig. 3-1). The average final OD$_{600}$ of the *m*-Tyr^R strains was used as

a proxy for their level of resistance to *m*-Tyr. The resistance assay revealed that the strains had a

variety of levels of resistance, all higher than *pheT(G318W)* negative control. Some showed

resistance levels lower than the WT control, such as Rmt1, Rmt2, and Rmt4. Contrastingly,

Rmt5 and Rmt7 showed greater than WT levels of growth. Most of the *m*-Tyr^R strains had a

higher variance in their final OD$_{600}$ than the WT control, indicating that their mechanisms of

resistance could be more stochastic than PheRS editing.

We performed whole genome sequencing on the 8 strains and the *pheT(G318W)* parental

strain and searched for SNPs that could explain the strains' resistance to *m*-Tyr. Sample

genomic DNA was digested enzymatically and labeled via barcode ligation onto the ends of

DNA fragments[29]. The samples were then sequenced using the Illumina® NextSeq™ with 75 bp long, pair end reads. The sequences were sorted to their correct strain automatically using a custom python script[29]. SNPs were identified with a minimum requirement of 5x coverage of a given base and 80% agreement on the mutation. In total, there were 156 non-silent and intergenic SNPs identified across the 8 unique strains (Table 3-2). Notably, there were no WT revertants among them. Candidate m-Tyr^R mutations were identified by searching for genes and loci that were mutated in multiple strains, and by examining mutated genes' functions for plausible resistance mechanisms (e.g. amino acid metabolism, amino acid transport, stress response, etc.). Using allele replacement and the m-Tyr resistance assay, we determined that mutations in three genes were the main drivers of resistance in these strains: $aroP$, $rhtC$, and $tyrA$. See Appendix A for a full SNP list.
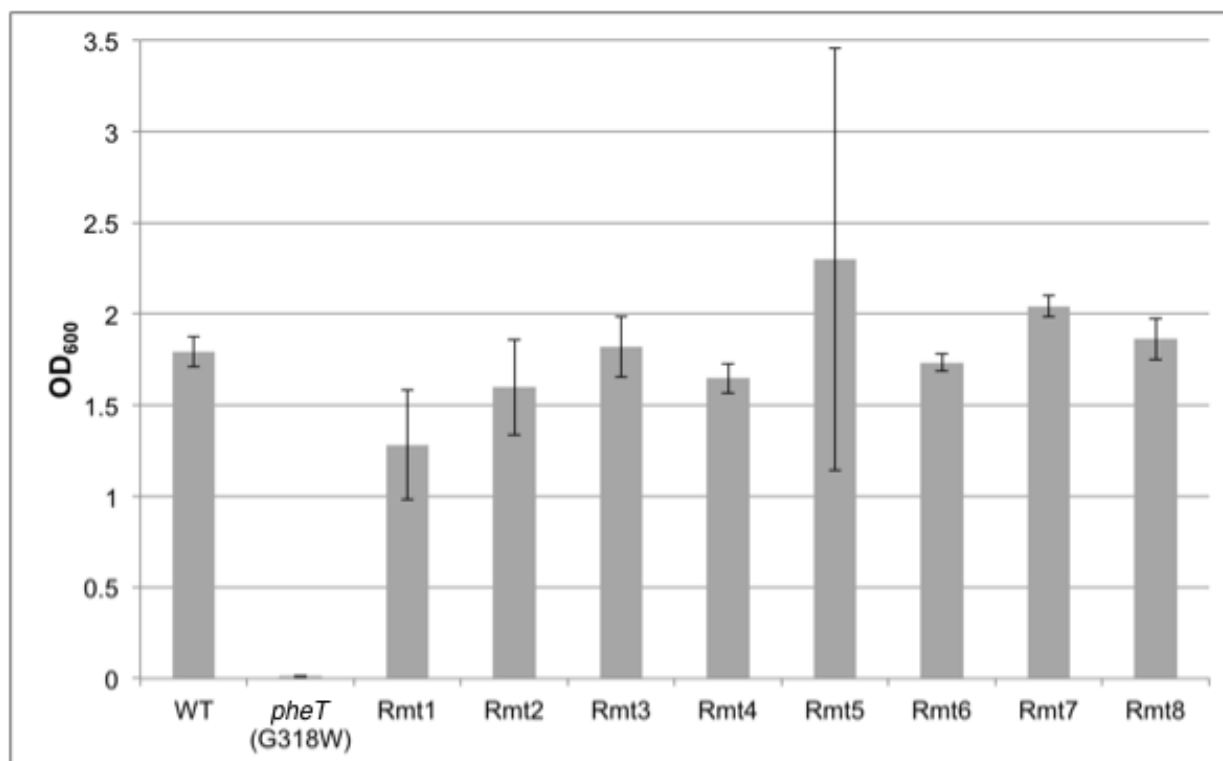
Figure 3-1. Growth of the 8 isolated m-Tyr^R strains compared to wild type and $pheT(G318W)$ strains. Strains Rmt1 and Rmt2 were isolated from the same mutagenesis assay. All others were isolated from independent mutagenesis assays. Bars are the average of three biological repeats. Error bars are standard deviation.

Table 3-2. m-Tyr[R] strains and their mutations in the three major sources of m-Tyr[R].

Mutant Strain	Outgrowth[a]	Total # of Mutations[b]	Mutations[c]		
			aroP	*rhtC*	*tyrA*
Rmt1	M9	17	W436C		
Rmt2	M9	46	Q42(Am)		
Rmt3	M9	3	S298F		
Rmt4	LB	14		C(-43)T	
Rmt5	LB	9		C(-43)T	
Rmt6	LB	43	W100(Op)		
Rmt7	LB	19		C(-43)T	
Rmt8	LB	5			G106S

[a] Growth Media used after cells were mutagenized, but before selection in media containing m-Tyr
[b] Non-silent and intergenic SNPs were identified by whole genome sequencing. The sequences were then aligned to the *E. coli* MG1655 reference genome (NC_000913) using Burrow-Wheeler Aligner and SAMtools[30,31]. SNPs were identified with a minimum requirement of 5x coverage of a given base and 80% agreement on the mutation.
[c] Mutations identified as being the major contributors to the strains' resistance to m-Tyr. This was determined by allelic replacement and subsequent m-Tyr[R] assays.

Loss of Function Mutations in *aroP* Impart Resistance to *m*-Tyr

The aromatic amino acid transporter gene *aroP* was mutated in 4/8 of the m-Tyr[R] strains.
These mutations all appeared to be loss of function mutations, two of which are nonsense
mutations truncating the protein to just 42 and 100 residues long respectively (Table 3-2.).
Because of this, we hypothesized that these *aroP* mutations are loss of function mutations that
impart resistance to m-Tyr to the m-Tyr[R] strains. To test this, we created an *aroP* knock out in a
clean *pheT(G318W)* strain background and tested the strain's resistance to m-Tyr. This *aroP*
knock out showed elevated m-Tyr resistance, however its level of resistance did not equal those
displayed by the Rmt mutant strains containing *aroP* mutations (Fig. 3-2). To assess the
contribution of each *aroP* mutation to the resistance of its m-Tyr[R] strain, we replaced the mutated
aroP alleles with the WT version in the m-Tyr[R] strain backgrounds and tested the resistance of
the resulting strains. These WT replacements severely reduced m-Tyr resistance in 3/4 of the
strains (Rmt1, Rmt3, and Rmt6), and made another (Rmt2) extremely variable, sometimes
appearing to be unaffected by the replacement and other times appearing to have completely lost
its resistance (Fig. 3-2).

A non-functional *aroP* as a source of resistance makes intuitive sense, since *m*-Tyr, as an aromatic amino acid, could be one of AroP's substrates. The variability in Rmt2 is most likely due to secondary resistance mutation(s) that provide extremely stochastic resistance without the mutated *aroP* allele. Rmt1 completely lost its resistance to *m*-Tyr when it was given a WT *aroP*, and yet its resistance levels with the mutant *aroP* appeared to be higher than a straight *aroP* knock out. This could be due to one of the 16 other mutations in this strain background that provide a growth benefit when *m*-Tyr is excluded from entering the cell, or it could be because the *aroP(W436C)* mutation allows for better discrimination against *m*-Tyr import, while still maintaining some aromatic amino acid transport function for canonical amino acids.

rhtC Promoter Mutation Imparts Resistance to *m*-Tyr

RhtC has been reported to be a threonine efflux pump[38]. In our *m*-Tyr^R screen, the same mutation 43 bp upstream of the gene *rhtC* (C-43T) was isolated three times independently in Rmt4, Rmt5, and Rmt7. The mutated base is located 1 bp downstream of the -35 promoter sequence and 10 bp upstream of the -10 promoter sequence. The facts that this mutation occurred in the promoter region of a known amino acid efflux pump and that it was isolated three separate times was a strong indication that this mutation might be responsible for the *m*-Tyr^R phenotype in these three strains. We tested whether this mutation was responsible by homologously recombining the upstream mutation and the *rhtC* gene out (Δ-59-621) and
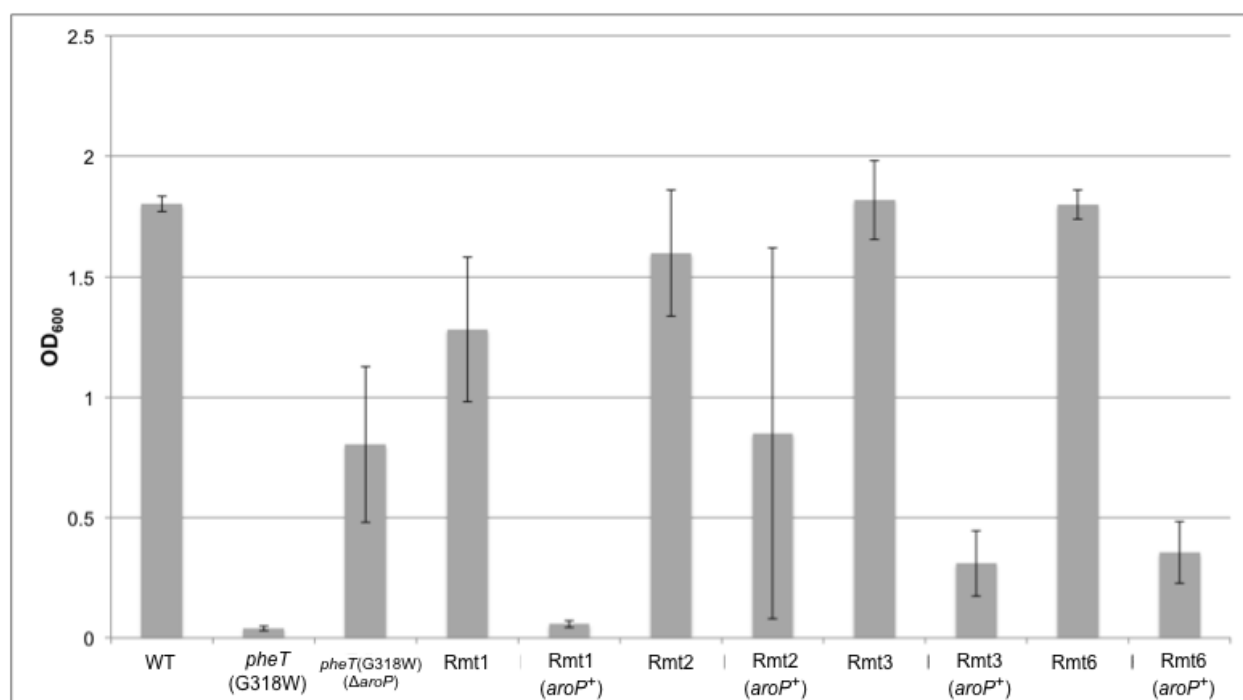
Figure 3-2. The impact of *aroP* mutations on resistance to *m*-Tyr. An *aroP* deletion in a clean *pheT(G318W)* background imparted *m*-Tyr^R. This *m*-Tyr^R did not equal any of the resistance levels seen in the mutagenized strains. However, strains Rmt1, Rmt3, and Rmt6 had the majority of their *m*-Tyr resistance eliminated when their *aroP* alleles were replaced with the WT version. Strain Rmt2's resistance was negatively impacted and was made highly variable by the WT *aroP* replacement. Bars are the average of three biological repeats. Error bars are standard deviation.

replacing it with the *cat-sacB* cassette on the chromosomes of the *m*-Tyr^R strains. In all three strain backgrounds, removing *rhtC* and the upstream mutation eliminated their resistance to *m*-Tyr. We also inserted the mutant sequence into a clean *pheT(G318W)* background, which provided the strain with *m*-Tyr resistance levels similar to the mutants (Fig. 3-3). To show that the *rhtC* open reading frame was necessary for the upstream mutation to confer resistance to *m*-Tyr, we replaced the *rhtC* gene with the *cat-sacB* cassette, leaving the upstream mutation in place. This also eliminated resistance from all three strain backgrounds (Fig. 3-3).

These results strongly suggest that the *rhtC(C-43T)* mutation increases expression of the *rhtC* gene. This mutation is 1 bp downstream of the putative -35 σ^{28} promoter sequence, which has a run of 3 T's at the end of the consensus sequence, but is "TGC" in *rhtC*'s promoter (Fig. 3-4) [39,40]. It's therefore possible that this C to T change could increase expression of *rhtC* by

45
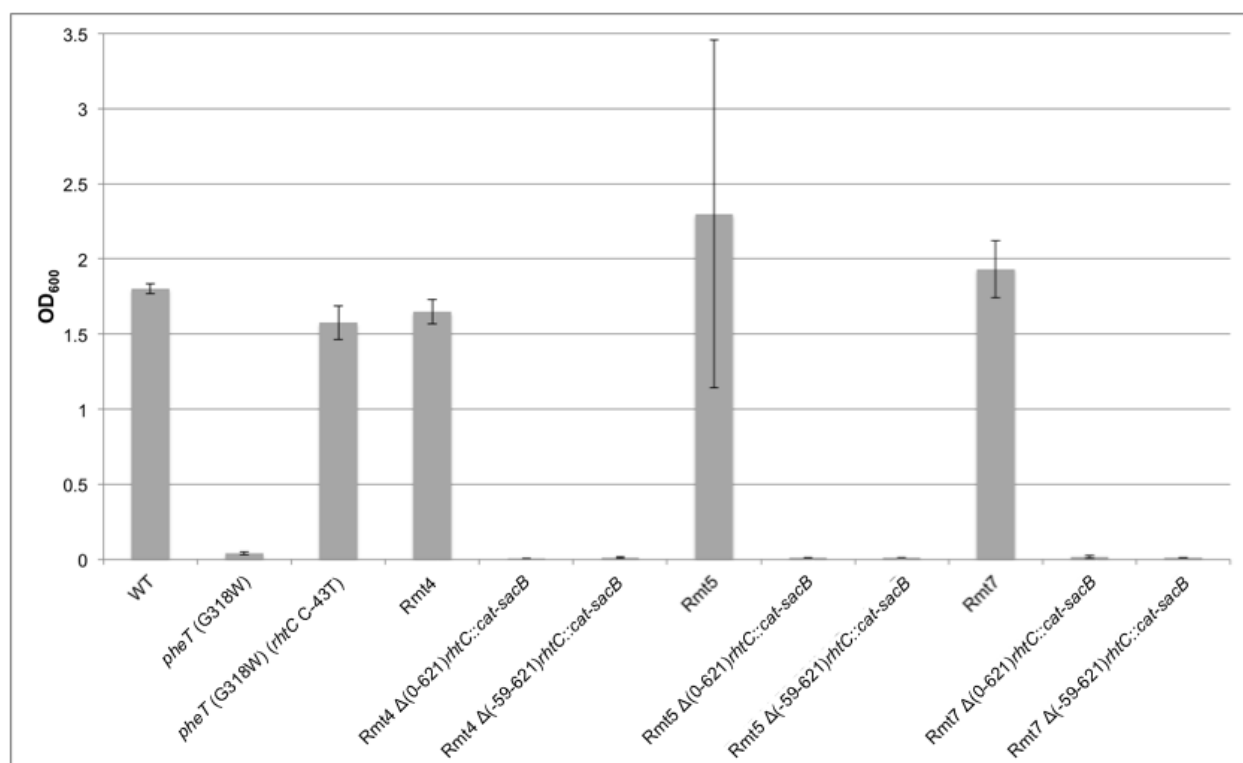
Figure 3-3. The impact of the *rhtC(C-43T)* resistance to *m*-Tyr. Introducing the *rhtC(C-43T)* mutation into a clean *pheT(G318W)* strain background imparted resistance to *m*-Tyr similar to those seen in Rmt4, Rmt5, and Rmt7. Replacing just the *rhtC* gene or the *rhtC* gene and the *rhtC(C-43T)* mutation with the *cat-sacB* cassette both eliminated the resistance to *m*-Tyr of the mutagenized strains. Bars are the average of three biological repeats. Error bars are standard deviation.

compensating for a lack of T's at the end of the -35 sequence. Because RhtC has been shown to

be a threonine efflux pump, it would seem likely that this mutation increases expression of *rhtC*

and that RhtC has a broader range of amino acid substrates than previously thought, allowing it

to pump *m*-Tyr[38].

Figure 3-4. The consensus σ^{28} promoter sequence as compared to the promoter sequence of WT *rhtC* and *rhtC(C-43T)*[39]. The underlined base pairs show the loci of the *m*-Tyr resistance mutation. It is possible that the C-43T mutation compensates for *rhtC*'s -35 promoter sequence's divergence from the consensus sequence, thereby increasing expression of *rhtC*.

46

Mutation in *tyrA* Imparts Resistance to *m*-Tyr

One *m*-Tyr[R] strain (Rmt8) only had 5 mutations, which allowed us to quickly identify a

mutation in *tyrA* (G106S) as the source of its resistance to *m*-Tyr. When the mutant version of

tyrA is replaced with the WT version in Rmt8, the strain became sensitive to *m*-Tyr (Fig. 3-5).

When the *tyrA(G106S)* mutation was introduced into a clean *pheT(G318W)* background, the

strain was resistant at the same level as Rmt8 (Fig. 3-5). TyrA is a bifunctional protein that acts

as a chorismate mutase and as a prephenate dehydrogenase, which is part of the Tyr and Phe

biosynthetic pathways[41,42]. The *tyrA(G106S)* mutation cannot be a complete loss of function,

because TyrA function is required for growth in minimal media and this mutation does not

prevent that [43]. The mutation is located in a region of the protein that is annotated as having the

prephenate dehydrogenase activity[44]. This mutation may lower the efficiency of TyrA's

prephenate dehydrogenase activity, increasing prephenate levels in the cell. As prephenate feeds

into the Phe biosynthetic pathway, the intracellular phenylalanine concentration may be

increased (Fig. 3-6), which could compete with *m*-Tyr to be charged onto tRNA[Phe], thereby

limiting its negative impact.

The three mutated genes that provided resistance to *m*-Tyr discussed above (*aroP*, *rhtC*,

and *tyrA*) explain the resistance of 5 of the 8 *m*-Tyr[R] strains, in that their *m*-Tyr resistance was

completely eliminated by replacing their mutant alleles with the WT versions. Rmt3 and Rmt6

had their resistance drastically reduced by giving them a WT allele of *aroP*, although a small

amount of resistance persisted. A WT *aroP* allele also made Rmt2's resistance very erratic,

although we cannot say it was eliminated completely. The strategies for resisting *m*-Tyr that

these mutated genes represent are to keep *m*-Tyr out of the cell (*aroP*), to get *m*-Tyr out of the

cell once it is inside (*rhtC*), and to increase intracellular Phe pools (*tyrA*).
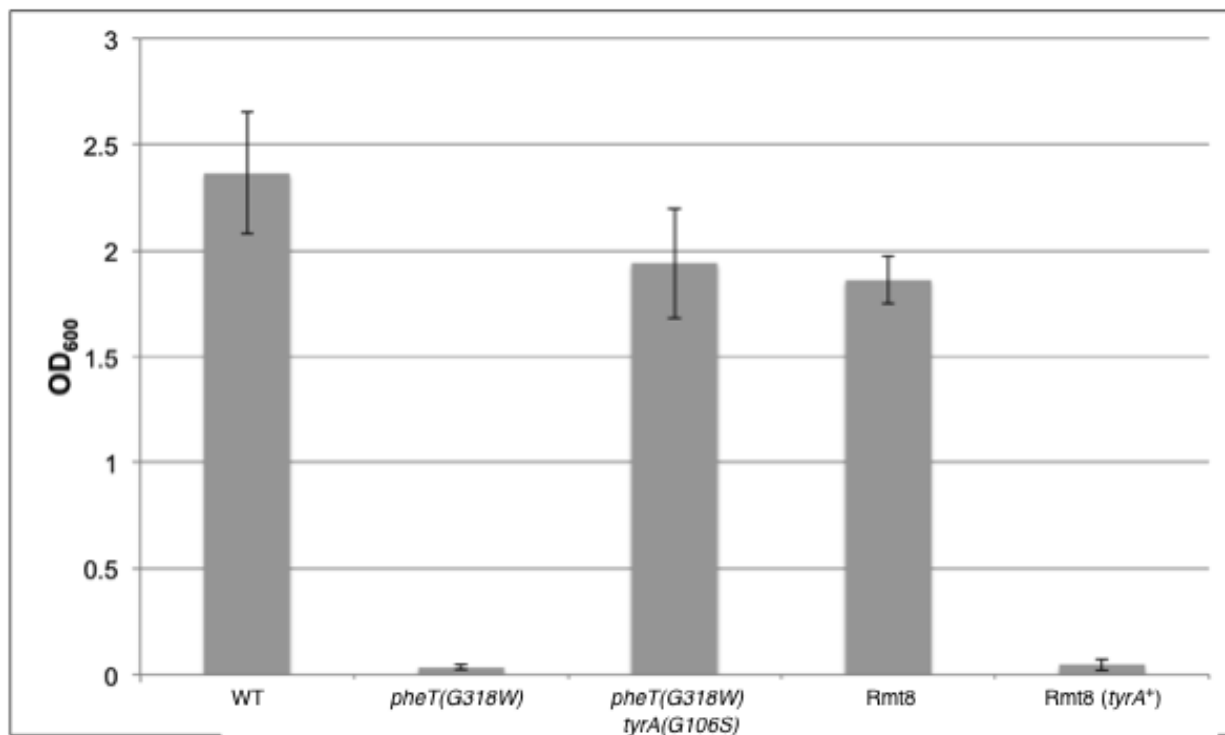
Figure 3-5. The impact of the *tyrA* mutation on resistance to *m*-Tyr. Introducing the *tyrA(G106S)* mutation into a clean *pheT(G318W)* strain background imparted *m*-Tyr resistance levels equivalent to strain Rmt8. Conversely, replacing the *tyrA(G106S)* mutation in Rmt8 with the WT allele completely eliminated its resistance to *m*-Tyr. Bars are the average of three biological repeats. Error bars are standard deviation.
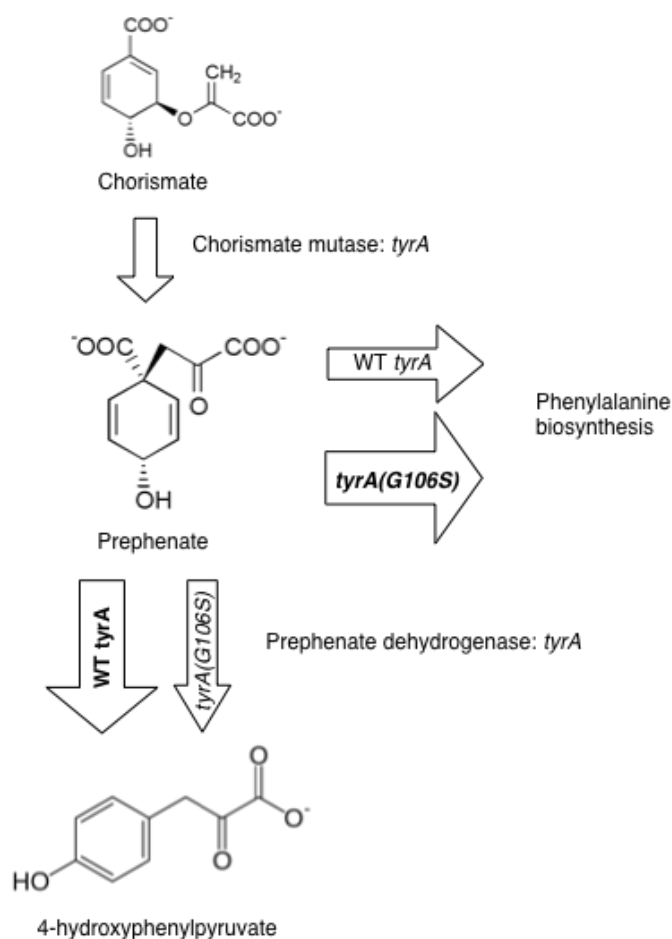
Figure 3-6. Model of *tyrA(G106S)* induced m-Tyr resistance. The less efficient prephenate dehydrogenase activity of *tyrA(G106S)* causes more prephenate to be diverted to the phenylalanine biosynthesis pathway, thereby increasing the concentration of phenylalanine inside the cell.

PheRS Editing-Defective *E. coli* Grown with *m*-Tyr are More Sensitive to Heat than WT

If *m*-Tyr is toxic to *pheT(G318W) E. coli* cells because it replaces Phe in proteins, thereby making the resulting proteins less thermally stable, then we would expect these cells to be more sensitive to heat. To test this, we grew *pheT(G318W)* and WT cells in M9 minimal media with a sub-lethal concentration of *m*-Tyr overnight. We washed the cells in 0.9% NaCl and standardized their OD_{600} to 1.0. We then incubated the cells in a thermocycler at 60°C, taking samples out periodically to plate, so that the remaining viable cell counts could be assessed. As was expected, the *pheT(G318W)* cells died much more rapidly than WT when
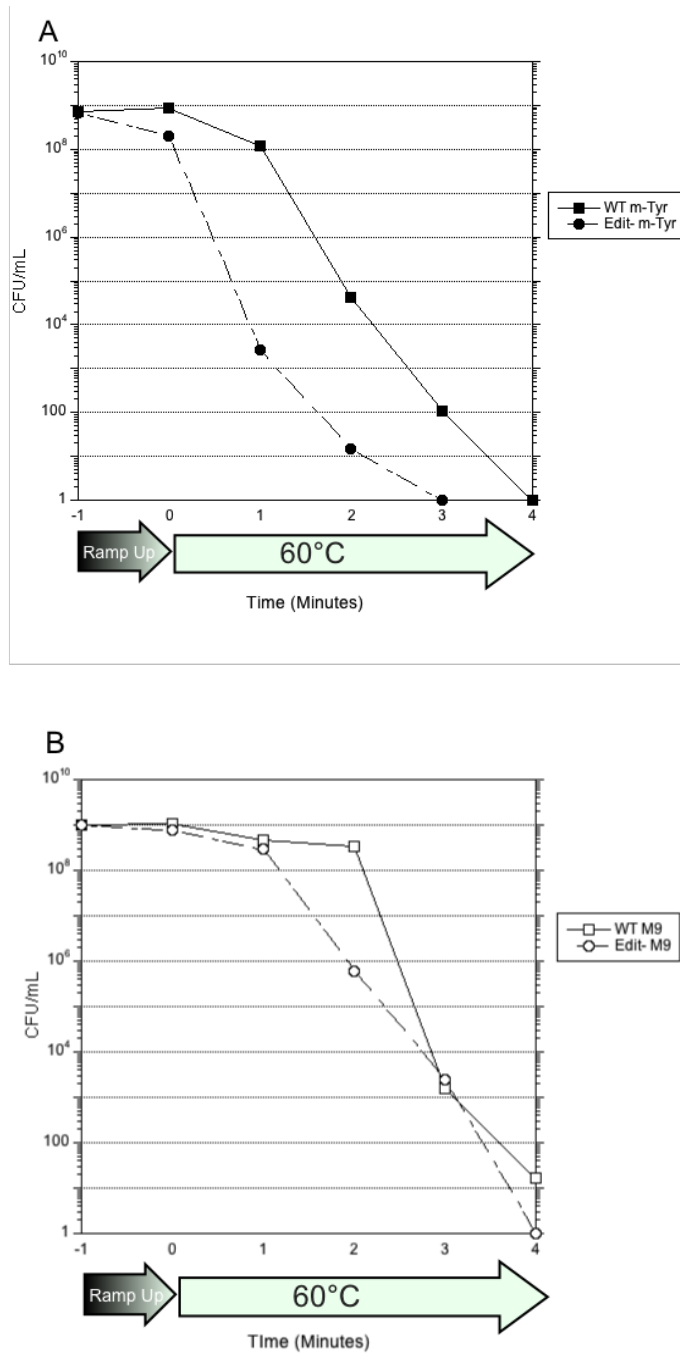
Figure 3-7. Heat sensitivity of *pheT(G318W)* editing-defective *E. coli*. When grown in the presence of a sub-lethal *m*-Tyr concentration (A), the PheRS editing defective strain dies more quickly than WT when exposed to a heat stress. The difference in death rate disappears when the strains are grown in plain M9 minimal media (B).

exposed to a heat stress after being grown in the presence of *m*-Tyr (Fig. 3-7A). A control

experiment in which both strains were grown in media lacking *m*-Tyr before undergoing the heat

stress eliminated the difference (Fig. 3-7B). This is consistent with the hypothesis that *m*-Tyr is toxic because of its effect on the stability of the proteins it is integrated into.

PheRS Editing-Defective *E. coli* Grown with *m*-Tyr Develop Inclusion Body-like Protein Aggregates

If replacing Phe with *m*-Tyr in proteins compromises the stability of those proteins, then it is possible that signs of proteome disruption could be visible via microscopy. WT and *pheT(G318W)* strains were grown in M9 minimal media and dosed with different *m*-Tyr concentrations or no *m*-Tyr. Time points from each culture were taken right before the addition of *m*-Tyr (t=0), and 30, 60, 120, and 300 minutes afterwards. Microscopy specimens were examined with a DIC microscope.

As can be seen in Fig. 3-8, the *pheT(G318W)* cells exposed to *m*-Tyr developed dark spots that localized to the poles of the cells, while the WT strain showed very few polar dark spots. Additionally, the *pheT(G318W)* cells became elongated during later time points of the experiment. To quantify these observed changes, 50 cells from each time point were measured and the number of visible spots was recorded. This quantification revealed that *pheT(G318W)* cells developed many more spots than WT and became elongated (Fig. 3-9). The appearance of the spots was shown to be dose dependent. For a 5 fold increase in *m*-Tyr concentration from 0.1 mM to 0.5 mM, *pheT(G318W)* had 28% more spots at 60 minutes, 62% more spots at 120 minutes, and 52% more spots at 300 minutes. The cell elongation over time of the *pheT(G318W)* strain indicates that the cells are still metabolically active and growing, but either cannot divide or cell division has been arrested due to internal regulatory signals. The quantification also revealed a baseline level of spots around 0.2 spots per cell in the WT strain with and without *m*-Tyr and in the *pheT(G318W)* strain without *m*-Tyr.
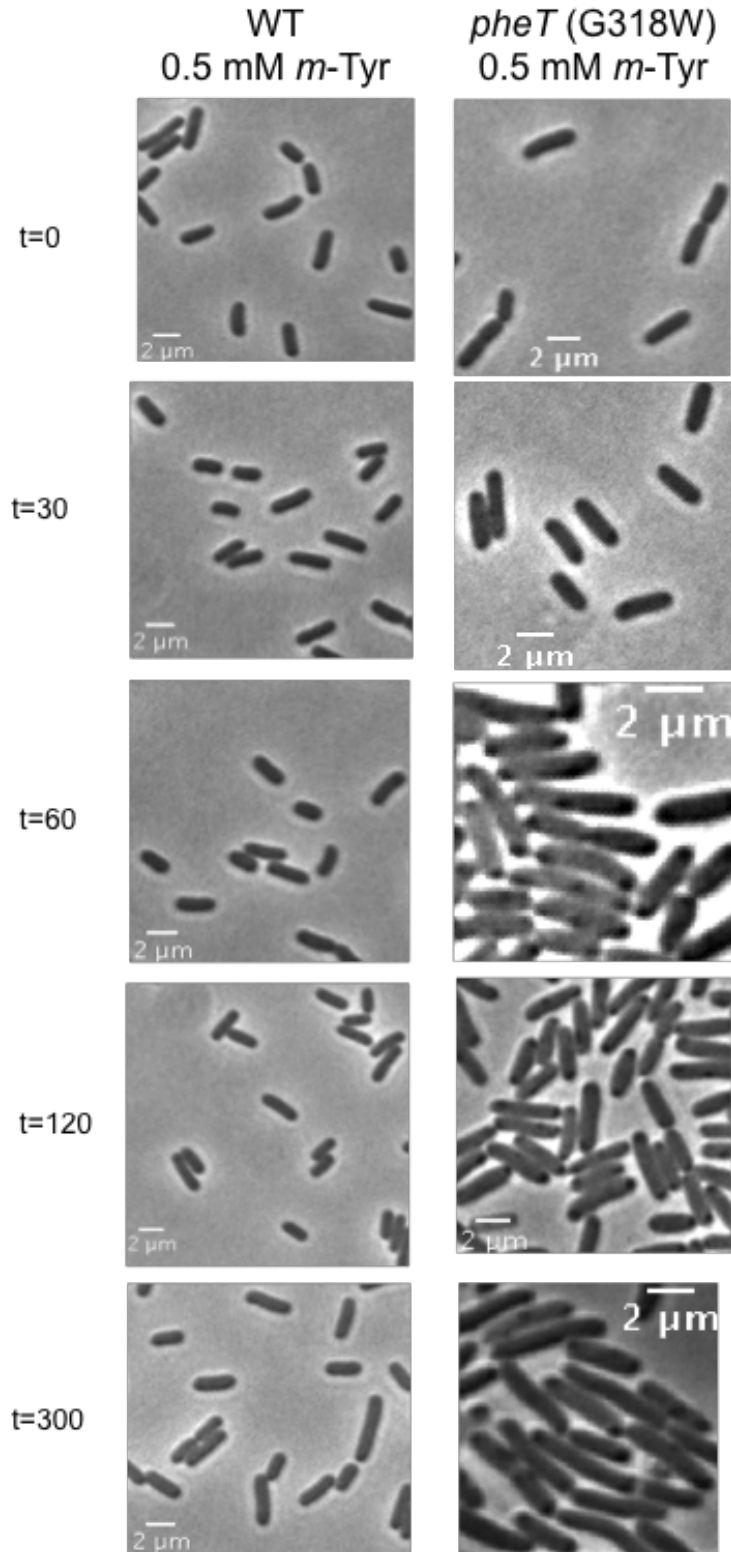
Figure 3-8. DIC Microscopy of *m*-Tyr treated *E. coli*. *pheT(G318W)* and WT *E. coli* were grown in M9 minimal media to an OD_{600} of 0.5 (t=0) and then dosed with *m*-Tyr to a concentration of 0.5 mM. The *pheT(G318W)* cells begin to develop dark polar spots after a half hour and the spots grow in number and intensity over time. The WT cells show no signs of being negatively affected by the *m*-Tyr.
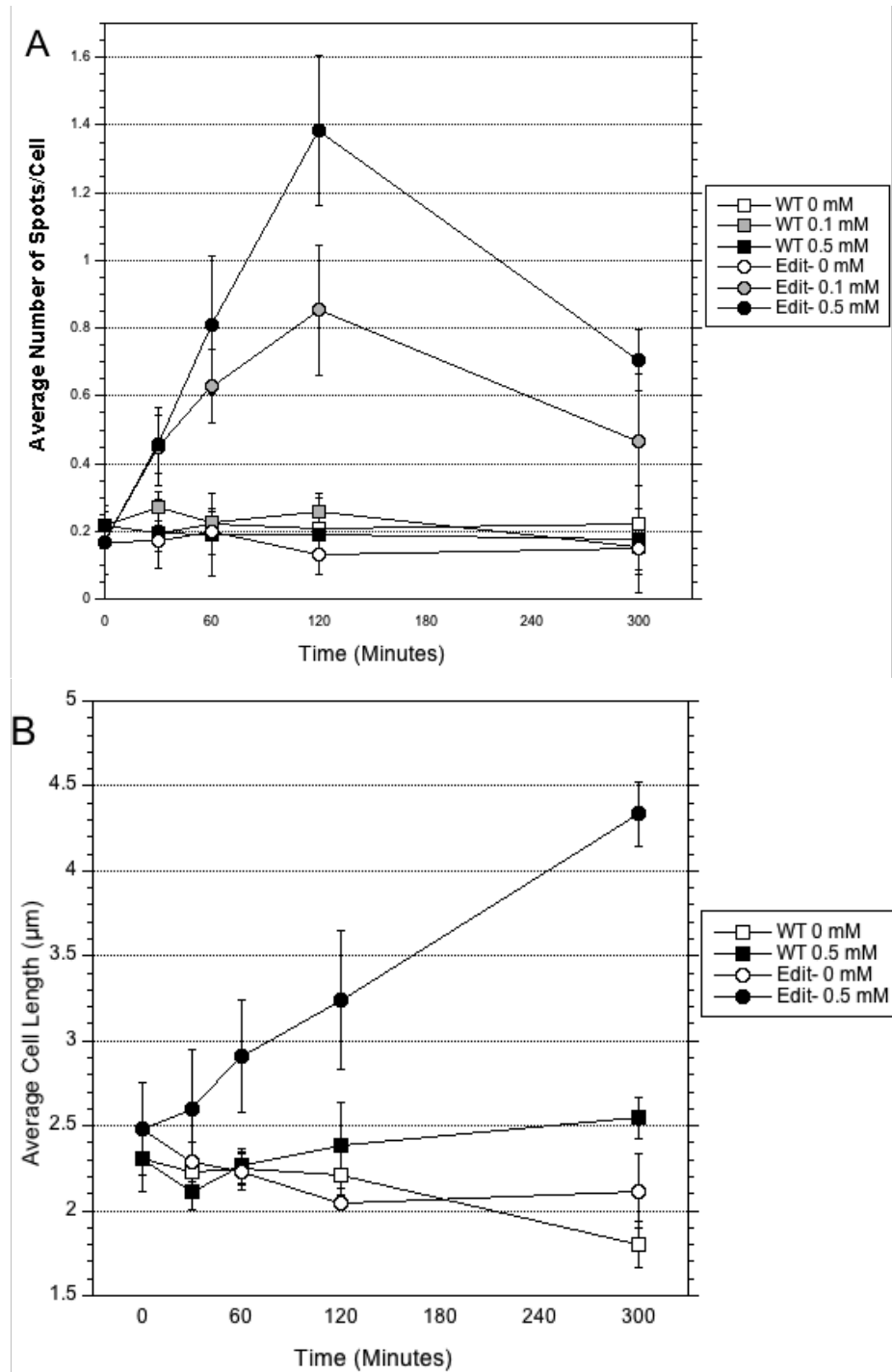
Figure 3-9. Quantification of DIC microscopy. The *m*-Tyr added to the *pheT(G318W)* cultures increased the number of visible polar spots in a dose dependent matter (A). *m*-Tyr also caused the *pheT(G318W)* cells to become elongated, while the WT remained unaffected (B). Data points are averages of three biological replicates and the error bars are standard deviation.

We hypothesized that these dark polar spots are protein aggregates formed by the cell to deal with a large number of unfolded proteins that were destabilized by the incorporation of *m*-Tyr. To test this hypothesis, we performed Transmission Electron Microscopy (TEM) on sectioned samples of *pheT(G318W)* cells grown in M9 and exposed to 0.5 mM *m*-Tyr for 120 minutes (Fig. 3-10). Thirteen cells were analyzed by TEM, and the images revealed the same polar localization of the spots that we observed with the DIC microscopy. The spots have an electron density and disorganized shape consistent with large protein aggregates[45,46]. The spots came in a variety of sizes; some having what appears to be satellite protein aggregates that could be in the process of being added to the larger aggregate (Fig. 3-10B). These results are consistent with the hypothesis that *pheT(G318W)* cells experience a large-scale proteome destabilization when grown in the presence of *m*-Tyr.
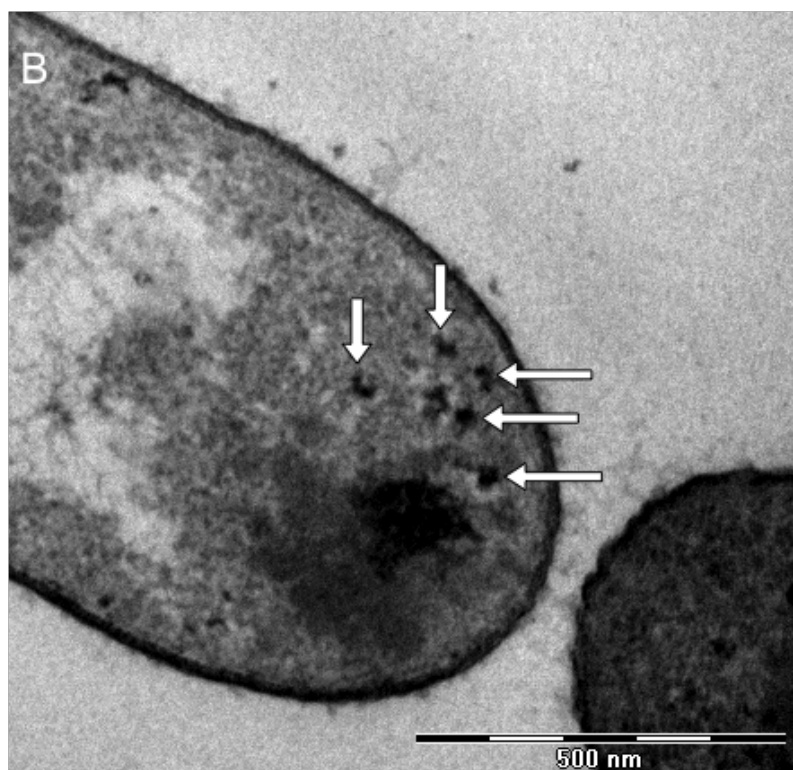
Figure 3-10. Transmission Electron Microscopy of *pheT(G318W) E. coli* treated with *m*-Tyr. Large protein aggregates localize to the poles (A). In some cases small satellite dark spots around the main protein aggregate were observed (arrows) (B). These appear to be smaller aggregates in the process of assembling into the larger one.

Transcriptomic Analysis of *pheT(G318W)* Cells Treated with *m*-Tyr Reveal the Activation of Various Stress Responses and Downregulation of Aromatic Amino Acid Synthesis

We used RNA-seq and transcriptomic analysis to try to understand what kind of stresses *pheT(G318W)* cells undergo when exposed to *m*-Tyr. Understanding the stress responses that are induced after *m*-Tyr exposure could reveal the mechanism of *m*-Tyr toxicity to PheRS editing-defective *E. coli*. Cultures of the *pheT(G318W)* strain were prepared similarly to the microscopy cultures. Minimal media cultures were dosed with *m*-Tyr to a final concentration of 0.5 mM. Samples for RNA extraction were taken at 0, 30, 60 and 120 minutes after *m*-Tyr treatment. When compared to t=0 minutes, the other times points had hundreds of differentially transcribed genes using the cut off of $p<0.005$. However, when compared to the previous time point, t=60

and t=120 only had 16 and 20 differentially expressed genes that made the cutoff, respectively.

See Appendix B for full dataset.

Aromatic Amino Acid Biosynthesis

The addition of *m*-Tyr to the *pheT(G318W)* culture induced a downregulation of many genes in the three aromatic amino acid biosynthesis pathways (Figure 3-11) (Table 3-3). This confirms and expands upon observations reported by Bullwinkle, et al. (2016) that showed mischarging of *m*-Tyr onto tRNA[Phe] interfered with the regulatory function of deacylated tRNA[Phe] in promoting Phe biosynthesis and in being a signal transducer for the stringent response[47]. It is possible that *m*-Tyr is also interfering with mechanisms of biosynthesis regulation of the other two aromatic amino acids, *p*-Tyr and Trp which also rely on the presence of deacylated tRNAs or free-floating amino acid[48,49].

Table 3-3. Transcriptional $\log_2$ fold change relative to t=0 of the aromatic amino acid biosynthesis superpathway. $p<0.005$ unless otherise noted.

Gene	Function	t=30	t=60	t=120
aroA	3-Phosphoshikimate-1-carboxyvinyltransferase is involved in the chorismate pathway[50]	-2.102	-2.190	-2.193
aroE	Shikimate dehydrogenase converts 3-dehydroshikimate to shikimate by catalyzing the NADPH linked reduction of 3-dehydro-shikimate[51]	-2.475	-2.331	-2.016
pheA	Bifunctional chorismate mutase/prephenate dehydratase[52]	-1.951	-2.568	-2.250
trpA	The TrpA protein is the α subunit of the tetrameric (α_2-β_2) tryptophan synthase complex[53]	-2.200	-3.068	-3.445
trpB	The TrpB protein is the β subunit of the tetrameric (α_2-β_2) tryptophan synthase complex[54]	-3.057	-3.652	-4.007
trpC	Bifunctional phosphoribosylanthranilate isomerase and indole-3-glycerol phosphate synthase performs the third and fourth steps in tryptophan biosynthesis[55]	-2.505	-3.424	-3.975
trpD	Anthranilate phosphoribosyl transferase performs the second step in tryptophan biosynthesis that generates N-(5'-phosphoribosyl)-anthranilate[56]	-2.225	-3.050	-3.652
trpE	Anthranilate synthase, forms complex with TrpD to	-2.617	-3.711	-3.070

	perform reaction[56]			
tyrA	Bifunctional chorismate mutase/prephenate dehydrogenase[57]	-3.492	-3.746	-2.268
tyrB	Aromatic-amino acid aminotransferase, broad-specificity enzyme that performs the final step in tyrosine, leucine, and phenylalanine biosynthesis[58]	-1.766	-2.159	-1.966

Unfolded Protein Response

Following the addition of *m*-Tyr, the *pheT(G318W)* cells underwent a very robust

unfolded protein response (Table 3-4). Dozens of protein chaperones and proteases had very

elevated levels of transcription. *rpoH*, the gene that encodes the heat shock response sigma

factor (σ^{32}) and is responsible for globally regulating the unfolded protein response, experienced

more than 400 fold increase in transcription in the first 30 minutes after *m*-Tyr treatment. That

initial spike came back down by the 60 minute time-point, but still maintained an elevated level

as compared to t=0. Many groups of chaperones and proteases that are known to work in concert

were upregulated to a similar degree such as *dnaK*, *dnaJ*, and *grpE*. This lends support to the

notion that these gene expression results are functionally significant.

These results corroborate what we observed via DIC microscopy and TEM. Over the

same time period that RNA samples were taken, we observed increasingly visible protein

aggregates, indicating that the unfolded protein stress did not subside and possibly increased.

This is reflected in the transcription levels of various proteases and chaperones observed over the

time course. Most maintained a similarly elevated level or increased steadily over every time-

point. Most of the few genes that did reduce their transcription levels over the time course, still

maintained an elevated level of expression relative to t=0. Some of the heat shock genes are

3-dehydroquinate

aroD

3-dehydroshikimate

ydiB   aroE ■ ydiB

shikimate

aroL aroK

shikimate 3-phosphate

aroA ■

5-enolpyruvoyl-shikimate 3-phosphate

aroC

chorismate

trpE ■ trpD ■   tyrA ■ pheA

anthranilate   prephenate

trpD ■   pheA   tyrA ■

N-(5-phosphoribosyl)-anthranilate   2-oxo-3-phenylpropanoate   4-hydroxyphenylpyruvate

trpC ■   ilvE aspC tyrB   aspC tyrB

1-(o-carboxyphenylamino)-1'-deoxyribulose 5'-phosphate

trpC ■   L-phenylalanine   L-tyrosine

(1S,2R)-1-C-(indol-3-yl)glycerol 3-phosphate

trpA ■

L-serine   indole

trpB ■

L-tryptophan

Figure 3-11. Biosynthetic map of the aromatic amino acid biosynthesis superpathway with overlaid transcriptomic data comparing t=30 with t=0. Blue squares indicate lowered transcription for each gene. Many different steps of the three biosynthetic pathways are slowed down after the addition of *m*-Tyr to the *pheT(G318W)* culture.

specifically known to localize to inclusion bodies (*ibpB*, *lon*), or protein aggregates (*degP*, *clpB*,

clpS), or inclusion bodies at the poles of the cell (*ibpA*)[59-66].

Table 3-4. Transcriptional log$_2$ fold change relative to t=0 of unfolded protein response genes. *p*<0.005 unless otherwise noted.

Gene	Function	t=30	t=60	t=120
uspG	Universal stress protein	8.767	2.097	2.028
rpoH[e]	σ^{32} Heat shock response sigma factor	8.118	2.594	2.645
cpxP[e]	Periplasmic regulator of the CpxAR two component regulatory system. Acts as an adaptor for the DegP-mediated proteolysis. Important for resistance to high pH[67-69].	4.791	4.656	4.730
cpxR[e]	Response regulator of the CpxAR two component regulatory system, which senses protein misfolding and activates expression of proteases and chaperones.[70]	2.067	0.434[d]	0.262[d]
degP[e]	Periplasmic serine protease required for survival at high temperatures. Degrades oxidatively damaged and aggregated proteins in periplasm. [71-73]	4.235	4.408	3.904
hslV	Part of the HslVU protease that is expressed during heat shock and helps clear defective proteins. [74-76]	4.761	4.689	4.425
hslU	Part of the HslVU protease that is expressed during heat shock and helps clear defective proteins. [74-76]	2.758	2.796	2.543
dnaK	Hsp70 chaperone protein assisted by DnaJ and GrpE	4.439	5.138	4.905
grpE	Nucleotide exchange factor for DnaK, facilitating use of ATP for chaperone functions[77]	4.387	3.637	3.549
dnaJ	Co-chaperone protein with DnaK	4.048	4.005	3.516
hflC	Inner membrane protein regulating FtsH protease[78]	4.343	1.567	1.445
ftsH	Membrane-bound metalloprotease that degrades misfolded membrane and some cytoplasmic proteins.[79]	2.357	2.080	1.833
hslO	Hsp33 chaperone, expressed during heat shock and oxidative stress.[80]	4.087	3.501	3.446
ibpA	Heat shock chaperone protein that localizes to inclusion bodies and binds to aggregated proteins at the cell poles. [59-61]	3.953	8.082	7.269
ibpB	Small heat shock protein, binds to protein aggregates, denatured proteins, and inclusion bodies. [60,61,64]	8.767	8.712	8.121
hslR	Hsp15, expressed during heat shock. Interacts with the 50S ribosomal subunit when it contains a nascent polypeptide and helps recycle them. [81-83]	3.921	4.571	4.876
groS	Co-chaperonin with GroEL, thought to be part of stressed induced mutagenesis system[84]	4.235	4.553	4.036
groL	GroEL chaperonin with GroES induced by heat	4.048	4.519	4.202

	shock.[85]			
htpG	Hsp90 family of proteins, induced during heat shock.[86,87]	3.239	3.399	3.303
spy[e]	Periplasmic protein chaperone	3.069	4.239	4.553
hspQ	Heat shock protein, binds hemimethylated DNA[88]	2.654	3.850	4.021
clpB	Heat shock induced chaperone protein that is able to resolubilize aggregated proteins.[65]	2.453	4.658	4.540
lon	Protease that degrades misfolded proteins and regulatory proteins. Also participates in the degradation of inclusion bodies. [62,63]	1.987	2.465	2.200
htpX[e]	Heat shock integral membrane protein, putative metalloproteinase.[89]	1.775	4.361	4.522
clpP	Serine protease, part of the ClpAP, ClpAPX, and ClpXP protease complexes. [90-92]	0.899	1.579	1.636
clpX	Chaperone that serves as a substrate specificity adaptor for ClpP.[93]	0.657	1.197	1.476
clpS	Substrate specificity adaptor for ClpAP, targeting the ClpAP complex to aggregated proteins.[66]	0.084[d]	0.527[c]	0.891
clpA	Chaperone that serves as a substrate adaptor for ClpAP and ClpAXP protease complexes.[94]	0.007[d]	0.361[d]	0.653[a]

[a] $p < 0.01$
[b] $p < 0.05$
[c] $p < 0.10$
[d] $p > 0.10$
[e] Regulated by the CpxAR two component regulatory system

Oxidative Stress and DNA Damage Response

A small number of ROS stress response genes and DNA damage repair genes showed elevated expression in response to the *m*-Tyr treatment (Table 3-5). SoxS is a transcriptional activator that helps remove superoxide. Its transcription is regulated by SoxR, which only activates the transcription of *soxS* when it detects superoxide[95]. *SoxS* peaked its transcription at 30 minutes and slowly lowered over the time course. Conversely, the expression of *mfd* (unknown regulators) and *mutM* (σ^{32}-regulated), both genes responsible for dealing with DNA lesions induced by ROS, increased steadily over the time course. Despite these possibly conflicting pieces of evidence about when the presence of ROS stress peaked in the cells, it seems likely that ROS caused problems for the cells after *m*-Tyr treatment. One possible reason

for this could be misfolding of electron transport chain proteins, causing the frequency of

monovalent reductions of O_2 to increase.

Table 3-5. Transcriptional $\log_2$ fold change relative to t=0 of oxidative stress and DNA damage response genes. $p<0.005$ unless otherwise noted.

Gene	Function	t=30	t=60	t=120
soxS	Transcriptional activator, and helps remove superoxide.[95] Transcribed when SoxR detects superoxide.	4.470	3.312	2.108
sodB	Superoxide dismutase (Fe)	-0.037[d]	0.174[d]	2.563
mfd	"Mutation Frequency Decline" protein, is responsible for removal of stalled RNA polymerase from DNA lesions[96]	1.201	1.547	1.703
mutM	DNA glycosylase that is part of the base excision repair pathway. Helps repair free radical-induced DNA lesions. [97,98]	2.360	3.493	4.112
recA	SOS response regulator. Catalyzes strand exchange for homologous recombination repair.[99]	1.055[c]	1.241[b]	0.701[d]
recD	Component of RecBCD exonuclease V complex that is essential for recombination repair.[100]	1.441	1.252	1.085

[a] $p<0.01$
[b] $p<0.05$
[c] $p<0.10$
[d] $p>0.10$

Membrane Damage and Ion Stress Response

Transcription patterns seem to indicate that the cells experienced membrane damage and

possibly as a result cannot maintain ion homeostasis (Table 3-6). Expression of the gene for the

σ^{24} membrane and periplasmic protein stress response sigma factor was elevated throughout the

time course. Phage Shock Protein A (PspA) has been shown to stabilize membranes and stop

proton leakage, and *pspA* transcription was very elevated during every time point after *m*-Tyr

treatment. The CpxAR two component regulatory system senses both membrane damage and

periplasmic misfolded proteins, so its higher transcription rate is not conclusive that membrane

damage was occurring, but in the context of the other results, it seems likely. Various genes

regulated by the Cpx response regulator CpxR showed altered expression including *ompF*, *htpX*,

rpoH, *spy*, and *degP* (Table 3-4 and 3-6). Proton antiporters that pump out sodium, potassium,

and lithium all were upregulated indicating elevated internal ion concentrations, since regulation

of these antiporters is dependent on either osmolarity or the presence of its ion substrate inside

the cell[101,102]. Also, porins, ion channels, and potassium import proteins were all downregulated.

Table 3-6. Transcriptional $\log_2$ fold change relative to t=0 of membrane damage and ion stress response genes. $p<0.005$ unless otherwise noted.

Gene	Function	t=30	t=60	t=120
rpoE	σ^{24} membrane and periplasmic protein stress response sigma factor	0.973[b]	1.000[b]	0.715[a]
pspA	"Phage Shock Protein A," regulates *psp* operon and stabilizes membranes.[103,104]	3.832	3.592	2.762
cpxP[c]	Periplasmic regulator of the CpxAR two component regulatory system. Acts as an adaptor for the DegP-mediated proteolysis. Important for resistance to high pH.[67-69]	4.791	4.656	4.730
cpxR[c]	Cytoplasmic response regulator of the CpxAR two component regulatory system. The system activates gene transcription in response to envelope damage.[70]	2.067	0.434[a]	0.262[a]
chaA	Sodium/potassium ion: proton antiporter[105,106]	5.624	5.310	4.122
nhaA	Sodium/lithium ion: proton antiporter[107,108]	3.668	3.672	3.068
nhaR	Sodium ion antiporter regulator, responds to alkaline pH and sodium concentration.[101]	2.058	2.452	2.059
kch	Potassium ion channel[109]	-2.756	-2.628	-3.237
trkA	NAD-binding component of Trk potassium ion transporters, required for transport.[110,111]	-2.065	-2.104	-1.984
ompF[c]	Outer membrane porin[112]	-1.896	-1.619	-1.230
kup	Potassium ion transporter[113]	-1.703	-1.657	-1.517

[a] $p>0.10$
[b] $p<0.10$
[c] cpxAR regulated gene

Discussion

The Intracellular Ratio of Phe to *m*-Tyr is the Key to *m*-Tyr Toxicity and Resistance

Mechanisms in *pheT(G318W) E. coli*

The results we presented here showed that a common thread among all of the *m*-Tyr

resistance mechanisms we identified was the alteration of the Phe:*m*-Tyr ratio to make Phe

concentrations as high as possible in comparison to *m*-Tyr concentrations . Two of the mutated

genes we identified that confer m-Tyr^R (*rhtC* and *aroP*) appear to work by either pumping m-Tyr out of the cell or preventing it from getting into the cell in the first place. The third m-Tyr^R gene we identified (*tyrA*) appears to work on the other side of the ratio by altering the aromatic amino acid precursor flow to increase the amount of Phe that is produced by the cell. Our transcriptomic results showed that m-Tyr could exacerbate its toxicity by causing the cell to downregulate Phe (and other aromatic amino acid) biosynthesis. This means that the presence of m-Tyr inside a PheRS editing-defective cell also decreases the Phe:m-Tyr ratio by causing the intracellular Phe concentration to decrease.

Results from previous research tend to corroborate this view of m-Tyr resistance and toxicity mechanisms. It was reported that exogenous supplementation with proteogenic amino acids, Phe being the most effective, could partially rescue root growth of plants grown in soil with m-Tyr[23]. Also, a m-Tyr^R *A. thaliana* mutant was reported to resist m-Tyr by increasing Phe production[114]. In *pheT(G318W) E. coli*, Bullwinkle, et al. (2016) showed that mischarging of tRNA^{Phe} with m-Tyr caused the inhibition of Phe biosynthesis and the inhibition of the stringent response, because uncharged tRNA^{Phe} is a regulatory signal for Phe starvation[47].

Thermal Sensitivity of *pheT(G318W) E. coli* Grown with *m*-Tyr

We showed that PheRS editing-defective *E. coli* had a higher sensitivity to heat than WT *E. coli* when grown with m-Tyr. We hypothesize that this is due to both the lower thermal stability of proteins containing m-Tyr, and the fact that the heat shock and unfolded protein responses were already induced and unable to handle additional unfolded proteins. Our transcriptomic results showed a strong induction of the unfolded protein response quickly after the addition of m-Tyr to the growth media. The large number of inclusion body-like protein

aggregates that we observed developing over time under the same growth conditions via DIC and electron microscopy showed that a significant fraction of the cells' proteome was locked away in these large polar protein aggregates. Strikingly, our observed polar aggregates bare a strong resemblance to protein aggregates reported by Rokney, et al. (2009) in *E. coli* after a heat shock[115]. They were able to track the formation of polar aggregates with a temperature-sensitive protein and GFP fusion. They reported the formation of these aggregates was energy dependent, and the localization to the poles required *dnaK* and *dnaJ*[115]. Our transcriptomic results showed high *dnaK* and *dnaJ* expression, which provides more support for the comparison between the two observed protein aggregates. Since the *m*-Tyr-containing protein that are not yet aggregated would not be able to be refolded by chaperones, its possible that these unstable proteins would prevent the chaperones from effectively dealing with proteins unfolded by the heat shock that might hypothetically be effectively refolded.

Previous Research Underestimated the Rate of *m*-Tyr Incorporation into Proteins by *pheT(G318W) E. coli*

Bullwinkle, et al. (2014) reported that the rate of *m*-Tyr incorporation into proteins was ~2.5% for *pheT(G318W) E. coli* and ~1.5% for WT *E. coli* when grown in minimal media with 0.5 mM *m*-Tyr[25]. However, the methods they used to purify the protein would have excluded insoluble proteins like the large aggregates we observed under the same growth conditions. Given that these aggregates probably contain protein with disproportionately more *m*-Tyr in them than the soluble protein, this could lead to a large underestimation of *m*-Tyr incorporation in the *pheT(G318W)* strain. WT *E. coli* did not have any visible protein aggregates under DIC microscopy, which could mean that the incorporation estimate of 1.5% is closer to the true rate.

Bullwinkle, et al. also reported the intracellular concentration of *m*-Tyr (2.7 μM) and Phe

(0.9 μM) in *pheT(G318W)* grown in minimal media with 0.5 mM *m*-Tyr[25]. This, along with the

reported K_m and K_{cat} values for editing-defective PheRS charging *m*-Tyr (K_m=247 μM, K_{cat}=2.1

s^{-1}) and Phe (K_m=18 μM, K_{cat}=5.2 s^{-1}) onto tRNA^{Phe}, can be used to estimate the speed of the two

charging reactions with the Michaelis-Menten competitive inhibition equation (Fig. 3-12)[25]. (At

low substrate concentrations relative to K_m, the sum of the two competing reactions is

approximately equal to what their sum would be if the reactions were run separately, in the

absence of the competing substrate. Further, it is permissible to substitute the K_m of the

competitor substrate for K_i in the competitive inhibition expression for the velocity of the other

substrate[116].) K_i for the two amino acids are their K_ms, the V_0 for Phe being charged onto

tRNA^{Phe} is 0.245 s^{-1} and the V_0 for *m*-Tyr being charged onto tRNA^{Phe} is 0.022 s^{-1}. These results

mean that we should expect *m*-Tyr to be charged onto tRNA^{Phe} approximately 9% as fast as Phe

in vivo under the growth conditions described. Since the *pheT(G318W)* strain does not have any

QC mechanisms to eliminate *m*-Tyr-tRNA^{Phe} before *m*-Tyr is added to a polypeptide, 9% is a

good estimation of the true misincorporation rate until more direct measurements can be

performed.

$$V_0 = \frac{V_{max}[S]}{K_m \left(1 + \frac{[I]}{K_i}\right) + [S]}$$

Figure 3-12. Michaelis-Menten competitive inhibition equation

Model for *m*-Tyr Toxicity

Based on our findings, we propose a model for the mechanism of *m*-Tyr toxicity in

pheT(G318W) E. coli that involves a chain reaction of self-reinforcing cellular damage (Fig. 3-

13). It is possible that the incorporation of *m*-Tyr could destabilize and cause the malfunction of electron transport proteins. This would lead to an increase in the generation of ROS as the process of reducing O_2 becomes less efficient. Our transcriptomic results provide supporting evidence for this, because we observed elevated transcription from genes that require the presence of ROS to be expressed. ROS can damage DNA directly and indirectly by membrane lipid peroxidation[117]. Elevated ROS concentrations could also produce even more *m*-Tyr, thereby intensifying the negative effects[25]. Large protein aggregates and the peroxidation of membrane lipids could both cause membrane destabilization and leakage, which would lead to a loss of ion homeostasis, reduced proton motive force, and possibly lysis[117-119]. This is supported by the observed increased expression of cation antiporters, membrane damage response regulators, the membrane stabilizing gene *pspA*, and P_i starvation genes. This model of a cascading, branching series of cellular stresses explains the importance of PheRS editing function to keep *m*-Tyr out of the proteome.
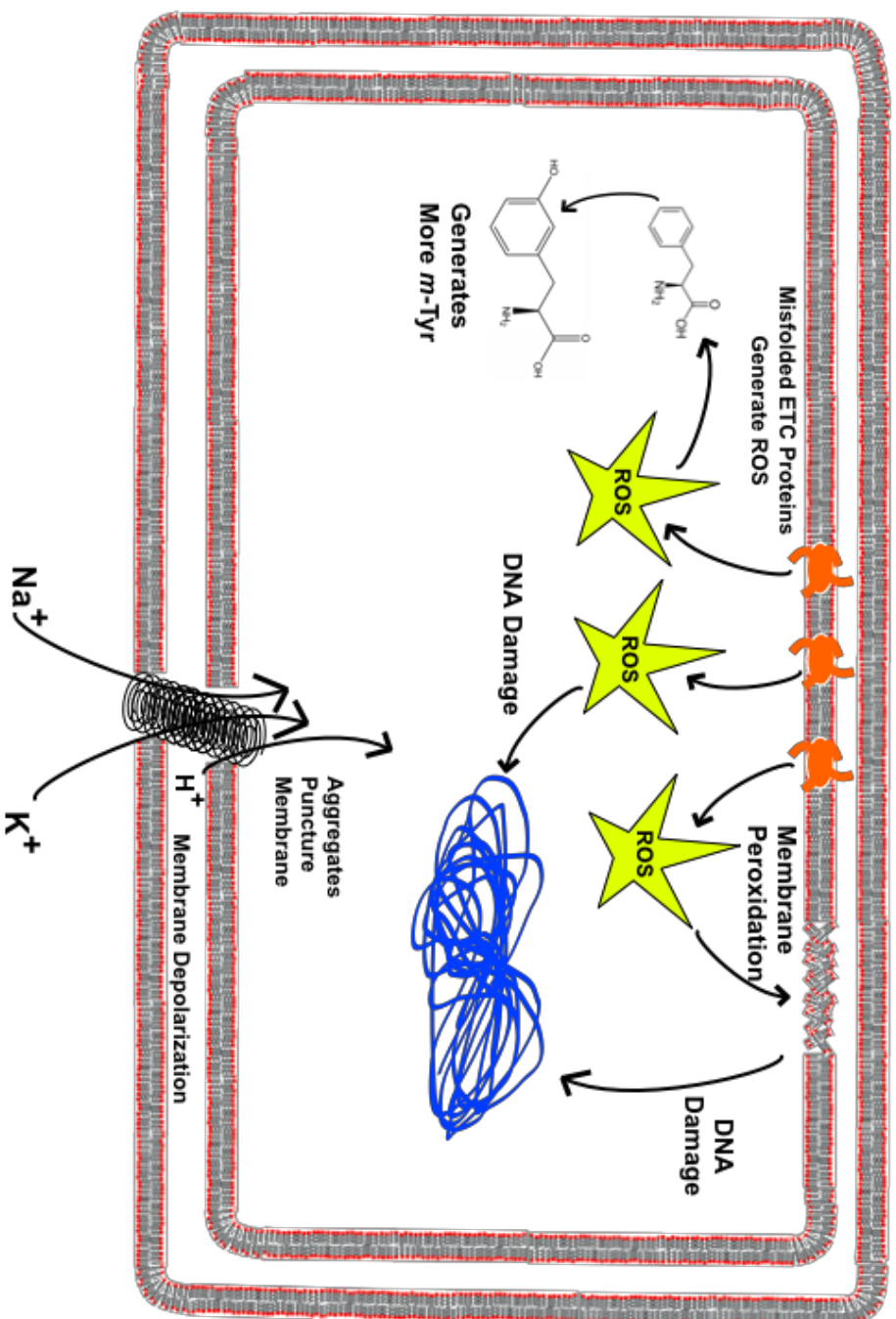
Figure 3-13. Model of *pheT(G318W) E. coli* cell death due to *m*-Tyr. Incorporation of *m*-Tyr into proteins causes some proteins to form large protein aggregates that puncture the membrane. Puncturing of the membrane then allows ions to flow into the cell and for a loss of proton motive force (PMF). Other proteins, such as Electron Transport Chain (ETC) proteins are made less efficient and as a result produce reactive oxygen species (ROS) from monovalent reductions of O_2. These ROS can then produce more *m*-Tyr, damage DNA directly, or cause membrane peroxidation. Membrane peroxidation produces mutagenic aldehydes, which can then also damage the cell's DNA. Membrane peroxidation can also cause the membrane to destabilize and allow for more proton leakage.

References

1.   Mascarenhas, A. P., An, S., Rosen, A. E. & Martinis, S. A. Fidelity mechanisms of the aminoacyl-tRNA synthetases. *Protein ...* (2009).

2.   Wong, F. C., Beuning, P. J., Silvers, C. & Musier-Forsyth, K. An Isolated Class II Aminoacyl-tRNA Synthetase Insertion Domain Is Functional in Amino Acid Editing. *J Biol Chem* **278,** 52857–52864 (2003).

3.   An, S. & Musier-Forsyth, K. Trans-editing of Cys-tRNAPro by Haemophilus influenzae YbaK Protein. *J Biol Chem* **279,** 42359–42362 (2004).

4.   Ahel, I., Korencic, D. & Ibba, M. Trans-editing of mischarged tRNAs. in (2003).

5.   Chong, Y. E., Yang, X.-L. & Schimmel, P. Natural homolog of tRNA synthetase editing domain rescues conditional lethality caused by mistranslation. *J Biol Chem* **283,** 30073–30078 (2008).

6.   Reynolds, N. M., Lazazzera, B. A. & Ibba, M. Cellular mechanisms that control mistranslation. *Nature Publishing Group* **8,** 849–856 (2010).

7.   Loftfield, R. B. & Vanderjagt, D. The frequency of errors in protein biosynthesis. *Biochem. J.* **128,** 1353–1356 (1972).

8.   Baker, S. J. *et al.* Therapeutic potential of boron-containing compounds. *Future Medicinal Chemistry* **1,** 1275–1288 (2009).

9.   Baker, S. J., Tomsho, J. W. & Benkovic, S. J. Boron-containing inhibitors of synthetases. *Chem. Soc. Rev.* **40,** 4279–8 (2011).

10.   Yaremchuk, A., Lincecum, T. L., Jr & Tukalo, M. *Structural and Mechanistic Basis of Pre-and Posttransfer Editing by Leucyl-tRNA Synthetase.* (Molecular cell, 2003).

11.   Alley, M. R., Baker, S. J., Beutner, K. R. & Plattner, J. Recent progress on the topical therapy of onychomycosis. *Expert Opinion on Investigational Drugs* **16,** 157–167 (2007).

12.   Seiradake, E. *et al.* Crystal Structures of the Human and Fungal Cytosolic Leucyl-tRNA Synthetase Editing Domains: A Structural Basis for the Rational Design of Antifungal Benzoxaboroles. *Journal of Molecular Biology* **390,** 196–207 (2009).

13.   Pohlmann, J. & Brotz-Oesterhelt, H. New aminoacyl-tRNA synthetase inhibitors as antibacterial agents. *Curr Drug Targets Infect Disord* **4,** 261–272 (2004).

14.   Bacher, J. M. & Schimmel, P. An editing-defective aminoacyl-tRNA synthetase is mutagenic in aging bacteria via the SOS response. *Proceedings of the National Academy of Sciences of the United States of America* **104,** 1907–1912 (2007).

15. Lee, J. W. *et al.* Editing-defective tRNA synthetase causes protein misfolding and neurodegeneration. *Nature* **443,** 50–55 (2006).

16. Nangle, L. A., Motta, C. M. & Schimmel, P. Global effects of mistranslation from an editing defect in mammalian cells. *Chem. Biol.* **13,** 1091–1100 (2006).

17. Wang, Y. *et al.* A Human Disease-causing Point Mutation in Mitochondrial Threonyl-tRNA Synthetase Induces Both Structural and Functional Defects. *J Biol Chem* **291,** 6507–6520 (2016).

18. Jakubowski, H. Translational accuracy of aminoacyl-tRNA synthetases: implications for atherosclerosis. *The Journal of nutrition* (2001).

19. Jakubowski, H. Misacylation of tRNALys with noncognate amino acids by lysyl-tRNA synthetase. *Biochemistry* **38,** 8088–8093 (1999).

20. Jakubowski, H. Quality control in tRNA charging -- editing of homocysteine. *Acta Biochim. Pol.* **58,** 149–163 (2011).

21. Cabiscol, E., Tamarit, J. & Ros, J. Oxidative stress in bacteria and protein damage by reactive oxygen species. *International Microbiology* **3,** 3–8 (2010).

22. Gurer-Orhan, H. *et al.* Misincorporation of free m-tyrosine into cellular proteins: a potential cytotoxic mechanism for oxidized amino acids. *Biochem. J.* **395,** 277–284 (2006).

23. Bertin, C. *et al.* Grass roots chemistry: meta-tyrosine, an herbicidal nonprotein amino acid. *Proceedings of the National Academy of Sciences of the United States of America* **104,** 16964–16969 (2007).

24. Klipcan, L., Moor, N., Kessler, N. & Safro, M. G. Eukaryotic cytosolic and mitochondrial phenylalanyl-tRNA synthetases catalyze the charging of tRNA with the meta-tyrosine. *Proceedings of the National Academy of Sciences* **106,** 11045–11048 (2009).

25. Bullwinkle, T. J. *et al.* Oxidation of cellular amino acid pools leads to cytotoxic mistranslation of the genetic code. *Elife* **3,** (2014).

26. Miller, J. H. Experiments in molecular genetics. (1972).

27. Costantino, N. & Court, D. L. Enhanced levels of lambda Red-mediated recombinants in mismatch repair mutants. *Proceedings of the National Academy of Sciences of the United States of America* **100,** 15748–15753 (2003).

28. Sawitzke, J. A. *et al.* Recombineering: using drug cassettes to knock out genes in vivo. *Methods Enzymol* **533,** 79–102 (2013).

29.   Ratib, N., Seidl, F., Ehrenreich, I. & Finkel, S. E. *Genetic diversity and population structure of E. coli during evolution during long-term batch culture. Manuscript in preparation*

30.   Li, H. & Durbin, R. Fast and accurate short read alignment with Burrows–Wheeler transform. *Bioinformatics* **25,** 1754–1760 (2009).

31.   Li, H. *et al.* The sequence alignment/map format and SAMtools. *Bioinformatics* **25,** 2078–2079 (2009).

32.   Trapnell, C., Pachter, L. & Salzberg, S. L. TopHat: discovering splice junctions with RNA-Seq. *Bioinformatics* **25,** 1105–1111 (2009).

33.   Anders, S., Pyl, P. T. & Huber, W. HTSeq–a Python framework to work with high-throughput sequencing data. *Bioinformatics* btu638 (2014).

34.   Love, M. I., Huber, W. & Anders, S. Moderated estimation of fold change and dispersion for RNA-seq data with DESeq2. *Genome Biol* **15,** 1 (2014).

35.   Paley, S. M. & Karp, P. D. The pathway tools cellular overview diagram and omics viewer. *Nucleic acids research* **34,** 3771–3778 (2006).

36.   Schneider, C. A., Rasband, W. S. & Eliceiri, K. W. NIH Image to ImageJ: 25 years of image analysis. *Nature Methods* **9,** 671–675 (2012).

37.   Schindelin, J. *et al.* Fiji: an open-source platform for biological-image analysis. *Nature Methods* **9,** 676–682 (2012).

38.   D, K. *et al.* Influence of threonine exporters on threonine production in Escherichia coli. *Applied microbiology and biotechnology* **59,** 205–210 (2002).

39.   Ide, N., Ikebe, T. & Kutsukake, K. Reevaluation of the promoter structure of the class 3 flagellar operons of Escherichia coli and Salmonella. *Genes & genetic systems* (1999).

40.   Karp, P. D., Riley, M., Paley, S. M. & Pelligrini-Toole, A. EcoCyc: an encyclopedia of Escherichia coli genes and metabolism. *Nucleic acids research* **24,** 32–39 (1996).

41.   Chen, S., Vincent, S., Wilson, D. B. & Ganem, B. Mapping of chorismate mutase and prephenate dehydrogenase domains in the Escherichia coli T-protein. *European Journal of Biochemistry* **270,** 757–763 (2003).

42.   Sampathkumar, P. & Morrison, J. F. Chorismate mutase-prephenate dehydrogenase from Escherichia coli purification and properties of the bifunctional enzyme. *Biochimica et Biophysica Acta (BBA)-Protein Structure and Molecular Enzymology* **702,** 204–211 (1982).

43. Patrick, W. M., Quandt, E. M., Swartzlander, D. B. & Matsumura, I. Multicopy suppression underpins metabolic evolvability. *Molecular biology and evolution* **24,** 2716–2722 (2007).

44. Consortium, U. UniProt: a hub for protein information. *Nucleic acids research* gku989 (2014).

45. Wasmer, C. *et al.* Solid-State NMR Spectroscopy Reveals that E. coliInclusion Bodies of HET-s(218 -289) are Amyloids. *Angew. Chem. Int. Ed.* **48,** 4858–4860 (2009).

46. Rokney, A. *et al.* E. coli Transports Aggregated Proteins to the Poles by a Specific and Energy-Dependent Process. *Journal of Molecular Biology* **392,** 589–601 (2009).

47. Bullwinkle, T. J. & Ibba, M. Translation quality control is critical for bacterial responses to amino acid stress. *Proceedings of the National Academy of Sciences of the United States of America* **113,** 2252–2257 (2016).

48. Pittard, A. J. & Davidson, B. E. TyrR protein of Escherichia coli and its role as repressor and activator. *Molecular Microbiology* **5,** 1585–1592 (1991).

49. Gunsalus, R. P. & Yanofsky, C. Nucleotide sequence and expression of Escherichia coli trpR, the structural gene for the trp aporepressor. *Proceedings of the National Academy of Sciences of the United States of America* **77,** 7117–7121 (1980).

50. Anderson, K. S., Sikorski, J. A. & Johnson, K. A. Evaluation of 5-enolpyruvoylshikimate-3-phosphate synthase substrate and inhibitor binding by stopped-flow and equilibrium fluorescence measurements. *Biochemistry* **27,** 1604–1610 (1988).

51. Yaniv, H. & Gilvarg, C. Aromatic biosynthesis XIV. 5-Dehydroshikimic reductase. *J Biol Chem* **213,** 787–795 (1955).

52. GETHING, M. J. & DAVIDSON, B. E. Chorismate Mutase/Prephenate Dehydratase from Escherichia coli K12. *European Journal of Biochemistry* **78,** 103–110 (1977).

53. Miles, E. W. & Moriguchi, M. Tryptophan synthase of Escherichia coli. Removal of pyridoxal 5'-phosphate and separation of the alpha and beta2 subunits. *J Biol Chem* **252,** 6594–6599 (1977).

54. Hathaway, G. M. & Crawford, I. P. Association of β-chain monomers of Escherichia coli tryptophan synthetase. *Biochemistry* **9,** 1801–1808 (1970).

55. Smith, O. H. Structure of the trpC cistron specifying indoleglycerol phosphate synthetase, and its localization in the tryptophan operon of Escherichia coli. *Genetics* **57,** 95 (1967).

56. Gonzalez, J. E. & Somerville, R. L. The anthranilate aggregate of Escherichia coli:

kinetics of inhibition by tryptophan of phosphoribosyltransferase. *Biochemistry and Cell Biology* **64,** 681–691 (1986).

57.   Pittard, J. & Wallace, B. J. Distribution and function of genes concerned with aromatic biosynthesis in Escherichia coli. *Journal of Bacteriology* **91,** 1494–1508 (1966).

58.   Powell, J. T. & Morrison, J. F. Role of the Escherichia coli aromatic amino acid aminotransferase in leucine biosynthesis. *Journal of Bacteriology* **136,** 1–4 (1978).

59.   Lindner, A. B., Madden, R., Demarez, A., Stewart, E. J. & Taddei, F. Asymmetric segregation of protein aggregates is associated with cellular aging and rejuvenation. *Proceedings of the National Academy of Sciences of the United States of America* **105,** 3076–3081 (2008).

60.   Laskowska, E., Wawrzynow, A. & Taylor, A. IbpA and IbpB, the new heat-shock proteins, bind to endogenous Escherichia coli proteins aggregated intracellularly by heat shock. *Biochimie* **78,** 117–122 (1996).

61.   Allen, S. P., Polazzi, J. O., Gierse, J. K. & Easton, A. M. Two novel heat shock genes encoding proteins produced in response to heterologous protein expression in Escherichia coli. *Journal of Bacteriology* **174,** 6938–6947 (1992).

62.   Vera, A., Arís, A., Carrió, M., González-Montalbán, N. & Villaverde, A. Lon and ClpP proteases participate in the physiological disintegration of bacterial inclusion bodies. *Journal of Biotechnology* **119,** 163–171 (2005).

63.   Higashitani, A., Ishii, Y., Kato, Y. & Horiuchi, K. Functional dissection of a cell-division inhibitor, SulA, of Escherichia coli and its negative regulation by Lon. *Molecular and General Genetics MGG* **254,** 351–357 (1997).

64.   Veinger, L., Diamant, S., Buchner, J. & Goloubinoff, P. The small heat-shock protein IbpB from Escherichia coli stabilizes stress-denatured proteins for subsequent refolding by a multichaperone network. *J Biol Chem* **273,** 11032–11037 (1998).

65.   Mogk, A., Deuerling, E., Vorderwülbecke, S., Vierling, E. & Bukau, B. Small heat shock proteins, ClpB and the DnaK system form a functional triade in reversing protein aggregation. *Molecular Microbiology* **50,** 585–595 (2003).

66.   Dougan, D. A., Reid, B. G., Horwich, A. L. & Bukau, B. ClpS, a substrate modulator of the ClpAP machine. *Molecular cell* **9,** 673–683 (2002).

67.   Raivio, T. L., Popkin, D. L. & Silhavy, T. J. The Cpx envelope stress response is controlled by amplification and feedback inhibition. *Journal of Bacteriology* **181,** 5263–5272 (1999).

68.   Buelow, D. R. & Raivio, T. L. Cpx signal transduction is influenced by a conserved N-

72

terminal domain in the novel inhibitor CpxP and the periplasmic protease DegP. *Journal of Bacteriology* **187,** 6622–6630 (2005).

69.   Danese, P. N. & Silhavy, T. J. CpxP, a stress-combative member of the Cpx regulon. *Journal of Bacteriology* **180,** 831–839 (1998).

70.   Vogt, S. L. & Raivio, T. L. Just scratching the surface: an expanding view of the Cpx envelope stress response. *FEMS microbiology letters* **326,** 2–11 (2012).

71.   Skorko-Glonek, J. *et al.* The Escherichia coli heat shock protease HtrA participates in defense against oxidative stress. *Molecular and General Genetics MGG* **262,** 342–350 (1999).

72.   Laskowska, E., Kuczyńska Wiśnik, D., Skórko Glonek, J. & Taylor, A. Degradation by proteases Lon, Clp and HtrA, of Escherichia coli proteins aggregated in vivo by heat shock; HtrA protease action in vivo and in vitro. *Molecular Microbiology* **22,** 555–571 (1996).

73.   Strauch, K. L., Johnson, K. & Beckwith, J. Characterization of degP, a gene required for proteolysis in the cell envelope and essential for growth of Escherichia coli at high temperature. *Journal of Bacteriology* **171,** 2689–2696 (1989).

74.   Missiakas, D., Schwager, F., Betton, J. M., Georgopoulos, C. & Raina, S. Identification and characterization of HsIV HsIU (ClpQ ClpY) proteins involved in overall proteolysis of misfolded proteins in Escherichia coli. *The EMBO Journal* **15,** 6899 (1996).

75.   Peruski, L. F. & Neidhardt, F. C. Identification of a conditionally essential heat shock protein in Escherichia coli. *Biochimica et Biophysica Acta (BBA)-Protein Structure and Molecular Enzymology* **1207,** 165–172 (1994).

76.   Yoo, S. J. *et al.* Purification and characterization of the heat shock proteins HslV and HslU that form a new ATP-dependent protease in Escherichia coli. *J Biol Chem* **271,** 14035–14040 (1996).

77.   Liberek, K., Marszalek, J., Ang, D., Georgopoulos, C. & Zylicz, M. Escherichia coli DnaJ and GrpE heat shock proteins jointly stimulate ATPase activity of DnaK. *Proceedings of the National Academy of Sciences of the United States of America* **88,** 2874–2878 (1991).

78.   Kihara, A., Akiyama, Y. & Ito, K. A protease complex in the Escherichia coli plasma membrane: HflKC (HflA) forms a complex with FtsH (HflB), regulating its proteolytic activity against SecY. *The EMBO Journal* **15,** 6122 (1996).

79.   Akiyama, Y. & Ito, K. Roles of multimerization and membrane association in the proteolytic functions of FtsH (HflB). *The EMBO Journal* **19,** 3888–3895 (2000).

80.   Vijayalakshmi, J., Mukhergee, M. K., Graumann, J., Jakob, U. & Saper, M. A. The 2.2 Å crystal structure of Hsp33: a heat shock protein with redox-regulated chaperone activity. *Structure* **9,** 367–375 (2001).

81.   Korber, P., Stahl, J. M., Nierhaus, K. H. & Bardwell, J. C. Hsp15: a ribosome-associated heat shock protein. *The EMBO Journal* **19,** 741–748 (2000).

82.   Jiang, L. *et al.* Recycling of aborted ribosomal 50S subunit-nascent chain-tRNA complexes by the heat shock protein Hsp15. *Journal of Molecular Biology* **386,** 1357–1367 (2009).

83.   Korber, P., Zander, T., Herschlag, D. & Bardwell, J. C. A new heat shock protein that binds nucleic acids. *J Biol Chem* **274,** 249–256 (1999).

84.   Mamun, Al, A. A. M. *et al.* Identity and function of a large gene network underlying mutagenic repair of DNA breaks. **338,** 1344–1348 (2012).

85.   Fayet, O., Ziegelhoffer, T. & Georgopoulos, C. The groES and groEL heat shock gene products of Escherichia coli are essential for bacterial growth at all temperatures. *Journal of Bacteriology* **171,** 1379–1385 (1989).

86.   Bardwell, J. C. & Craig, E. A. Eukaryotic Mr 83,000 heat shock protein has a homologue in Escherichia coli. *Proceedings of the National Academy of Sciences of the United States of America* **84,** 5177–5181 (1987).

87.   Heitzer, A., Mason, C. A. & Hamer, G. Heat shock gene expression in continuous cultures of Escherichia coli. *Journal of Biotechnology* **22,** 153–169 (1992).

88.   d'Alençon, E. *et al.* Isolation of a new hemimethylated DNA binding protein which regulates dnaA gene expression. *Journal of Bacteriology* **185,** 2967–2971 (2003).

89.   Shimohata, N., Chiba, S., Saikawa, N., Ito, K. & Akiyama, Y. The Cpx stress response system of Escherichia coli senses plasma membrane proteins and controls HtpX, a membrane protease with a cytosolic active site. *Genes to Cells* **7,** 653–662 (2002).

90.   Arribas, J. & Castaño, J. G. A comparative study of the chymotrypsin-like activity of the rat liver multicatalytic proteinase and the ClpP from Escherichia coli. *J Biol Chem* **268,** 21165–21171 (1993).

91.   Wang, J., Hartling, J. A. & Flanagan, J. M. The structure of ClpP at 2.3 Å resolution suggests a model for ATP-dependent proteolysis. *Cell* **91,** 447–456 (1997).

92.   Ortega, J., Lee, H. S., Maurizi, M. R. & Steven, A. C. ClpA and ClpX ATPases bind simultaneously to opposite ends of ClpP peptidase to form active hybrid complexes. *Journal of structural biology* **146,** 217–226 (2004).

93. Levchenko, I., Smith, C. K., Walsh, N. P., Sauer, R. T. & Baker, T. A. PDZ-like domains mediate binding specificity in the Clp/Hsp100 family of chaperones and protease regulatory subunits. *Cell* **91,** 939–947 (1997).

94. Neuwald, A. F., Aravind, L., Spouge, J. L. & Koonin, E. V. AAA+: A class of chaperone-like ATPases associated with the assembly, operation, and disassembly of protein complexes. *Genome Research* **9,** 27–43 (1999).

95. Semchyshyn, H., Bagnyukova, T. & Lushchak, V. Involvement of soxRS regulon in response of Escherichia coli to oxidative stress induced by hydrogen peroxide. *Biochemistry (Moscow)* **70,** 1238–1244 (2005).

96. Park, J.-S., Marr, M. T. & Roberts, J. W. E. coli transcription repair coupling factor (Mfd protein) rescues arrested complexes by promoting forward translocation. *Cell* **109,** 757–767 (2002).

97. Tchou, J. *et al.* 8-Oxoguanine (8-hydroxyguanine) DNA glycosylase and its substrate specificity. *Proceedings of the National Academy of Sciences of the United States of America* **88,** 4690–4694 (1991).

98. Michaels, M. L., Pham, L., Cruz, C. & Miller, J. H. MutM, a protein that prevents GC→TA transversions, is formamidopyrimidine-DNA glycosylase. *Nucleic acids research* **19,** 3629–3632 (1991).

99. Cole, R. S. Inactivation of Escherichia coli, F′ episomes at transfer, and bacteriophage lambda by psoralen plus 360-nm light: significance of deoxyribonucleic acid cross-links. *Journal of Bacteriology* **107,** 846–852 (1971).

100. Chen, H.-W., Ruan, B., Yu, M. & Julin, D. A. The RecD subunit of the RecBCD enzyme from Escherichia coli is a single-stranded DNA-dependent ATPase. *J Biol Chem* **272,** 10072–10079 (1997).

101. Padan, E. *et al.* The molecular mechanism of regulation of the NhaA Na+/H+ antiporter of Escherichia coli, a key transporter in the adaptation to Na+ and H. 183–199 (1999).

102. Shijuku, T. *et al.* Expression of chaA, a sodium ion extrusion system of Escherichia coli, is regulated by osmolarity and pH. *Biochim. Biophys. Acta* **1556,** 142–148 (2002).

103. Kobayashi, R., Suzuki, T. & Yoshida, M. Escherichia coli phage–shock protein A (PspA) binds to membrane phospholipids and repairs proton leakage of the damaged membranes. *Molecular Microbiology* **66,** 100–109 (2007).

104. Weiner, L., Brissette, J. L. & Model, P. Stress-induced expression of the Escherichia coli phage shock protein operon is dependent on sigma 54 and modulated by positive and negative feedback mechanisms. *Genes & development* **5,** 1912–1923 (1991).

105.   Ivey, D. M. *et al.* Cloning and characterization of a putative Ca2+/H+ antiporter gene from Escherichia coli upon functional complementation of Na+/H+ antiporter-deficient strains by the overexpressed gene. *J Biol Chem* **268,** 11296–11303 (1993).

106.   Radchenko, M. V. *et al.* Potassium/proton antiport system of Escherichia coli. *J Biol Chem* **281,** 19822–19829 (2006).

107.   圭, 稲. *et al.* Lithium toxicity and Na+ (Li+)/H+ antiporter in Escherichia coli. *Biological and Pharmaceutical Bulletin* **17,** 395–398 (1994).

108.   Taglicht, D., Padan, E. & Schuldiner, S. Overproduction and purification of a functional Na+/H+ antiporter coded by nhaA (ant) from Escherichia coli. *J Biol Chem* **266,** 11289–11294 (1991).

109.   Voges, D. & Jap, B. K. Recombinant expression, purification and characterization of Kch, a putative Escherichia coli potassium channel protein. *FEBS Letters* **429,** 104–108 (1998).

110.   Schlosser, A., Hamann, A., Bossemeyer, D., Schneider, E. & Bakker, E. P. NAD+ binding to the Escherichia coli K+-uptake protein TrkA and sequence similarity between TrkA and domains of a family of dehydrogenases suggest a role for NAD+ in bacterial transport. *Molecular Microbiology* **9,** 533–543 (1993).

111.   Dosch, D. C., Helmer, G. L., Sutton, S. H., Salvacion, F. F. & Epstein, W. Genetic analysis of potassium transport loci in Escherichia coli: evidence for three constitutive systems mediating uptake potassium. *Journal of Bacteriology* **173,** 687–696 (1991).

112.   Cowan, S. W. *et al.* Crystal structures explain functional properties of two E. coli porins. *Nature* **358,** 727–733 (1992).

113.   Trchounian, A. & Kobayashi, H. Kup is the major K+ uptake system in Escherichia coli upon hyper-osmotic stress at a low pH. *FEBS Letters* **447,** 144–148 (1999).

114.   Huang, T., Tohge, T., Lytovchenko, A., Fernie, A. R. & Jander, G. Pleiotropic physiological consequences of feedback-insensitive phenylalanine biosynthesis in Arabidopsis thaliana. *The Plant Journal* **63,** 823–835 (2010).

115.   Rokney, A. *et al.* E. coli Transports Aggregated Proteins to the Poles by a Specific and Energy-Dependent Process. *Journal of Molecular Biology* **392,** 589–601 (2009).

116.   Segel, I. H. Enzyme Kinetics: Behavior and Analysis of Rapid Equilibrium and Steady-State Enzyme Systems. (1993).

117.   Akasaka, S. & Yamamoto, K. Mutagenesis resulting from DNA damage by lipid peroxidation in the supF gene of Escherichia coli. *Mutation Research/DNA Repair* **315,** 105–112 (1994).

118. Caughey, B. & Lansbury, P. T., Jr. Protofibrils, pores, fibrils, and neurodegeneration: Separating the responsible protein aggregates from the innocent bystanders*. *Annual review of neuroscience* **26,** 267–298 (2003).

119. Marnett, L. J. Lipid peroxidation—DNA damage by malondialdehyde. *Mutation Research/Fundamental and Molecular Mechanisms of Mutagenesis* **424,** 83–95 (1999).

Chapter 4:

Future Directions

<u>Mutation Rate of *pheT(G318W)* E. coli compared to WT</u>

Because *E. coli* is unlikely to regularly experience the high concentrations of *m*-Tyr used in the experiments reported here (at least 0.1 mM), it would be illuminating to investigate more subtle negative effects *E. coli* lacking PheRS editing function experiences during more normal growth. It has been shown that *m*-Tyr is generated inside *E. coli* when exposed to H_2O_2, and that aerobic growth naturally generates ROS including H_2O_2 inside *E. coli*[1,2]. The concentration of *m*-Tyr generated by naturally produced ROS will be low compared to the concentration achieved by addition of exogenous *m*-Tyr to the growth media. This makes minimal media the most likely growth condition to have a detectable negative effect, because the intracellular Phenylalanine (Phe) concentration will be low compared to growth in rich media.

An elevated mutation rate is a promising candidate for a negative growth effect in *pheT(G318W)* grown in minimal media. It has been shown that aging *E. coli* cells that lack IleRS editing function had an elevated mutation rate caused by the SOS response[3]. It was also reported that translation stress-induced mutagenesis occurs in *E. coli* treated with an antibiotic that affects translation fidelity[4]. Using a crude assay, we performed some initial experiments where we grew *pheT(G318W)* and WT *E. coli* in minimal media cultures and plated them on rifampicin (rif) containing LB plates to estimate the mutation rate (Fig. 4-1). These initial results were promising enough that we have begun pursuing the more sophisticated Luria-Delbrück fluctuation assay that uses parallel cultures that are plated onto rif plates to determine the mutation rate[5-7]. The results thus far (Fig. 4-2) show a higher mutation rate for the *pheT(G318W)* strain ($p<0.01$). We have also engineered knock outs of the three error prone DNA polymerases in both WT and *pheT(G318W)* strain backgrounds. Determining the mutation rate of these

strains will help us determine if any of these error prone DNA polymerases are responsible for

the differences in mutation rate.
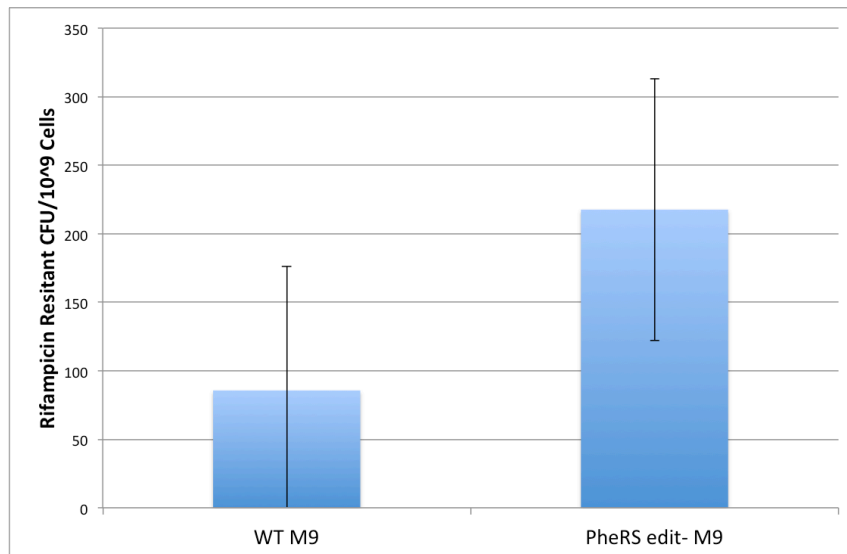
Figure 4-1. Initial mutation rate estimate of WT and *pheT(G318W) E. coli* grown in M9 minimal media. Bars are averages of three replicates, and error bars are standard deviation.
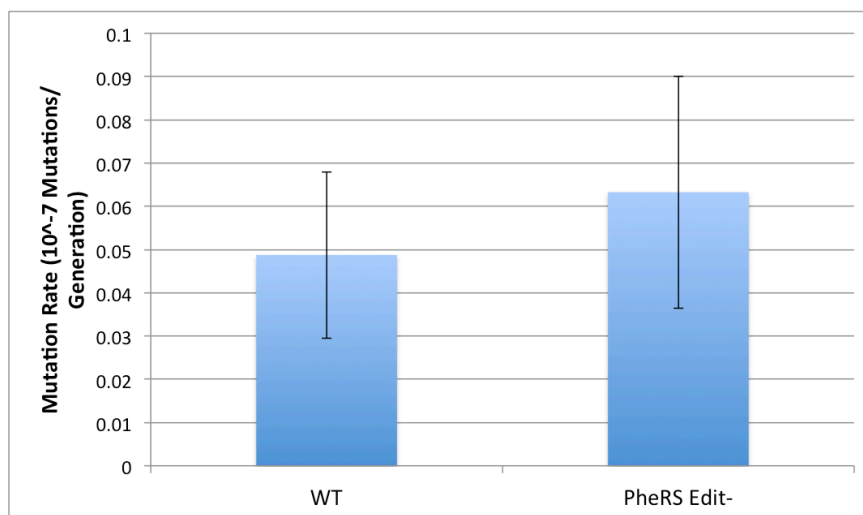
Figure 4-2. Mutation rates of WT and *pheT(G318W) E. coli* grown in M9 minimal media as calculated by the Luria-Delbrück fluctuation assay. Bars are averages of 7 replicates, and error bars are standard deviation.

Characterization of Soluble and Insoluble Protein in *pheT(G318W) E. coli* Treated with *m*-Tyr

As discussed in Chapter 3, it is highly likely that Bullwinkle, et al. (2014) underestimated the rate of *m*-Tyr being misincorporation due to insoluble protein aggregates being excluded from the protein purification methods used[1]. It would be valuable to repeat the liquid chromatography tandem mass spectrometry with multiple reaction monitoring (LC-MS/MS-MRM) used in Bullwinkle, et al. (2014) to measure the *m*-Tyr presence in the true total protein content of these cells. This would give a better idea of how close to the theoretical misincorporation rate outlined in Chapter 3 the actual rate of *m*-Tyr misincorporation is. It would also be interesting to see what the difference in *m*-Tyr misincorporation is between the soluble protein fraction and the insoluble protein aggregate fraction. This might provide an insight into what the average threshold of *m*-Tyr misincorporation is for *E. coli* proteins to unfold because of destabilization.

Another useful area to explore would be to identify and study the proteins that make up the large polar aggregates that form in the *pheT(G318W)* strain when grown with *m*-Tyr. It seems likely that some proteins would be more sensitive to *m*-Tyr destabilization than others, and would therefore be disproportionately represented in the protein aggregates. The protein aggregates could be purified using previously described methods, and the constituent proteins could be identified either by 2D gel electrophoresis or mass spectrometry[8-10]. Once the proteins that make up the polar aggregates are identified, we could study their thermal stability when produced with or without *m*-Tyr. This could be accomplished using basic protein purification methods and Differential Scanning Fluorimetry, which allows for the accurate determination of the melting temperature of a given protein[11]. This could allow us to quantify the destabilizing effects of *m*-Tyr in proteins.

References

1.   Bullwinkle, T. J. *et al.* Oxidation of cellular amino acid pools leads to cytotoxic mistranslation of the genetic code. *Elife* **3,** (2014).

2.   González-Flecha, B. & Demple, B. Metabolic sources of hydrogen peroxide in aerobically growing Escherichia coli. *J Biol Chem* **270,** 13681–13687 (1995).

3.   Bacher, J. M. & Schimmel, P. An editing-defective aminoacyl-tRNA synthetase is mutagenic in aging bacteria via the SOS response. *Proceedings of the National Academy of Sciences of the United States of America* **104,** 1907–1912 (2007).

4.   Balashov, S. & Humayun, M. Z. Mistranslation induced by streptomycin provokes a RecABC/RuvABC-dependent mutator phenotype in Escherichia coli cells. *Journal of Molecular Biology* **315,** 513–527 (2002).

5.   Luria, S. E. & Delbrück, M. Mutations of bacteria from virus sensitivity to virus resistance. *Genetics* **28,** 491 (1943).

6.   Foster, P. L. Methods for determining spontaneous mutation rates. *Methods in enzymology* **409,** 195–213 (2006).

7.   Hall, B. M., Ma, C.-X., Liang, P. & Singh, K. K. Fluctuation AnaLysis CalculatOR: a web tool for the determination of mutation rate using Luria–Delbrück fluctuation analysis. *Bioinformatics* **25,** 1564–1565 (2009).

8.   García-Fruitós, E. Insoluble Proteins: Methods and Protocols. (2015).

9.   Peng, J., Elias, J. E., Thoreen, C. C., Licklider, L. J. & Gygi, S. P. Evaluation of multidimensional chromatography coupled with tandem mass spectrometry (LC/LC-MS/MS) for large-scale protein analysis: the yeast proteome. *Journal of proteome research* **2,** 43–50 (2003).

10.   Henzel, W. J. *et al.* Identifying proteins from two-dimensional gels by molecular mass searching of peptide fragments in protein sequence databases. *Proceedings of the National Academy of Sciences of the United States of America* **90,** 5011–5015 (1993).

11.   Niesen, F. H., Berglund, H. & Vedadi, M. The use of differential scanning fluorimetry to detect ligand interactions that promote protein stability. *Nature Protocols* **2,** 2212–2221 (2007).

Chapter 5:

Appendices

Appendix A: Whole Genome Sequencing Results of Non-Silent and Intergenic SNPs From *m*-Tyr[R] Mutants. Position refers to the chromosomal locus of the mutated base. The mutations are listed as the original base and then the replacement base of the mutation. For example "CT" would indicate a C changed to a T.

Strain	Outgrowth Media	Position	Gene	Mutation	Amino Acid Substitution
Rmt1	M9	2498100	*alaC*	CT	D66N
Rmt1	M9	120245	*aroP*	CT	W436C
Rmt1	M9	498233	*hemH*	GA	R60H
Rmt1	M9	174598	*hemL*	CT	M95I
Rmt1	M9	2686487	*hmp*	GA	R218H
Rmt1	M9	2607185	*hyfF*	CT	T90I
Rmt1	M9	2836303	*hypF*	GA	R375W
Rmt1	M9	2236904	*mglC*	CT	G284R
Rmt1	M9	233879	*mltD*	GA	A26V
Rmt1	M9	530295	*mnmH*	GA	T311M
Rmt1	M9	602431	*pheP*	GA	G158D
Rmt1	M9	1185300	*potA*	CT	A99T
Rmt1	M9	2314538	*rcsD*	CT	R351C
Rmt1	M9	2120789	*wcaJ*	CT	V256I
Rmt1	M9	573274	*ybcO*	GA	R64H
Rmt1	M9	829171	*ybhG*	GA	R268S
Rmt1	M9	966240	*ycaI*	CT	P641S
Rmt2	M9	121428	*aroP*	GA	Q42STOP
Rmt2	M9	325996	*betA*	CT	E418K
Rmt2	M9	2789708	*csiD*	CT	R242C
Rmt2	M9	2569169	*eutG*	CT	G115S
Rmt2	M9	3232833	*fadH*	CT	A390V
Rmt2	M9	3123349	*glcB*	CT	A153T
Rmt2	M9	2920371	*gudX*	CT	A126T
Rmt2	M9	1591669	*hipA*	GA	P170S
Rmt2	M9	4585396	*hsdR*	CT	V456I
Rmt2	M9	3010959	*hyuA*	CT	A311E
Rmt2	M9	87136	*ilvI*	GA	D503N
Rmt2	M9	1520463	*mcbR*	CT	P68S
Rmt2	M9	2377193	*menH*	GA	R134C
Rmt2	M9	3337151	*mlaB*	CT	V36M
Rmt2	M9	3105147	*mltC*	CT	H239Y
Rmt2	M9	100556	*murG*	GA	E305K
Rmt2	M9	1539623	*narZ*	CT	E990STOP
Rmt2	M9	3308894	*nlpI*	CT	A11T
Rmt2	M9	1462554	*paaK*	GA	G144R
Rmt2	M9	300687	*paoC*	GA	A83V
Rmt2	M9	3219687	*patA*	CT	A65V

Rmt2	M9	2805248	*proV*	CT	A145V
Rmt2	M9	3170719	*qseC*	GA	G79D
Rmt2	M9	3170796	*qseC*	GA	G105R
Rmt2	M9	21773	*ribF*	GA	V123I
Rmt2	M9	213752	*rof*	GA	R61C
Rmt2	M9	3214472	*rpoD*	CT	R476C
Rmt2	M9	1654833	*rspA*	CT	M103I
Rmt2	M9	3061157	*scpA*	CT	S103F
Rmt2	M9	4630946	*slt*	CT	Q72STOP
Rmt2	M9	3239818		CT	
Rmt2	M9	1763600	*sufB*	CT	G137D
Rmt2	M9	4579614	*symE*	GA	A76V
Rmt2	M9	3205718	*ttdR*	GA	P180L
Rmt2	M9	3208014		GA	
Rmt2	M9	4555155	*uxuR*	CT	R194C
Rmt2	M9	292483	*yagK*	GA	H156Y
Rmt2	M9	1274061	*ychO*	CT	A93V
Rmt2	M9	1325902	*yciQ*	CT	P386L
Rmt2	M9	1780331	*ydiQ*	CT	P239S
Rmt2	M9	1867235	*yeaG*	GA	G110E
Rmt2	M9	2550043	*yfeX*	CT	G168D
Rmt2	M9	3362868	*yhcD*	CT	A21V
Rmt2	M9	3368196	*yhcG*	CT	P124S
Rmt2	M9	2985905	*yqeG*	CT	A20V
Rmt2	M9	4612123	*ytjA*	CT	
Rmt3	M9	120659	*aroP*	GA	S298F
Rmt3	M9	1087266	*pgaC*	CT	R194H
Rmt3	M9	4296380		A->ACG	
Rmt4	LB	1296149	*adhE*	GA	A658V
Rmt4	LB	3741084		GA	
Rmt4	LB	3900953	*bglH*	CT	G423I
Rmt4	LB	4044059		CT	
Rmt4	LB	3361101	*gltF*	CT	
Rmt4	LB	3460367	*gspF*	CT	A184V
Rmt4	LB	4598298	*opgB*	GA	P382S
Rmt4	LB	302618		GA	
Rmt4	LB	4007714		CT	
Rmt4	LB	4181279	*rpoB*	GA	R12H
Rmt4	LB	1298991	*ychE*	GA	G132R
Rmt4	LB	1299487	*ychE*	GA	
Rmt4	LB	1995827	*yecF*	CT	P4S
Rmt4	LB	3831628	*yicH*	GA	R391H
Rmt5	LB	3920551	*atpF*	GA	R113H
Rmt5	LB	3872515	*dgoD*	GA	A162T
Rmt5	LB	3839861	*nlpA*	GA	D45N

Rmt5	LB	3803945	*waaB*	GA	G65S
Rmt5	LB	3676814	*yhjG*	GA	G513S
Rmt5	LB	3896778	*yieH*	CT	S2F
Rmt5	LB	633489		CA	
Rmt5	LB	3925817		CT	
Rmt5	LB	4007714		CT	
Rmt6	LB	544517	*allC*	CT	P259L
Rmt6	LB	121252	*aroP*	GA	W100STOP
Rmt6	LB	807991	*bioA*	GA	D423N
Rmt6	LB	809764	*bioB*	CT	R141C
Rmt6	LB	4377382	*blc*	GA	G114D
Rmt6	LB	651799	*citC*	GA	E20K
Rmt6	LB	4364943	*dsbD*	GA	D100N
Rmt6	LB	4515410	*fecA*	GA	R423H
Rmt6	LB	4512737	*fecC*	GA	D225N
Rmt6	LB	173005	*fhuB*	CT	S515L
Rmt6	LB	4278680	*ghxP*	GA	A68T
Rmt6	LB	2919800	*gudX*	GA	W316STOP
Rmt6	LB	4584204	*hsdR*	GA	S853N
Rmt6	LB	3955505	*ilvA*	CT	H59Y
Rmt6	LB	3595755	*livH*	GA	A217T
Rmt6	LB	277021	*mmuM*	CT	R103C
Rmt6	LB	301845	*paoB*	GA	A15T
Rmt6	LB	3113577	*pppA*	GA	G259D
Rmt6	LB	4125598	*priA*	CT	P405S
Rmt6	LB	4126645	*priA*	CT	P56S
Rmt6	LB	4263459	*qorA*	CT	S258L
Rmt6	LB	3937427	*rbsK*	CT	A45V
Rmt6	LB	2950854	*recD*	GA	M536I
Rmt6	LB	3966408	*rho*	CT	
Rmt6	LB	734550	*rhsO*	CT	R140C
Rmt6	LB	4409327	*rlmB*	CT	A18V
Rmt6	LB	4182715	*rpoB*	GA	D491N
Rmt6	LB	4187549	*rpoC*	GA	A733T
Rmt6	LB	2709829	*rpoE*	GA	D62N
Rmt6	LB	4043337	*srkA*	CT	A308E
Rmt6	LB	4423745	*ulaF*	CT	P16S
Rmt6	LB	3806401	*waaG*	GA	E223K
Rmt6	LB	130704	*yacH*	GA	G186D
Rmt6	LB	335614	*yahD*	CT	A112V
Rmt6	LB	3236784	*ygjQ*	CT	A82V
Rmt6	LB	4045501	*yihF*	CT	Q434STOP
Rmt6	LB	4073016	*yihU*	GA	A186C
Rmt6	LB	2923988	*yqcC*	GA	M42I
Rmt6	LB	2062043		CT	

Rmt6	LB	2491995		CT	
Rmt6	LB	3941335		CT	
Rmt6	LB	4382553		CT	
Rmt6	LB	4614609		CT	
Rmt7	LB	3902635	*bglB*	CT	P356L
Rmt7	LB	3897902	*cbrB*	GA	V133M
Rmt7	LB	3898472	*cbrC*	CA	L151I
Rmt7	LB	3720139	*cspA*	TC	F91L
Rmt7	LB	3787258	*envC*	GA	E141K
Rmt7	LB	3722711	*glyS*	CT	R563C
Rmt7	LB	3774904	*mtlD*	GA	V161I
Rmt7	LB	3938241	*rbsR*	AT	K5N
Rmt7	LB	4193745	*thiE*	GA	E154K
Rmt7	LB	3999493	*uvrD*	CT	T504M
Rmt7	LB	2900245	*ygcW*	CT	S10L
Rmt7	LB	3835503	*yicJ*	CT	Q143STOP
Rmt7	LB	4573191	*yjiT*	GA	E260K
Rmt7	LB	485685		GA	
Rmt7	LB	3599924		CT	
Rmt7	LB	3840045		GT	
Rmt7	LB	3922617		GA	
Rmt7	LB	4007714		CT	
Rmt7	LB	4296380		A-ACG	
Rmt8	LB	4092682	*frvA*	CT	R48C
Rmt8	LB	4115935	*glpK*	CT	R430C
Rmt8	LB	3963149	*gpp*	CT	L361F
Rmt8	LB	2739754	*tyrA*	GA	G106S
Rmt8	LB	2025143	*yodD*	CT	T53I

Appendix B: RNA-seq Results from *pheT(G318W) E. coli* After *m*-Tyr Exposure

Table Terms

Base mean: the average of the normalized count values, dividing by size factors, taken over all samples in the data set

Log$_2$ Fold Change: is the effect size estimate. It tells us how much the gene's expression seems to have changed due to the *m*-Tyr treatment in comparison another sample from the time course. This value is reported on a logarithmic scale to base 2: for example, a log$_2$ fold change of 3 means that the gene's expression is increased by a multiplicative factor of $2^3 = 8$.

lfcSE: the Log2 Fold Change Standard Error

stat: the Wald statistic. It is the LFC divided by its standard error. This Wald statistic is used to calculate *p*-values

***p* value:** indicates the probability that a fold change as strong as the observed one, or even stronger, would be seen under the situation described by the null hypothesis.

padj: Benjamini-Hochberg adjustment applied to the *p* value. It answers the following question: if one called significant all genes with an adjusted *p* value less than or equal to this gene's adjusted *p* value threshold, what would be the fraction of false positives among them?

t=30 vs. t=0 (p<0.005)

Gene	BaseMean	log$_2$ Fold Change	lfcSE	stat	*p*-value	padj
aceB	324.6456	-0.9727	0.3297	-2.9499	0.0032	0.0192
ackA	180.3401	1.4341	0.4953	2.8956	0.0038	0.0221
acnA	50.2069	-1.1868	0.3523	-3.3691	7.54E-04	0.0060
acS	38.9100	2.0338	0.3240	6.2774	3.44E-10	1.63E-08
acuI	21.3695	-2.1536	0.5988	-3.5965	3.23E-04	0.0030
adhE	103.0873	-1.1321	0.3654	-3.0985	0.0019	0.0130
adhP	21.8856	-4.1659	0.5818	-7.1598	8.08E-13	6.39E-11
ahR	11.7657	-3.4677	0.5970	-5.8084	6.31E-09	2.21E-07
aidB	12.8906	-3.4091	0.5789	-5.8893	3.88E-09	1.48E-07

alaW	17.7307	1.6451	0.5294	3.1075	0.0019	0.0127
aldB	4.6081	-3.2580	0.7829	-4.1617	3.16E-05	4.45E-04
amiA	71.2954	2.1864	0.5692	3.8413	1.22E-04	0.0014
amiC	77.2977	1.7641	0.5373	3.2829	0.0010	0.0077
amN	38.1308	-1.3272	0.4638	-2.8614	0.0042	0.0240
amyA	20.9495	-3.1303	0.5258	-5.9538	2.62E-09	1.04E-07
araC	58.0605	2.2933	0.3337	6.8720	6.33E-12	4.12E-10
argA	573.4813	3.7101	0.5803	6.3936	1.62E-10	8.28E-09
argB	162.2474	3.5197	0.5551	6.3406	2.29E-10	1.12E-08
argC	544.7538	4.1272	0.5837	7.0703	1.55E-12	1.12E-10
argD	192.4090	2.1416	0.5281	4.0556	5.00E-05	6.44E-04
argE	353.4858	3.2384	0.5427	5.9674	2.41E-09	9.89E-08
argF	224.6939	4.2756	0.5514	7.7544	8.88E-15	1.02E-12
argG	1067.2312	3.2855	0.8368	3.9263	8.62E-05	0.0010
argH	337.7552	3.4278	0.4563	7.5125	5.80E-14	5.67E-12
argI	190.4276	4.1358	0.5541	7.4639	8.40E-14	7.75E-12
argY	93.3163	1.7199	0.4940	3.4812	4.99E-04	0.0043
argZ	51.3680	1.7141	0.4347	3.9431	8.04E-05	9.58E-04
arnT	5.2623	-2.3060	0.7322	-3.1492	0.0016	0.0115
aroA	53.5643	-2.1018	0.5173	-4.0629	4.85E-05	6.32E-04
aroE	25.3601	-2.4746	0.6188	-3.9992	6.36E-05	7.91E-04
aroG	327.2786	-2.2702	0.5908	-3.8426	1.22E-04	0.0014
aroM	21.9340	-1.6179	0.5525	-2.9283	0.0034	0.0202
aroP	109.3223	-2.5375	0.4125	-6.1515	7.67E-10	3.45E-08
arrS	2.3709	-4.4648	1.1323	-3.9431	8.05E-05	9.58E-04
artI	110.0126	1.5189	0.4490	3.3830	7.17E-04	0.0058
artJ	890.1429	4.3151	0.6475	6.6647	2.65E-11	1.63E-09
artM	35.3219	1.1604	0.3633	3.1940	0.0014	0.0100
artP	88.3271	1.4925	0.4100	3.6398	2.73E-04	0.0027
asnA	115.8790	2.7907	0.5949	4.6913	2.71E-06	5.43E-05
aspA	65.9784	1.0609	0.3055	3.4726	5.15E-04	0.0044
aspS	118.8384	1.0361	0.3550	2.9188	0.0035	0.0207
aspV	26.4039	1.4349	0.4653	3.0836	0.0020	0.0135
atpB	230.9551	1.5119	0.5258	2.8755	0.0040	0.0231
atpC	164.2234	1.4762	0.2991	4.9358	7.98E-07	1.87E-05
atpG	107.6051	0.6603	0.2149	3.0732	0.0021	0.0139
atpI	91.8862	1.9119	0.5039	3.7939	1.48E-04	0.0016
bcsC	14.9794	-1.3605	0.4612	-2.9502	0.0032	0.0192
bcsE	26.5329	-1.6035	0.4332	-3.7015	2.14E-04	0.0022
bcsG	11.9896	-2.1034	0.4760	-4.4189	9.92E-06	1.62E-04
bcsQ	5.8364	-2.4572	0.8335	-2.9480	0.0032	0.0193
betB	76.5106	1.6850	0.4610	3.6548	2.57E-04	0.0026
betI	65.5681	2.0211	0.4251	4.7547	1.99E-06	4.15E-05
betT	75.8656	1.4655	0.3805	3.8514	1.17E-04	0.0013
bioB	76.1983	-0.8840	0.2544	-3.4750	5.11E-04	0.0044
bioD	21.3015	-1.3725	0.4798	-2.8608	0.0042	0.0240
bisC	27.1451	-1.3302	0.4223	-3.1497	0.0016	0.0115
blC	5.3204	-3.4537	0.9086	-3.8014	1.44E-04	0.0015
bolA	69.1033	-1.6168	0.4052	-3.9898	6.61E-05	8.14E-04
borD	160.1467	4.3283	0.7282	5.9442	2.78E-09	1.07E-07
brnQ	57.9731	1.1600	0.3127	3.7092	2.08E-04	0.0021
bssS	249.8527	3.0840	0.5183	5.9504	2.67E-09	1.05E-07
btuE	26.0777	-3.9049	0.6657	-5.8658	4.47E-09	1.69E-07

caN	233.1977	-1.7835	0.3495	-5.1024	3.35E-07	8.57E-06
cbpA	12.9718	-2.5103	0.7760	-3.2349	0.0012	0.0090
cfA	92.6151	-2.9646	0.7090	-4.1813	2.90E-05	4.15E-04
chaA	1801.5463	5.6241	0.5480	10.2627	1.04E-24	3.83E-22
chaB	6.5901	-2.6977	0.6917	-3.8999	9.62E-05	0.0011
clpB	2232.3087	3.9529	0.4212	9.3839	6.36E-21	1.17E-18
clpP	171.4154	0.8994	0.2623	3.4292	6.05E-04	0.0050
clpX	374.5339	0.6566	0.2247	2.9218	0.0035	0.0206
clsB	5.2879	-3.5090	0.7669	-4.5754	4.75E-06	8.63E-05
cohE	49.8958	1.4862	0.4730	3.1418	0.0017	0.0117
cpxP	1421.5659	4.7910	0.5535	8.6565	4.87E-18	7.70E-16
cpxR	112.4011	0.9712	0.2672	3.6349	2.78E-04	0.0027
creC	30.7791	-3.0649	0.8517	-3.5986	3.20E-04	0.0030
crfC	12.7291	-3.8763	0.9505	-4.0781	4.54E-05	5.96E-04
csgE	3.8345	-5.4013	1.0416	-5.1857	2.15E-07	5.72E-06
csgF	2.5030	-4.9121	1.0978	-4.4746	7.65E-06	1.32E-04
csgG	9.4775	-1.8981	0.5296	-3.5842	3.38E-04	0.0032
csiD	6.9070	-3.1506	0.6694	-4.7069	2.52E-06	5.10E-05
cspA	248.2614	3.2940	0.6315	5.2159	1.83E-07	4.98E-06
cstA	76.0891	0.7978	0.2562	3.1138	0.0018	0.0125
curA	14.8910	-2.3927	0.5711	-4.1898	2.79E-05	4.03E-04
cusA	25.5696	-1.9158	0.6484	-2.9545	0.0031	0.0191
cusS	19.6410	-2.1870	0.6294	-3.4750	5.11E-04	0.0044
cutC	91.8922	1.4989	0.3809	3.9355	8.30E-05	9.85E-04
cvpA	162.2143	2.3346	0.5130	4.5510	5.34E-06	9.49E-05
cysS	103.5158	1.1082	0.3396	3.2627	0.0011	0.0082
damX	85.7220	-1.5332	0.3583	-4.2786	1.88E-05	2.88E-04
dcP	74.4693	-1.3527	0.3644	-3.7117	2.06E-04	0.0021
dedA	74.3600	1.0846	0.2990	3.6272	2.86E-04	0.0028
degP	955.0686	4.4385	0.4658	9.5298	1.58E-21	3.49E-19
deoA	17.4026	-2.3624	0.6322	-3.7365	1.87E-04	0.0019
dgcZ	377.3155	4.9592	0.6642	7.4662	8.25E-14	7.75E-12
dkgA	5.7852	-2.8538	0.7274	-3.9235	8.73E-05	0.0010
dkgB	6.1448	-1.9676	0.6324	-3.1112	0.0019	0.0126
dlD	54.6736	-1.1191	0.3616	-3.0946	0.0020	0.0132
dnaA	326.3602	1.2175	0.3344	3.6413	2.71E-04	0.0027
dnaJ	361.8432	3.6944	0.3843	9.6129	7.05E-22	1.67E-19
dnaK	4429.9742	4.7606	0.2498	19.0550	5.98E-81	6.62E-78
dosC	11.2787	-2.8097	0.5184	-5.4203	5.95E-08	1.73E-06
dosP	9.2437	-2.8199	0.6968	-4.0471	5.19E-05	6.63E-04
dpS	168.7634	-2.9921	0.8863	-3.3761	7.35E-04	0.0059
dsbA	263.4807	2.8434	0.5901	4.8187	1.45E-06	3.16E-05
dtpB	9.4400	-3.0912	0.7612	-4.0608	4.89E-05	6.35E-04
eamA	22.4494	-1.4738	0.3826	-3.8518	1.17E-04	0.0013
ecnB	46.9753	-4.2008	0.8676	-4.8420	1.29E-06	2.89E-05
efeB	23.8871	-3.2446	0.6135	-5.2887	1.23E-07	3.53E-06
efeO	28.2223	-5.5898	0.7249	-7.7113	1.25E-14	1.29E-12
efeU	17.9876	-4.9964	0.6477	-7.7142	1.22E-14	1.29E-12
efeU	4.8893	-2.4470	0.7985	-3.0644	0.0022	0.0142
elaB	65.6709	-3.6448	0.9583	-3.8036	1.43E-04	0.0015
eptB	36.5605	2.3033	0.3836	6.0036	1.93E-09	8.11E-08
fabD	134.2225	-1.5230	0.5096	-2.9886	0.0028	0.0174
fabF	628.7953	1.3538	0.4530	2.9886	0.0028	0.0174

fadA	8.5909	1.6107	0.5542	2.9063	0.0037	0.0214
fbaB	58.4233	-2.8088	0.8282	-3.3915	6.95E-04	0.0057
fdhF	28.3324	2.1250	0.4837	4.3935	1.12E-05	1.79E-04
fdoG	78.0274	1.4645	0.2521	5.8094	6.27E-09	2.21E-07
fepE	3.6929	-3.1727	1.1242	-2.8221	0.0048	0.0265
fiU	98.2584	-2.6543	0.6468	-4.1038	4.06E-05	5.38E-04
fldB	35.8218	1.1083	0.3661	3.0278	0.0025	0.0158
fliD	5.7629	-3.8083	1.0190	-3.7374	1.86E-04	0.0019
folE	69.7526	-2.1159	0.4493	-4.7089	2.49E-06	5.08E-05
ftnB	71.9762	3.2956	0.5322	6.1927	5.91E-10	2.77E-08
ftsH	1021.4470	1.7748	0.2874	6.1743	6.65E-10	3.07E-08
ftsZ	167.4045	-0.5424	0.1916	-2.8309	0.0046	0.0260
fuR	153.7327	0.6739	0.2388	2.8220	0.0048	0.0265
fxsA	326.8943	3.1116	0.7308	4.2580	2.06E-05	3.10E-04
gabD	6.3291	-2.9525	0.7805	-3.7828	1.55E-04	0.0017
gabT	7.8461	-2.7155	0.5925	-4.5827	4.59E-06	8.42E-05
gadA	13.7680	-4.7198	0.9632	-4.9001	9.58E-07	2.19E-05
gadB	22.3374	-4.9729	0.8772	-5.6688	1.44E-08	4.78E-07
gadC	36.9329	-4.7214	0.5978	-7.8975	2.85E-15	3.64E-13
gadE	11.9782	-5.5936	1.0319	-5.4209	5.93E-08	1.73E-06
gadW	13.9756	-3.5531	0.7806	-4.5515	5.33E-06	9.49E-05
gadX	25.0536	-2.5322	0.8798	-2.8782	0.0040	0.0229
galM	78.6021	-1.3333	0.3089	-4.3157	1.59E-05	2.48E-04
gcD	39.4542	-2.7339	0.4752	-5.7535	8.74E-09	2.99E-07
gcvB	106.5418	2.9775	0.5659	5.2614	1.43E-07	3.99E-06
ggT	8.4322	-3.9850	0.6884	-5.7887	7.09E-09	2.45E-07
ghrB	48.7207	-2.5359	0.5003	-5.0688	4.00E-07	9.92E-06
glcA	6.4212	-1.8105	0.6137	-2.9502	0.0032	0.0192
glcB	12.4920	-1.4489	0.4931	-2.9385	0.0033	0.0198
glcC	20.7198	1.9291	0.4642	4.1556	3.24E-05	4.51E-04
glgA	37.2273	-1.4651	0.3836	-3.8195	1.34E-04	0.0015
glgB	100.2297	-1.5707	0.3903	-4.0246	5.71E-05	7.27E-04
glgC	34.1668	-1.4099	0.2870	-4.9129	8.97E-07	2.07E-05
glnE	32.4117	-0.9806	0.3209	-3.0558	0.0022	0.0146
glnU	15.7699	2.0735	0.6938	2.9886	0.0028	0.0174
glnV	8.1865	2.1454	0.7307	2.9359	0.0033	0.0199
glsA	7.2168	-3.7595	0.7376	-5.0967	3.46E-07	8.77E-06
gltA	849.7028	2.2302	0.4508	4.9472	7.53E-07	1.80E-05
gltP	55.4565	1.4477	0.4189	3.4555	5.49E-04	0.0046
gltW	221.4872	1.1714	0.3168	3.6981	2.17E-04	0.0022
glvC	2.4009	-3.1585	1.0092	-3.1296	0.0018	0.0120
glyV	106.6975	1.8090	0.6061	2.9846	0.0028	0.0176
glyX	25.3220	2.0741	0.5941	3.4909	4.81E-04	0.0042
gntP	22.1217	2.5673	0.6467	3.9697	7.20E-05	8.76E-04
gntX	33.5307	1.5998	0.4237	3.7763	1.59E-04	0.0017
gpH	21.1385	-1.9248	0.5497	-3.5017	4.62E-04	0.0041
gpsA	49.0238	-1.5889	0.3822	-4.1569	3.23E-05	4.51E-04
gpT	82.9911	1.2956	0.3962	3.2703	0.0011	0.0080
greA	63.9211	1.6067	0.5082	3.1618	0.0016	0.0111
groL	3826.4466	4.0478	0.4595	8.8098	1.25E-18	2.08E-16
groS	1062.6779	4.2353	0.2817	15.0330	4.47E-51	3.71E-48
grpE	1019.9289	3.0694	0.7251	4.2328	2.31E-05	3.42E-04
gsS	31.5094	-1.9176	0.3420	-5.6068	2.06E-08	6.58E-07

guaC	70.4250	-1.5555	0.3221	-4.8291	1.37E-06	3.02E-05
gyrA	360.5763	1.0026	0.3221	3.1130	0.0019	0.0126
hchA	16.7830	-3.1272	0.6471	-4.8323	1.35E-06	2.99E-05
hdeA	137.1506	-5.4500	0.7451	-7.3143	2.59E-13	2.20E-11
hdeB	67.1532	-6.3321	0.9684	-6.5390	6.20E-11	3.49E-09
hdeD	27.6560	-5.9963	0.9252	-6.4810	9.11E-11	4.88E-09
hemD	17.2744	-1.9936	0.6930	-2.8768	0.0040	0.0230
hemF	25.1717	1.4137	0.4940	2.8618	0.0042	0.0240
hemL	243.1335	1.3262	0.4213	3.1480	0.0016	0.0115
hflC	195.3413	1.4065	0.2163	6.5030	7.87E-11	4.29E-09
hflX	463.6176	1.7445	0.4205	4.1482	3.35E-05	4.56E-04
hhA	71.4556	2.5865	0.6326	4.0884	4.34E-05	5.73E-04
hisD	38.2602	1.5776	0.5279	2.9886	0.0028	0.0174
hisG	69.7516	2.0181	0.5730	3.5222	4.28E-04	0.0038
hisJ	231.7730	2.5810	0.5311	4.8598	1.17E-06	2.67E-05
hsdR	23.6117	-1.3328	0.4137	-3.2214	0.0013	0.0093
hslO	118.2126	2.4539	0.5766	4.2556	2.08E-05	3.12E-04
hslR	45.4486	3.9208	0.6383	6.1430	8.10E-10	3.59E-08
hslU	204.1247	2.6541	0.4103	6.4688	9.88E-11	5.21E-09
hslV	195.3605	4.3865	0.3130	14.0144	1.27E-44	8.46E-42
hspQ	587.3926	3.2390	0.7254	4.4652	8.00E-06	1.36E-04
htpG	1246.1117	2.7589	0.5977	4.6158	3.92E-06	7.39E-05
htpX	1656.5956	4.0868	0.4000	10.2171	1.66E-24	5.52E-22
ibpA	2628.8038	8.1180	0.4003	20.2780	2.01E-91	6.69E-88
ibpB	2288.1887	8.7671	0.4451	19.6980	2.24E-86	3.73E-83
ilvC	148.0484	-4.1080	0.9131	-4.4989	6.83E-06	1.19E-04
ilvH	18.7467	-1.6784	0.4738	-3.5428	3.96E-04	0.0036
ilvI	40.9462	-1.6349	0.5099	-3.2061	0.0013	0.0097
ilvN	19.4295	-2.6157	0.6834	-3.8274	1.30E-04	0.0014
infC	1722.1083	1.9106	0.5467	3.4949	4.74E-04	0.0042
insL1	52.1856	2.7377	0.3986	6.8686	6.49E-12	4.14E-10
insL1-1	24.6771	2.1791	0.5250	4.1505	3.32E-05	4.54E-04
intF	88.1297	2.5140	0.4289	5.8614	4.59E-09	1.71E-07
intS	18.4393	-2.6552	0.8187	-3.2432	0.0012	0.0087
ivY	75.3203	-1.6875	0.5605	-3.0109	0.0026	0.0165
katE	16.2156	-3.4583	0.5797	-5.9653	2.44E-09	9.89E-08
kcH	21.9150	-2.7562	0.7517	-3.6666	2.46E-04	0.0025
kdgK	29.8456	1.2897	0.3462	3.7257	1.95E-04	0.0020
kefC	7.2674	-1.9149	0.5647	-3.3909	6.97E-04	0.0057
kuP	14.6701	-1.7025	0.4070	-4.1826	2.88E-05	4.14E-04
ldcC	13.5788	-2.4792	0.5288	-4.6884	2.75E-06	5.48E-05
ldtC	180.0621	4.0799	0.6405	6.3699	1.89E-10	9.38E-09
ldtE	37.5237	-1.5978	0.4764	-3.3537	7.97E-04	0.0063
leuQ	13.1400	1.6772	0.5954	2.8167	0.0049	0.0269
lexA	70.2417	1.5482	0.4349	3.5598	3.71E-04	0.0034
lhgO	4.8458	-2.8020	0.7422	-3.7753	1.60E-04	0.0017
lipA	166.1518	1.5490	0.4305	3.5982	3.20E-04	0.0030
livJ	91.8910	-3.4324	0.5244	-6.5456	5.92E-11	3.39E-09
loN	1368.7973	1.9867	0.5053	3.9314	8.44E-05	9.98E-04
lpoA	31.4509	-1.3129	0.4228	-3.1053	0.0019	0.0128
lpoB	19.5541	-1.4822	0.4280	-3.4632	5.34E-04	0.0045
lptB	33.9022	-2.4667	0.7863	-3.1371	0.0017	0.0118
lpxD	164.8784	-0.7453	0.2236	-3.3327	8.60E-04	0.0067

lpxT	12.1432	1.6215	0.5736	2.8269	0.0047	0.0262
lrhA	125.6188	1.4814	0.3938	3.7614	1.69E-04	0.0018
lysA	14.5986	-2.4646	0.6085	-4.0503	5.11E-05	6.56E-04
lysP	223.6144	2.3180	0.4860	4.7694	1.85E-06	3.91E-05
lysQ	28.7330	1.7545	0.5605	3.1301	0.0017	0.0120
lysT	365.7474	1.5835	0.4127	3.8371	1.25E-04	0.0014
lysZ	133.0509	1.8473	0.4659	3.9650	7.34E-05	8.83E-04
macA	14.1422	-1.3372	0.4684	-2.8547	0.0043	0.0243
malI	16.3347	1.7291	0.4911	3.5211	4.30E-04	0.0038
malP	16.9295	-3.6823	0.7083	-5.1987	2.01E-07	5.38E-06
malT	136.2267	1.5668	0.3749	4.1789	2.93E-05	4.18E-04
mepM	46.7285	1.3314	0.3941	3.3783	7.29E-04	0.0059
metE	227.1578	-3.1913	0.4287	-7.4442	9.75E-14	8.75E-12
mfD	265.6321	1.2005	0.3319	3.6176	2.97E-04	0.0029
mglB	22.8025	2.0458	0.6022	3.3973	6.80E-04	0.0056
mgrB	76.3768	3.4142	0.6381	5.3504	8.77E-08	2.53E-06
mgrR	14.3310	2.4594	0.7450	3.3013	9.62E-04	0.0073
mgtA	2645.4046	3.8088	0.8771	4.3425	1.41E-05	2.23E-04
mgtL	469.5853	4.2003	0.7535	5.5744	2.48E-08	7.71E-07
miaA	1026.4875	2.7907	0.3930	7.1017	1.23E-12	9.17E-11
mipA	165.7631	1.6657	0.4955	3.3618	7.74E-04	0.0062
mlaF	108.2725	1.9771	0.4202	4.7053	2.54E-06	5.10E-05
mlC	82.6689	1.8951	0.2584	7.3346	2.22E-13	1.94E-11
mlrA	7.8020	-2.0196	0.6151	-3.2836	0.0010	0.0077
mltD	485.9148	1.2661	0.3509	3.6083	3.08E-04	0.0030
moaA	53.8765	-1.4341	0.4692	-3.0563	0.0022	0.0146
moaB	27.2209	-1.6642	0.3603	-4.6187	3.86E-06	7.33E-05
moaC	16.4231	-1.9510	0.4243	-4.5983	4.26E-06	7.95E-05
moaE	18.6211	-2.0545	0.4630	-4.4379	9.08E-06	1.51E-04
modF	27.9121	-1.7226	0.4481	-3.8444	1.21E-04	0.0014
mqsA	52.8469	1.9063	0.5355	3.5598	3.71E-04	0.0034
mqsR	62.2148	2.4670	0.4002	6.1636	7.11E-10	3.24E-08
mreB	224.6452	1.4354	0.4997	2.8728	0.0041	0.0232
mscL	59.2731	-1.8036	0.3210	-5.6178	1.93E-08	6.24E-07
mscS	211.0824	-1.6762	0.4271	-3.9245	8.69E-05	0.0010
msrB	98.6760	1.7736	0.5228	3.3925	6.93E-04	0.0057
msyB	26.0955	-3.2664	0.9023	-3.6202	2.94E-04	0.0029
mtlA	15.8921	-1.9294	0.5090	-3.7906	1.50E-04	0.0016
mtlD	20.5246	-1.3124	0.4494	-2.9203	0.0035	0.0206
murC	56.6153	-0.8637	0.2414	-3.5781	3.46E-04	0.0032
mutM	37.4293	2.3601	0.5004	4.7169	2.39E-06	4.91E-05
mzrA	29.7861	2.3060	0.5078	4.5412	5.59E-06	9.88E-05
nadA	61.1093	-1.2241	0.3017	-4.0578	4.95E-05	6.40E-04
nadR	28.4920	-1.4165	0.4412	-3.2108	0.0013	0.0096
narP	49.8583	1.6462	0.4520	3.6422	2.70E-04	0.0027
nhaA	443.8046	3.6680	0.2739	13.3930	6.64E-41	3.68E-38
nhaB	15.4050	-1.6279	0.4785	-3.4020	6.69E-04	0.0055
nhaR	80.6050	2.0583	0.2669	7.7121	1.24E-14	1.29E-12
nmpC	69.5198	1.7775	0.3614	4.9179	8.75E-07	2.03E-05
nnR	24.1333	-1.2506	0.3507	-3.5656	3.63E-04	0.0034
norR	22.9749	1.9290	0.5019	3.8434	1.21E-04	0.0014
nrdA	34.8821	-2.1731	0.4945	-4.3943	1.11E-05	1.79E-04
nrdF	32.8012	-1.6734	0.5179	-3.2314	0.0012	0.0090

nudC	15.8070	-2.1039	0.5069	-4.1505	3.32E-05	4.54E-04
nudE	112.4928	1.6865	0.4941	3.4134	6.42E-04	0.0053
nudF	21.5778	-1.4683	0.4726	-3.1071	0.0019	0.0127
ogT	7.3251	1.9641	0.6599	2.9765	0.0029	0.0180
ompF	876.5537	-1.8960	0.3386	-5.6001	2.14E-08	6.78E-07
opgB	110.2024	2.0451	0.2968	6.8908	5.55E-12	3.76E-10
opgD	101.9575	1.2553	0.2970	4.2271	2.37E-05	3.48E-04
osmB	562.2381	2.4827	0.6361	3.9029	9.50E-05	0.0011
osmE	71.8239	-2.3199	0.8028	-2.8898	0.0039	0.0224
osmF	9.1397	-2.9918	0.6510	-4.5956	4.31E-06	8.01E-05
osmY	82.3883	-3.4343	0.7357	-4.6680	3.04E-06	5.98E-05
otsA	28.8326	-2.7031	0.5664	-4.7723	1.82E-06	3.88E-05
otsB	14.5063	-3.2599	1.0127	-3.2189	0.0013	0.0094
parC	70.2432	0.8466	0.2992	2.8301	0.0047	0.0260
patA	46.9852	-3.4509	0.7798	-4.4252	9.63E-06	1.58E-04
pcK	84.6685	2.2892	0.3462	6.6120	3.79E-11	2.25E-09
pdhR	61.3035	1.0968	0.3252	3.3723	7.46E-04	0.0060
pdxH	33.2436	-1.9449	0.5114	-3.8031	1.43E-04	0.0015
pdxJ	33.1834	-1.1280	0.3171	-3.5569	3.75E-04	0.0034
pdxK	17.5108	-2.5753	0.5062	-5.0879	3.62E-07	9.04E-06
pdxY	18.9552	-1.5448	0.4821	-3.2040	0.0014	0.0097
pfkB	14.2034	-2.6734	0.5409	-4.9427	7.70E-07	1.82E-05
pflB	227.9401	-1.2146	0.2550	-4.7624	1.91E-06	4.02E-05
pfO	35.7367	-3.2056	0.5623	-5.7008	1.19E-08	4.00E-07
pgL	34.0496	-1.8864	0.5765	-3.2722	0.0011	0.0080
pheA	246.3539	-1.9512	0.5433	-3.5917	3.29E-04	0.0031
phoP	54.2082	1.0818	0.3440	3.1450	0.0017	0.0116
phR	8.9555	-1.9153	0.5716	-3.3509	8.05E-04	0.0064
potH	7.6819	-1.8204	0.6053	-3.0077	0.0026	0.0166
poxB	31.5305	-4.4354	0.5681	-7.8077	5.82E-15	7.16E-13
ppiA	96.9611	2.2158	0.5349	4.1426	3.43E-05	4.62E-04
prC	172.6114	-0.9229	0.2975	-3.1022	0.0019	0.0129
prkB	22.3715	-2.0704	0.6705	-3.0881	0.0020	0.0134
prpR	3.6931	-3.5822	0.8969	-3.9940	6.50E-05	8.05E-04
pspA	122.7713	3.8316	0.5747	6.6672	2.61E-11	1.63E-09
pspC	10.7286	2.1418	0.6066	3.5309	4.14E-04	0.0037
pspE	29.6213	2.7476	0.4870	5.6421	1.68E-08	5.52E-07
pspG	10.6075	2.7691	0.5864	4.7224	2.33E-06	4.81E-05
pssA	107.4887	-1.2676	0.3829	-3.3102	9.32E-04	0.0072
ptwF	4.2764	3.5263	0.9373	3.7620	1.69E-04	0.0018
purD	89.3002	1.5330	0.4919	3.1163	0.0018	0.0125
purF	166.8782	1.3098	0.3866	3.3884	7.03E-04	0.0057
purL	358.8707	1.3111	0.2945	4.4514	8.53E-06	1.42E-04
pykF	169.0487	-1.5657	0.3772	-4.1504	3.32E-05	4.54E-04
qorA	22.8718	-1.8556	0.4026	-4.6092	4.04E-06	7.58E-05
raiA	1468.4669	3.3942	0.4766	7.1223	1.06E-12	8.20E-11
rbsD	57.9053	2.7716	0.7154	3.8741	1.07E-04	0.0012
rclA	5.2196	-4.1215	0.8572	-4.8082	1.52E-06	3.29E-05
recD	58.5513	1.4411	0.3477	4.1442	3.41E-05	4.61E-04
relB	38.4067	2.1609	0.7139	3.0267	0.0025	0.0158
relE	49.1182	2.2227	0.6678	3.3286	8.73E-04	0.0068
rimM	1278.5966	2.2775	0.7466	3.0507	0.0023	0.0148
rlmE	495.6980	2.9488	0.6366	4.6321	3.62E-06	6.95E-05

rlmL	76.1451	1.1224	0.3539	3.1714	0.0015	0.0108
rluB	79.1984	1.0690	0.3641	2.9364	0.0033	0.0199
rnC	82.4497	1.0231	0.3553	2.8796	0.0040	0.0229
roxA	97.7697	0.6709	0.2320	2.8916	0.0038	0.0223
rpE	20.1052	-1.2988	0.4096	-3.1709	0.0015	0.0108
rplA	989.6979	1.5795	0.5135	3.0758	0.0021	0.0138
rplE	584.0206	1.5500	0.4467	3.4701	5.20E-04	0.0044
rplI	161.0359	1.3905	0.4322	3.2169	0.0013	0.0094
rplJ	1737.9112	2.6900	0.6457	4.1660	3.10E-05	4.40E-04
rplK	725.7552	1.5343	0.3428	4.4760	7.61E-06	1.32E-04
rplL	1328.8659	2.8566	0.7198	3.9688	7.22E-05	8.76E-04
rplN	948.1770	1.5896	0.5412	2.9373	0.0033	0.0199
rplO	460.2324	2.0290	0.4690	4.3260	1.52E-05	2.39E-04
rplQ	538.3331	1.3821	0.3103	4.4546	8.41E-06	1.42E-04
rplS	941.7046	2.3946	0.4417	5.4213	5.92E-08	1.73E-06
rplT	1854.3319	2.2431	0.6709	3.3436	8.27E-04	0.0065
rplU	694.1227	2.2547	0.6412	3.5165	4.37E-04	0.0039
rplX	279.3430	1.6633	0.4765	3.4908	4.82E-04	0.0042
rplY	238.6800	2.4807	0.5697	4.3545	1.33E-05	2.12E-04
rpmD	38.3253	1.5705	0.5323	2.9505	0.0032	0.0192
rpmE	1673.6222	3.4635	0.8050	4.3023	1.69E-05	2.62E-04
rpmH	319.6441	2.4253	0.6234	3.8904	1.00E-04	0.0011
rpmI	1269.4784	2.1174	0.6484	3.2656	0.0011	0.0081
rpmJ	216.9949	1.7409	0.3939	4.4197	9.89E-06	1.62E-04
rpoC	1031.6640	0.7507	0.2493	3.0116	0.0026	0.0165
rpoD	382.7254	1.1804	0.3298	3.5790	3.45E-04	0.0032
rpoH	651.0465	2.3574	0.4871	4.8394	1.30E-06	2.90E-05
rpsA	1727.8655	0.9059	0.2707	3.3469	8.17E-04	0.0064
rpsB	2435.6991	2.7879	0.3122	8.9294	4.28E-19	7.49E-17
rpsE	360.4873	1.2878	0.4025	3.1993	0.0014	0.0099
rpsK	399.5320	1.0360	0.3138	3.3012	9.63E-04	0.0073
rpsL	896.0547	1.7049	0.5902	2.8888	0.0039	0.0224
rpsM	736.0815	1.1728	0.3226	3.6356	2.77E-04	0.0027
rpsO	915.5335	2.3583	0.7091	3.3256	8.82E-04	0.0069
rpsP	680.3206	2.2925	0.7521	3.0479	0.0023	0.0149
rpsQ	222.7374	1.1692	0.3347	3.4931	4.77E-04	0.0042
rpsT	735.5870	0.9579	0.2897	3.3060	9.46E-04	0.0073
rpsU	1120.4577	2.0844	0.6970	2.9904	0.0028	0.0174
rrfH	481.5582	0.5733	0.1647	3.4811	4.99E-04	0.0043
rsmA	47.7250	-0.9088	0.3058	-2.9720	0.0030	0.0182
rsmB	40.4076	-3.0186	0.7517	-4.0158	5.92E-05	7.46E-04
rssA	24.3061	-1.2701	0.3323	-3.8220	1.32E-04	0.0014
rssB	34.6812	-2.5781	0.5812	-4.4360	9.16E-06	1.51E-04
rstA	78.7238	2.4852	0.3939	6.3088	2.81E-10	1.35E-08
rstB	49.9957	1.6816	0.3264	5.1520	2.58E-07	6.80E-06
sdaA	915.8868	4.9794	0.5112	9.7400	2.04E-22	5.20E-20
sdaB	36.4824	2.2628	0.5806	3.8976	9.72E-05	0.0011
sdaC	79.6355	2.8114	0.4815	5.8383	5.27E-09	1.90E-07
sdhA	163.4790	2.1716	0.2303	9.4277	4.19E-21	8.19E-19
sdhC	40.4426	2.4949	0.3862	6.4601	1.05E-10	5.43E-09
sdhD	12.0209	1.8881	0.4762	3.9650	7.34E-05	8.83E-04
secA	268.0939	0.8917	0.1879	4.7455	2.08E-06	4.32E-05
secD	237.1383	0.8941	0.2946	3.0352	0.0024	0.0154

secF	147.6545	1.2133	0.2915	4.1616	3.16E-05	4.45E-04
secY	2531.8522	1.8978	0.4419	4.2943	1.75E-05	2.71E-04
serC	341.2322	-1.4335	0.4000	-3.5835	3.39E-04	0.0032
skP	88.0796	-1.9084	0.3127	-6.1035	1.04E-09	4.53E-08
slyB	1218.0733	2.7060	0.8384	3.2276	0.0012	0.0091
solA	29.9008	-1.2396	0.3766	-3.2914	9.97E-04	0.0076
soxS	141.8499	4.4699	0.5932	7.5358	4.85E-14	4.89E-12
spY	192.9851	4.3426	0.6116	7.1007	1.24E-12	9.17E-11
srkA	172.5376	3.0879	0.6937	4.4515	8.53E-06	1.42E-04
stpA	34.3891	-2.8952	0.5842	-4.9555	7.21E-07	1.75E-05
sucA	145.3545	1.7089	0.3346	5.1069	3.27E-07	8.50E-06
sucC	101.5568	1.2129	0.2403	5.0467	4.50E-07	1.11E-05
sucD	95.9486	1.6809	0.5140	3.2704	0.0011	0.0080
sufD	46.5605	-1.3412	0.4342	-3.0889	0.0020	0.0133
talA	29.3545	-3.9573	0.5942	-6.6594	2.75E-11	1.66E-09
taM	5.8417	-2.3199	0.8179	-2.8365	0.0046	0.0256
taS	30.8528	-1.2398	0.4024	-3.0811	0.0021	0.0136
tehA	20.2298	-2.2278	0.7262	-3.0677	0.0022	0.0141
tesA	129.9320	3.3913	0.5175	6.5539	5.61E-11	3.27E-09
tff	461.2490	2.1899	0.4783	4.5786	4.68E-06	8.54E-05
tgT	433.9771	1.8580	0.6404	2.9012	0.0037	0.0217
thiE	48.9052	-1.6321	0.5313	-3.0719	0.0021	0.0140
tisB	25.5485	1.4753	0.5033	2.9311	0.0034	0.0201
tktA	233.7299	0.7158	0.2132	3.3574	7.87E-04	0.0063
tktB	27.8268	-3.8122	0.6524	-5.8436	5.11E-09	1.86E-07
tmcA	23.8815	-2.0208	0.5049	-4.0023	6.27E-05	7.83E-04
tolC	313.8664	0.8572	0.2874	2.9827	0.0029	0.0176
tomB	155.9341	3.2497	0.4500	7.2223	5.11E-13	4.24E-11
torR	15.8675	1.7496	0.5161	3.3901	6.99E-04	0.0057
tpiA	134.7403	-1.3770	0.4399	-3.1301	0.0017	0.0120
treA	5.4964	-1.8561	0.6347	-2.9245	0.0035	0.0204
treF	7.8897	-1.8202	0.5796	-3.1402	0.0017	0.0117
trkA	43.1615	-2.0650	0.5197	-3.9734	7.09E-05	8.65E-04
trmD	1521.8933	2.1810	0.7572	2.8803	0.0040	0.0229
trmJ	112.1810	1.9811	0.6126	3.2341	0.0012	0.0090
trpA	37.5440	-2.2001	0.5229	-4.2079	2.58E-05	3.76E-04
trpB	65.0196	-3.0566	0.4382	-6.9747	3.06E-12	2.12E-10
trpC	79.8260	-2.5050	0.3060	-8.1861	2.70E-16	3.90E-14
trpD	93.9514	-2.2253	0.5210	-4.2709	1.95E-05	2.95E-04
trpE	44.5957	-2.6175	0.5653	-4.6306	3.65E-06	6.96E-05
tsF	1040.8905	2.5201	0.3101	8.1266	4.42E-16	6.11E-14
tusB	65.6765	1.6360	0.5567	2.9390	0.0033	0.0198
tyrA	233.6352	-3.4922	0.6206	-5.6270	1.83E-08	5.97E-07
tyrB	37.0635	-1.7660	0.5497	-3.2125	0.0013	0.0095
tyrU	95.3600	1.5703	0.5141	3.0547	0.0023	0.0146
ugpA	4.2437	-3.9530	1.0992	-3.5964	3.23E-04	0.0030
ugpB	28.6655	-3.5014	0.7622	-4.5936	4.36E-06	8.04E-05
uhpT	3.2567	-2.6262	0.9224	-2.8472	0.0044	0.0247
uspB	17.1986	-1.8755	0.6305	-2.9744	0.0029	0.0181
uspC	10.3256	-2.2616	0.7903	-2.8617	0.0042	0.0240
uspG	39.7580	2.0675	0.5237	3.9476	7.89E-05	9.47E-04
uvrC	52.0899	-1.3393	0.4255	-3.1476	0.0016	0.0115
uxuB	31.2835	1.9256	0.6281	3.0659	0.0022	0.0142

uxuR	41.8549	1.6842	0.4670	3.6064	3.10E-04	0.0030
valT	70.5103	1.4847	0.4455	3.3322	8.62E-04	0.0067
waaF	20.6549	-1.1886	0.3523	-3.3743	7.40E-04	0.0060
wrbA	44.8201	-3.9028	0.7490	-5.2109	1.88E-07	5.08E-06
wzyE	6.2299	-2.3201	0.8119	-2.8576	0.0043	0.0241
xerC	12.7019	-1.6645	0.4784	-3.4789	5.04E-04	0.0043
yabI	31.2726	1.2972	0.3662	3.5421	3.97E-04	0.0036
yaeH	38.1982	-1.3291	0.4614	-2.8803	0.0040	0.0229
yagI	58.1086	2.7108	0.4153	6.5270	6.71E-11	3.71E-09
yagP	5.3761	2.2894	0.7953	2.8786	0.0040	0.0229
yagU	20.4831	-3.6704	0.8490	-4.3229	1.54E-05	2.41E-04
yahK	13.5970	-3.8292	0.7318	-5.2330	1.67E-07	4.58E-06
yajC	258.7349	2.2502	0.5415	4.1555	3.25E-05	4.51E-04
yajO	30.0130	-1.6146	0.3538	-4.5633	5.04E-06	9.04E-05
ybaL	102.3186	1.5994	0.3578	4.4703	7.81E-06	1.34E-04
ybaP	12.4493	-1.9819	0.5970	-3.3197	9.01E-04	0.0070
ybaT	16.0154	-3.5657	0.6095	-5.8498	4.92E-09	1.82E-07
ybaY	45.0979	-2.9122	0.7246	-4.0190	5.84E-05	7.38E-04
ybbA	52.1729	3.0557	0.5472	5.5837	2.35E-08	7.38E-07
ybbN	319.6311	2.6260	0.3266	8.0405	8.95E-16	1.19E-13
ybbP	76.0252	2.5957	0.4519	5.7440	9.25E-09	3.13E-07
ybdK	5.1376	-2.5549	0.7366	-3.4685	5.23E-04	0.0044
ybdR	6.9474	-2.8954	0.7000	-4.1365	3.53E-05	4.72E-04
ybeD	470.5137	3.7813	0.3328	11.3635	6.36E-30	3.02E-27
ybeY	50.7290	1.3880	0.4312	3.2191	0.0013	0.0094
ybeZ	251.9548	2.1937	0.2812	7.8014	6.12E-15	7.26E-13
ybfA	192.1723	2.4224	0.7973	3.0383	0.0024	0.0153
ybgA	4.7709	-2.7440	0.7881	-3.4819	4.98E-04	0.0043
ybhB	34.7242	-1.5201	0.3904	-3.8934	9.89E-05	0.0011
ybhP	5.2777	-3.9740	0.8253	-4.8155	1.47E-06	3.19E-05
ybiB	25.7281	-2.1255	0.5166	-4.1142	3.89E-05	5.16E-04
ybiC	74.6027	-1.8701	0.5734	-3.2616	0.0011	0.0082
ybiI	4.8606	-2.2699	0.6654	-3.4114	6.46E-04	0.0054
ybiJ	7.0377	-2.0517	0.5922	-3.4646	5.31E-04	0.0045
ybiU	15.2303	-2.1158	0.5280	-4.0074	6.14E-05	7.69E-04
ybiX	19.4367	-2.4524	0.6920	-3.5437	3.95E-04	0.0036
ybjG	109.4191	3.2444	0.6158	5.2688	1.37E-07	3.87E-06
ybjP	19.3429	-1.8806	0.5396	-3.4848	4.93E-04	0.0043
ybjX	252.3540	3.1991	0.3164	10.1095	5.01E-24	1.47E-21
ycaC	17.7904	-3.8808	0.8312	-4.6692	3.02E-06	5.98E-05
yccA	1014.4862	3.2055	0.7008	4.5742	4.78E-06	8.63E-05
yccE	3.2944	-2.9030	1.0291	-2.8209	0.0048	0.0266
yccJ	16.4828	-3.5622	0.6413	-5.5549	2.78E-08	8.54E-07
yccU	19.0161	-1.3362	0.3653	-3.6579	2.54E-04	0.0026
yceD	1019.2731	2.1216	0.5868	3.6155	3.00E-04	0.0029
yceI	63.7748	2.3115	0.6056	3.8166	1.35E-04	0.0015
yceK	8.8197	-3.3213	0.9466	-3.5085	4.51E-04	0.0040
ycfJ	245.2190	3.2341	0.6514	4.9645	6.89E-07	1.68E-05
ycfP	23.0595	-1.5659	0.4283	-3.6559	2.56E-04	0.0026
ycgB	21.2682	-3.7376	0.4437	-8.4244	3.63E-17	5.48E-15
ycgX	3.5970	-3.0728	1.0403	-2.9538	0.0031	0.0191
ychF	94.1521	1.0594	0.3632	2.9165	0.0035	0.0208
yciB	50.9651	2.1085	0.4010	5.2575	1.46E-07	4.04E-06

yciC	85.1343	1.9160	0.2727	7.0261	2.12E-12	1.50E-10
yciE	6.7506	-2.5075	0.7207	-3.4792	5.03E-04	0.0043
yciF	6.2061	-4.6096	0.9032	-5.1034	3.34E-07	8.57E-06
yciG	6.5057	-5.6051	0.9395	-5.9658	2.43E-09	9.89E-08
yciM	155.8727	1.3565	0.2465	5.5022	3.75E-08	1.13E-06
yciS	91.9568	2.0110	0.4694	4.2846	1.83E-05	2.82E-04
ycjX	259.0368	3.2567	0.4539	7.1745	7.26E-13	5.88E-11
ydaM	23.4328	-1.8454	0.3866	-4.7734	1.81E-06	3.88E-05
ydcK	9.4092	-3.0745	0.6607	-4.6534	3.27E-06	6.34E-05
ydcP	146.5753	2.4978	0.4102	6.0896	1.13E-09	4.88E-08
ydeP	28.8260	2.0199	0.4726	4.2744	1.92E-05	2.92E-04
ydeT	25.7932	2.6174	0.8647	3.0270	0.0025	0.0158
ydfV	7.7825	-2.7119	0.9013	-3.0088	0.0026	0.0166
ydgJ	46.0393	-1.1312	0.3438	-3.2904	0.0010	0.0076
ydhK	14.9531	-2.3072	0.7408	-3.1143	0.0018	0.0125
ydhL	4.6288	-2.2698	0.7703	-2.9465	0.0032	0.0194
ydhP	14.3599	-3.0801	0.7966	-3.8665	1.10E-04	0.0013
ydhS	9.8139	-2.2087	0.7006	-3.1525	0.0016	0.0114
ydhZ	10.4602	-2.3166	0.6443	-3.5953	3.24E-04	0.0030
ydiV	10.0829	-2.2962	0.6568	-3.4958	4.73E-04	0.0042
ydiZ	9.2429	-2.7702	0.7073	-3.9165	8.98E-05	0.0010
ydjF	24.5052	2.2403	0.5569	4.0230	5.75E-05	7.29E-04
yeaG	33.5109	-3.5657	0.5982	-5.9603	2.52E-09	1.01E-07
yeaH	6.9906	-3.0390	0.8355	-3.6372	2.76E-04	0.0027
yeaQ	37.0583	-2.9894	0.8214	-3.6392	2.73E-04	0.0027
yebE	453.8967	5.9418	0.5247	11.3243	9.94E-30	4.13E-27
yebO	136.0702	3.4312	0.6739	5.0913	3.56E-07	8.95E-06
yebT	44.6916	-2.6883	0.6392	-4.2056	2.60E-05	3.78E-04
yebV	44.8998	-4.1199	0.9409	-4.3785	1.19E-05	1.91E-04
yecS	7.8854	-2.8039	0.8540	-3.2832	0.0010	0.0077
yedE	23.5953	1.7220	0.4722	3.6465	2.66E-04	0.0027
yedP	9.4258	-2.0785	0.7026	-2.9581	0.0031	0.0189
yegE	23.3014	-1.1953	0.3596	-3.3237	8.88E-04	0.0069
yegH	18.6296	-2.4508	0.5944	-4.1229	3.74E-05	4.99E-04
yegP	20.7107	-3.3704	0.8477	-3.9760	7.01E-05	8.59E-04
yegS	11.6160	-2.7071	0.7385	-3.6658	2.47E-04	0.0025
yegX	12.3334	-2.4042	0.7590	-3.1677	0.0015	0.0109
yehE	8.5579	-3.2387	0.6955	-4.6565	3.22E-06	6.28E-05
yehW	4.0478	-2.6111	0.7525	-3.4697	5.21E-04	0.0044
yehX	6.5175	-4.0046	0.8640	-4.6349	3.57E-06	6.90E-05
yehY	4.6885	-2.6849	0.7567	-3.5482	3.88E-04	0.0035
yeiB	20.5481	-2.6707	0.7633	-3.4987	4.68E-04	0.0041
yejG	166.5280	2.8891	0.6424	4.4973	6.88E-06	1.20E-04
yejM	59.0550	0.9160	0.3033	3.0201	0.0025	0.0161
yfcF	9.1713	-2.7892	0.5643	-4.9430	7.69E-07	1.82E-05
yfcG	4.8794	-2.6132	0.7615	-3.4318	6.00E-04	0.0050
yfdC	8.2723	-2.4331	0.7637	-3.1858	0.0014	0.0103
yfeY	34.9789	0.8895	0.3081	2.8870	0.0039	0.0225
yfjK	19.2509	-1.4403	0.4362	-3.3021	9.60E-04	0.0073
ygaM	48.6382	-2.1667	0.5107	-4.2424	2.21E-05	3.29E-04
ygaY	11.9745	-2.6735	0.9348	-2.8601	0.0042	0.0240
ygdR	66.5415	1.6336	0.5467	2.9882	0.0028	0.0174
yggE	115.9607	-2.3787	0.6210	-3.8303	1.28E-04	0.0014

yggI	4.9260	-2.5982	0.8871	-2.9288	0.0034	0.0202
yggR	2.9910	-3.1936	1.0466	-3.0515	0.0023	0.0147
yghA	35.1465	-4.8476	0.8742	-5.5453	2.93E-08	8.94E-07
yghX	5.3086	-3.2697	0.7344	-4.4523	8.49E-06	1.42E-04
yghX	4.1335	-3.0957	0.8956	-3.4567	5.47E-04	0.0046
ygiB	107.7206	1.8765	0.4809	3.9017	9.55E-05	0.0011
ygiC	129.2387	1.7361	0.2523	6.8822	5.89E-12	3.92E-10
ygiM	45.1855	1.4847	0.3719	3.9927	6.53E-05	8.07E-04
yhbO	7.3121	-3.6612	1.0128	-3.6148	3.01E-04	0.0029
yhbW	7.9043	-2.8447	0.5747	-4.9498	7.43E-07	1.79E-05
yhcO	3.1886	-3.0633	1.0525	-2.9105	0.0036	0.0212
yheO	55.7899	-1.8800	0.6273	-2.9969	0.0027	0.0172
yheT	23.5891	-2.5973	0.7710	-3.3690	7.55E-04	0.0060
yhgF	26.7321	-1.0138	0.3615	-2.8045	0.0050	0.0279
yhiD	10.0077	-6.4340	1.0603	-6.0679	1.30E-09	5.52E-08
yhiM	6.2320	-3.6309	0.8063	-4.5033	6.69E-06	1.18E-04
yhjD	13.2136	-2.0891	0.6199	-3.3702	7.51E-04	0.0060
yhjG	9.5988	-2.9179	0.5530	-5.2767	1.32E-07	3.73E-06
yhjY	8.7726	-2.2962	0.5989	-3.8341	1.26E-04	0.0014
yibB	12.6421	-1.8033	0.5990	-3.0104	0.0026	0.0165
yibH	4.2174	-2.5780	0.8224	-3.1346	0.0017	0.0119
yicR	74.9785	1.2407	0.4347	2.8540	0.0043	0.0243
yidB	9.4343	-1.5931	0.5079	-3.1363	0.0017	0.0118
yigB	10.9073	-1.6188	0.5239	-3.0901	0.0020	0.0133
yiiM	15.9205	-1.8512	0.6190	-2.9905	0.0028	0.0174
yiiX	29.1367	1.7213	0.5764	2.9865	0.0028	0.0175
yijD	23.1787	1.7781	0.4927	3.6087	3.08E-04	0.0030
yjdC	15.1203	-1.7508	0.4810	-3.6396	2.73E-04	0.0027
yjdJ	2.6656	-3.0958	0.9227	-3.3551	7.93E-04	0.0063
yjdM	19.8612	1.8622	0.4491	4.1467	3.37E-05	4.57E-04
yjfN	68.1073	4.2591	0.7319	5.8189	5.92E-09	2.12E-07
yjfY	4.1578	-2.6998	0.8169	-3.3049	9.50E-04	0.0073
yjgH	4.4487	-3.8318	0.8682	-4.4135	1.02E-05	1.65E-04
yjgR	10.2843	-2.3561	0.5527	-4.2628	2.02E-05	3.05E-04
ylaB	11.9524	-1.9575	0.5703	-3.4324	5.98E-04	0.0050
yliI	11.3204	-2.9867	0.9129	-3.2716	0.0011	0.0080
ymgE	2.2580	-3.4035	0.9633	-3.5331	4.11E-04	0.0037
ynaJ	118.8299	1.0892	0.3525	3.0899	0.0020	0.0133
yncI	2.4659	-3.2070	1.0925	-2.9355	0.0033	0.0199
yncJ	186.8641	6.1862	0.6553	9.4404	3.71E-21	7.71E-19
yncL	8.2749	-2.5415	0.6773	-3.7522	1.75E-04	0.0018
yneK	3.7327	-4.0354	1.0916	-3.6969	2.18E-04	0.0022
yneM	4197.2269	5.1921	0.9545	5.4394	5.34E-08	1.60E-06
ynfD	42.7537	2.9449	0.6964	4.2285	2.35E-05	3.47E-04
yoaC	5.8583	-2.4548	0.6733	-3.6461	2.66E-04	0.0027
yobB	92.1889	3.3130	0.3279	10.1037	5.32E-24	1.47E-21
yodD	5.4371	-2.8319	0.8846	-3.2015	0.0014	0.0098
yohF	5.4090	-2.2892	0.6990	-3.2752	0.0011	0.0079
yohK	7.8111	-1.8163	0.6119	-2.9685	0.0030	0.0183
ypfJ	32.9984	-2.3049	0.6485	-3.5544	3.79E-04	0.0035
yqaA	32.7406	-2.3000	0.7351	-3.1287	0.0018	0.0120
yqaE	80.4429	2.3879	0.8267	2.8884	0.0039	0.0224
yqeF	24.3647	2.2033	0.4541	4.8522	1.22E-06	2.76E-05

yqjG	10.8148	-1.8506	0.6145	-3.0117	0.0026	0.0165
yqjI	42.2741	2.5782	0.4037	6.3865	1.70E-10	8.54E-09
yrbN	15.3361	2.3078	0.6952	3.3197	9.01E-04	0.0070
yrfG	93.6013	1.9923	0.4716	4.2250	2.39E-05	3.50E-04
ytfE	15.0410	1.7793	0.5618	3.1671	0.0015	0.0109
ytfK	276.7519	2.6204	0.6308	4.1541	3.27E-05	4.52E-04
ytjA	24.2736	-3.9203	0.7645	-5.1278	2.93E-07	7.67E-06
zitB	20.8477	-1.8269	0.6412	-2.8493	0.0044	0.0246
znuA	31.7726	1.5340	0.3774	4.0652	4.80E-05	6.28E-04

t=60 vs t=0 (p<0.005)

Gene	BaseMean	log$_2$ Fold Change	lfcSE	stat	*p*-value	padj
aaS	29.1386	-1.0740	0.3287	-3.2677	0.0011	0.0068
aceB	324.6456	-1.5863	0.3339	-4.7511	2.02E-06	3.33E-05
ackA	180.3401	1.8232	0.4962	3.6746	2.38E-04	0.0020
acnA	50.2069	-1.6997	0.3756	-4.5251	6.04E-06	8.39E-05
acuI	21.3695	-2.2714	0.6228	-3.6471	2.65E-04	0.0021
adhE	103.0873	-1.5586	0.3756	-4.1499	3.33E-05	3.74E-04
adhP	21.8856	-5.0768	0.7160	-7.0904	1.34E-12	8.67E-11
ahR	11.7657	-3.7012	0.6747	-5.4853	4.13E-08	1.13E-06
aidB	12.8906	-3.7221	0.6593	-5.6453	1.65E-08	4.98E-07
alaW	17.7307	1.7110	0.5408	3.1639	0.0016	0.0089
aldB	4.6081	-2.6303	0.7915	-3.3233	8.89E-04	0.0058
amiA	71.2954	2.5240	0.5710	4.4204	9.85E-06	1.28E-04
amN	38.1308	-1.3678	0.4771	-2.8670	0.0041	0.0201
amyA	20.9495	-2.3006	0.5230	-4.3990	1.09E-05	1.39E-04
ansP	20.1247	1.7254	0.5375	3.2101	0.0013	0.0079
appA	5.3693	-2.4563	0.8676	-2.8312	0.0046	0.0219
araC	58.0605	1.7761	0.3453	5.1433	2.70E-07	5.86E-06
araE	13.5140	1.5760	0.4829	3.2635	0.0011	0.0069
argA	573.4813	3.4021	0.5808	5.8582	4.68E-09	1.60E-07
argB	162.2474	3.2154	0.5569	5.7736	7.76E-09	2.60E-07
argC	544.7538	3.8448	0.5842	6.5812	4.67E-11	2.42E-09
argD	192.4090	1.7954	0.5298	3.3885	7.03E-04	0.0047
argE	353.4858	2.7839	0.5436	5.1212	3.04E-07	6.42E-06
argF	224.6939	3.9951	0.5527	7.2288	4.87E-13	3.53E-11
argG	1067.2312	3.2729	0.8369	3.9108	9.20E-05	8.47E-04
argH	337.7552	3.3061	0.4572	7.2307	4.80E-13	3.53E-11
argI	190.4276	3.8960	0.5556	7.0129	2.33E-12	1.45E-10
argV	34.7314	1.7284	0.6141	2.8143	0.0049	0.0228
argY	93.3163	2.0142	0.4958	4.0624	4.86E-05	5.11E-04
argZ	51.3680	2.1301	0.4376	4.8681	1.13E-06	1.97E-05
arnB	4.6883	-2.2729	0.8019	-2.8344	0.0046	0.0217
aroA	53.5643	-2.1902	0.5294	-4.1375	3.51E-05	3.92E-04
aroE	25.3601	-2.3313	0.6346	-3.6736	2.39E-04	0.0020
aroG	327.2786	-2.3689	0.5928	-3.9964	6.43E-05	6.42E-04
aroP	109.3223	-2.4747	0.4205	-5.8846	3.99E-09	1.40E-07
artI	110.0126	1.5370	0.4516	3.4031	6.66E-04	0.0045
artJ	890.1429	3.9064	0.6477	6.0308	1.63E-09	6.27E-08
artM	35.3219	1.1772	0.3745	3.1431	0.0017	0.0094
artP	88.3271	1.2714	0.4151	3.0626	0.0022	0.0117

asnA	115.8790	2.6975	0.5971	4.5180	6.24E-06	8.60E-05
asnS	451.7534	0.7361	0.2040	3.6077	3.09E-04	0.0024
aspS	118.8384	1.1250	0.3583	3.1397	0.0017	0.0095
aspV	26.4039	1.5580	0.4749	3.2809	0.0010	0.0065
atpC	164.2234	1.0782	0.3039	3.5476	3.89E-04	0.0029
atpI	91.8862	1.4934	0.5081	2.9390	0.0033	0.0165
bcsC	14.9794	-2.0828	0.5291	-3.9365	8.27E-05	7.80E-04
bcsE	26.5329	-2.0692	0.4691	-4.4110	1.03E-05	1.33E-04
bcsG	11.9896	-2.9624	0.5823	-5.0875	3.63E-07	7.46E-06
betA	31.8390	1.3765	0.3854	3.5712	3.55E-04	0.0027
betB	76.5106	1.9801	0.4639	4.2681	1.97E-05	2.37E-04
betI	65.5681	2.2162	0.4295	5.1597	2.47E-07	5.42E-06
betT	75.8656	2.1108	0.3817	5.5302	3.20E-08	9.14E-07
bioB	76.1983	-1.0607	0.2684	-3.9515	7.77E-05	7.44E-04
bisC	27.1451	-1.8418	0.4561	-4.0386	5.38E-05	5.56E-04
bolA	69.1033	-1.6975	0.4152	-4.0880	4.35E-05	4.65E-04
borD	160.1467	3.9051	0.7293	5.3543	8.59E-08	2.14E-06
brnQ	57.9731	1.2651	0.3204	3.9478	7.89E-05	7.51E-04
bssS	249.8527	3.9152	0.5183	7.5542	4.22E-14	3.45E-12
btuE	26.0777	-3.3949	0.6761	-5.0211	5.14E-07	9.99E-06
caN	233.1977	-2.1859	0.3555	-6.1490	7.80E-10	3.32E-08
cfA	92.6151	-2.7810	0.7135	-3.8974	9.72E-05	8.90E-04
chaA	1801.5463	5.3100	0.5482	9.6868	3.43E-22	5.62E-20
chaB	6.5901	-2.1946	0.7079	-3.1003	0.0019	0.0106
clpB	2232.3087	4.6582	0.4213	11.0574	2.02E-28	7.86E-26
clpP	171.4154	1.5791	0.2630	6.0049	1.91E-09	7.27E-08
clpX	374.5339	1.1973	0.2255	5.3089	1.10E-07	2.62E-06
clsB	5.2879	-3.9439	0.8794	-4.4847	7.30E-06	9.80E-05
cohE	49.8958	1.4859	0.4794	3.0993	0.0019	0.0107
corA	48.9412	1.6101	0.5673	2.8381	0.0045	0.0215
cpxP	1421.5659	4.6559	0.5537	8.4094	4.12E-17	4.75E-15
crfC	12.7291	-3.3274	0.9580	-3.4733	5.14E-04	0.0036
csgE	3.8345	-4.2457	1.0091	-4.2074	2.58E-05	3.00E-04
csiD	6.9070	-3.6652	0.7860	-4.6633	3.11E-06	4.73E-05
cspA	248.2614	3.9923	0.6317	6.3203	2.61E-10	1.25E-08
curA	14.8910	-2.6430	0.6153	-4.2955	1.74E-05	2.12E-04
cusS	19.6410	-2.6078	0.6643	-3.9254	8.66E-05	8.10E-04
cutC	91.8922	1.6797	0.3843	4.3710	1.24E-05	1.57E-04
cvpA	162.2143	2.6428	0.5139	5.1426	2.71E-07	5.86E-06
cysS	103.5158	1.2166	0.3435	3.5419	3.97E-04	0.0029
dacB	8.1085	-2.3123	0.8014	-2.8851	0.0039	0.0191
daM	31.9288	-1.4573	0.5024	-2.9004	0.0037	0.0183
damX	85.7220	-1.7360	0.3701	-4.6913	2.71E-06	4.29E-05
dapB	67.5693	-1.2634	0.4033	-3.1326	0.0017	0.0097
dapD	282.6125	-0.9853	0.3151	-3.1271	0.0018	0.0099
dcP	74.4693	-1.4892	0.3755	-3.9658	7.31E-05	7.07E-04
deaD	786.2489	2.2533	0.5427	4.1520	3.30E-05	3.72E-04
dedA	74.3600	1.7664	0.3002	5.8838	4.01E-09	1.40E-07
degP	955.0686	4.4076	0.4660	9.4573	3.16E-21	4.92E-19
degS	48.0690	-2.5155	0.7530	-3.3405	8.36E-04	0.0055
deoA	17.4026	-2.2806	0.6543	-3.4856	4.91E-04	0.0035
dgcZ	377.3155	4.7835	0.6647	7.1963	6.19E-13	4.31E-11
dkgA	5.7852	-2.4729	0.7530	-3.2839	0.0010	0.0065

dkgB	6.1448	-2.3665	0.7159	-3.3058	9.47E-04	0.0061
dlD	54.6736	-1.1872	0.3745	-3.1703	0.0015	0.0088
dnaA	326.3602	1.5056	0.3353	4.4902	7.12E-06	9.63E-05
dnaG	131.8946	1.4363	0.2841	5.0555	4.29E-07	8.57E-06
dnaJ	361.8432	4.0048	0.3849	10.4038	2.38E-25	6.18E-23
dnaK	4429.9742	5.1382	0.2499	20.5600	6.26E-94	1.95E-90
dosC	11.2787	-2.4338	0.5430	-4.4822	7.39E-06	9.87E-05
dosP	9.2437	-2.2979	0.7097	-3.2378	0.0012	0.0074
dpS	168.7634	-3.2966	0.8893	-3.7068	2.10E-04	0.0018
dsbA	263.4807	2.7255	0.5910	4.6119	3.99E-06	5.78E-05
dtpB	9.4400	-2.4775	0.7689	-3.2223	0.0013	0.0077
eamA	22.4494	-1.5019	0.4101	-3.6619	2.50E-04	0.0020
ecnB	46.9753	-4.9740	0.9045	-5.4989	3.82E-08	1.06E-06
efeB	23.8871	-3.1962	0.6410	-4.9867	6.14E-07	1.16E-05
efeO	28.2223	-4.2119	0.6813	-6.1826	6.31E-10	2.73E-08
efeU	17.9876	-2.7568	0.5274	-5.2272	1.72E-07	3.94E-06
efeU	4.8893	-2.8939	0.8764	-3.3022	9.59E-04	0.0062
elaB	65.6709	-4.2186	0.9704	-4.3471	1.38E-05	1.72E-04
envZ	9.6134	-1.6111	0.5521	-2.9183	0.0035	0.0174
eptB	36.5605	1.8615	0.3981	4.6763	2.92E-06	4.55E-05
fabF	628.7953	2.1915	0.4530	4.8382	1.31E-06	2.25E-05
fbaB	58.4233	-3.2857	0.8396	-3.9132	9.11E-05	8.44E-04
fdhF	28.3324	2.0169	0.4958	4.0682	4.74E-05	5.01E-04
fdoG	78.0274	1.5692	0.2593	6.0522	1.43E-09	5.56E-08
fecA	47.1225	-2.4646	0.7650	-3.2217	0.0013	0.0077
fepE	3.6929	-3.8014	1.1401	-3.3343	8.55E-04	0.0056
fiC	7.5139	-2.6171	0.7876	-3.3230	8.91E-04	0.0058
fiU	98.2584	-2.0599	0.6482	-3.1780	0.0015	0.0087
fliD	5.7629	-3.3772	1.0325	-3.2709	0.0011	0.0067
folE	69.7526	-1.9455	0.4572	-4.2555	2.09E-05	2.49E-04
fpR	6.7228	-2.3920	0.7490	-3.1936	0.0014	0.0083
ftnB	71.9762	2.1726	0.5400	4.0231	5.74E-05	5.84E-04
ftsH	1021.4470	2.0804	0.2878	7.2288	4.87E-13	3.53E-11
ftsZ	167.4045	-0.5775	0.1985	-2.9093	0.0036	0.0179
fuR	153.7327	0.6941	0.2432	2.8541	0.0043	0.0206
fusA	1603.4388	0.9774	0.2827	3.4571	5.46E-04	0.0038
fxsA	326.8943	3.3787	0.7310	4.6218	3.80E-06	5.56E-05
gabD	6.3291	-5.1582	1.0074	-5.1203	3.05E-07	6.42E-06
gabT	7.8461	-3.5675	0.7314	-4.8774	1.07E-06	1.92E-05
gadA	13.7680	-3.8965	0.9610	-4.0548	5.02E-05	5.24E-04
gadB	22.3374	-5.9543	0.9802	-6.0746	1.24E-09	4.96E-08
gadC	36.9329	-4.2018	0.6104	-6.8838	5.83E-12	3.42E-10
gadE	11.9782	-5.1009	1.0444	-4.8843	1.04E-06	1.87E-05
gadW	13.9756	-3.8189	0.8306	-4.5980	4.27E-06	6.12E-05
gadX	25.0536	-2.8543	0.8950	-3.1889	0.0014	0.0084
galM	78.6021	-1.6094	0.3235	-4.9756	6.50E-07	1.22E-05
gcD	39.4542	-2.6283	0.4934	-5.3273	9.97E-08	2.43E-06
gcvB	106.5418	4.2998	0.5636	7.6293	2.36E-14	2.04E-12
ggT	8.4322	-4.5051	0.8213	-5.4852	4.13E-08	1.13E-06
ghrB	48.7207	-2.9582	0.5250	-5.6349	1.75E-08	5.19E-07
glcA	6.4212	-2.2895	0.7005	-3.2682	0.0011	0.0068
glcB	12.4920	-2.1114	0.5612	-3.7626	1.68E-04	0.0014
glgA	37.2273	-2.0461	0.4143	-4.9387	7.86E-07	1.46E-05

glgB	100.2297	-2.2589	0.4042	-5.5892	2.28E-08	6.70E-07
glgC	34.1668	-1.8475	0.3242	-5.6990	1.20E-08	3.87E-07
glgP	78.4846	-1.5507	0.3398	-4.5634	5.03E-06	7.15E-05
glgX	64.0716	-1.6282	0.3540	-4.5991	4.24E-06	6.12E-05
glnE	32.4117	-1.2035	0.3460	-3.4780	5.05E-04	0.0036
glnU	15.7699	2.5831	0.6974	3.7042	2.12E-04	0.0018
glnV	8.1865	2.5079	0.7394	3.3919	6.94E-04	0.0046
glsA	7.2168	-5.4029	0.9687	-5.5774	2.44E-08	7.10E-07
gltA	849.7028	1.3952	0.4515	3.0898	0.0020	0.0109
gltB	272.2884	-1.3581	0.4290	-3.1656	0.0015	0.0089
gltP	55.4565	1.3589	0.4259	3.1904	0.0014	0.0084
gltS	63.6972	1.2602	0.3544	3.5559	3.77E-04	0.0028
gltW	221.4872	1.2673	0.3188	3.9759	7.01E-05	6.84E-04
glyX	25.3220	2.0497	0.6030	3.3993	6.76E-04	0.0045
gmK	149.6654	1.5907	0.4879	3.2601	0.0011	0.0069
gntP	22.1217	3.0333	0.6509	4.6598	3.17E-06	4.78E-05
gntX	33.5307	2.0637	0.4279	4.8226	1.42E-06	2.40E-05
gpH	21.1385	-1.8009	0.5678	-3.1719	0.0015	0.0088
gpsA	49.0238	-1.7985	0.3997	-4.4996	6.81E-06	9.26E-05
gpT	82.9911	1.5127	0.3993	3.7882	1.52E-04	0.0013
grcA	101.7551	2.4201	0.8155	2.9675	0.0030	0.0152
greA	63.9211	1.8479	0.5108	3.6173	2.98E-04	0.0023
groL	3826.4466	4.5189	0.4595	9.8344	8.01E-23	1.38E-20
groS	1062.6779	4.5531	0.2820	16.1441	1.25E-58	9.73E-56
grpE	1019.9289	3.6366	0.7252	5.0146	5.31E-07	1.03E-05
gshA	89.2596	-1.3875	0.4710	-2.9459	0.0032	0.0162
gsS	31.5094	-1.8432	0.3650	-5.0505	4.41E-07	8.74E-06
gstA	49.9369	-1.4407	0.4052	-3.5551	3.78E-04	0.0028
gstB	35.7960	-1.2093	0.4201	-2.8788	0.0040	0.0194
guaC	70.4250	-1.7956	0.3385	-5.3051	1.13E-07	2.64E-06
gyrA	360.5763	1.0387	0.3234	3.2117	0.0013	0.0079
gyrB	210.6058	0.8861	0.2073	4.2741	1.92E-05	2.32E-04
hchA	16.7830	-3.5616	0.7044	-5.0563	4.28E-07	8.57E-06
hdeA	137.1506	-5.8866	0.7752	-7.5940	3.10E-14	2.61E-12
hdeB	67.1532	-5.9974	0.9832	-6.0998	1.06E-09	4.41E-08
hdeD	27.6560	-6.8952	1.0302	-6.6932	2.18E-11	1.21E-09
helD	37.5432	-1.4877	0.4842	-3.0722	0.0021	0.0114
hemA	65.7330	1.1787	0.3518	3.3507	8.06E-04	0.0053
hemD	17.2744	-2.0085	0.7118	-2.8218	0.0048	0.0224
hemL	243.1335	1.2716	0.4227	3.0079	0.0026	0.0136
hemX	22.7090	-1.4760	0.4422	-3.3380	8.44E-04	0.0055
hflC	195.3413	1.5672	0.2194	7.1444	9.04E-13	5.99E-11
hflK	157.7513	0.9636	0.3264	2.9523	0.0032	0.0159
hflX	463.6176	1.7005	0.4213	4.0359	5.44E-05	5.61E-04
hhA	71.4556	2.6369	0.6350	4.1529	3.28E-05	3.72E-04
hicA	4.9648	2.5987	0.8162	3.1839	0.0015	0.0085
hisJ	231.7730	2.7541	0.5319	5.1783	2.24E-07	4.98E-06
hokD	66.6550	2.2234	0.6667	3.3351	8.53E-04	0.0056
hsdR	23.6117	-1.6565	0.4473	-3.7034	2.13E-04	0.0018
hslJ	68.2994	2.0507	0.5816	3.5257	4.22E-04	0.0031
hslO	118.2126	3.5013	0.5761	6.0780	1.22E-09	4.92E-08
hslR	45.4486	4.5706	0.6393	7.1495	8.71E-13	5.90E-11
hslU	204.1247	2.7956	0.4117	6.7904	1.12E-11	6.45E-10

hslV	195.3605	4.6891	0.3145	14.9103	2.82E-50	1.76E-47
hspQ	587.3926	3.8504	0.7255	5.3074	1.11E-07	2.62E-06
htpG	1246.1117	3.3987	0.5977	5.6858	1.30E-08	4.14E-07
htpX	1656.5956	4.3612	0.4002	10.8989	1.17E-27	3.63E-25
iaP	27.5401	1.5029	0.4781	3.1433	0.0017	0.0094
ibpA	2628.8038	8.0824	0.4005	20.1826	1.39E-90	2.17E-87
ibpB	2288.1887	8.7125	0.4452	19.5692	2.83E-85	2.94E-82
ilvC	148.0484	-4.7967	0.9233	-5.1951	2.05E-07	4.58E-06
ilvH	18.7467	-2.6202	0.5393	-4.8589	1.18E-06	2.05E-05
ilvI	40.9462	-1.8091	0.5245	-3.4495	5.62E-04	0.0039
ilvN	19.4295	-3.8751	0.7605	-5.0952	3.48E-07	7.28E-06
infC	1722.1083	2.2436	0.5468	4.1033	4.07E-05	4.42E-04
insL1	52.1856	3.4053	0.3997	8.5189	1.61E-17	2.01E-15
insL1-1	24.6771	2.5488	0.5305	4.8049	1.55E-06	2.59E-05
intF	88.1297	2.0219	0.4347	4.6514	3.30E-06	4.96E-05
katE	16.2156	-4.8221	0.7506	-6.4244	1.32E-10	6.75E-09
kcH	21.9150	-2.6282	0.7662	-3.4300	6.04E-04	0.0041
kdgK	29.8456	1.0948	0.3618	3.0257	0.0025	0.0130
kdgR	97.5088	0.8257	0.2544	3.2449	0.0012	0.0072
kefC	7.2674	-3.7377	0.7930	-4.7132	2.44E-06	3.91E-05
kuP	14.6701	-1.6574	0.4427	-3.7436	1.81E-04	0.0015
ldcC	13.5788	-1.9752	0.5421	-3.6436	2.69E-04	0.0021
ldhA	198.6914	1.9098	0.5693	3.3545	7.95E-04	0.0053
ldtB	249.3909	1.7907	0.3936	4.5499	5.37E-06	7.56E-05
ldtC	180.0621	4.0361	0.6415	6.2913	3.15E-10	1.48E-08
leuA	237.5274	-1.4226	0.4669	-3.0470	0.0023	0.0122
leuB	77.8666	-1.3836	0.4860	-2.8469	0.0044	0.0210
leuC	54.9912	-1.3344	0.4488	-2.9735	0.0029	0.0150
leuD	100.6599	-1.4528	0.4259	-3.4115	6.46E-04	0.0044
leuL	67.3598	-1.7580	0.3520	-4.9950	5.88E-07	1.12E-05
leuQ	13.1400	1.9146	0.6067	3.1558	0.0016	0.0091
leuW	10.8800	2.4672	0.6793	3.6320	2.81E-04	0.0022
lexA	70.2417	1.5318	0.4396	3.4843	4.93E-04	0.0035
lhgO	4.8458	-3.6139	0.8787	-4.1126	3.91E-05	4.29E-04
lipA	166.1518	1.7821	0.4320	4.1248	3.71E-05	4.10E-04
livF	35.0614	-1.3043	0.4117	-3.1679	0.0015	0.0089
livH	18.8207	-2.1703	0.6676	-3.2509	0.0012	0.0071
livJ	91.8910	-4.4866	0.5620	-7.9831	1.43E-15	1.43E-13
livK	103.1145	-1.7753	0.5182	-3.4258	6.13E-04	0.0042
livM	46.8520	-1.7954	0.5455	-3.2911	9.98E-04	0.0064
lldD	22.2430	-2.3096	0.7209	-3.2036	0.0014	0.0081
loN	1368.7973	2.4647	0.5054	4.8764	1.08E-06	1.92E-05
lpD	729.7311	0.9976	0.3247	3.0725	0.0021	0.0114
lpoA	31.4509	-1.3998	0.4413	-3.1723	0.0015	0.0088
lptB	33.9022	-2.7145	0.8001	-3.3930	6.91E-04	0.0046
lptD	152.8850	-0.6051	0.1988	-3.0437	0.0023	0.0123
lpxC	721.1082	1.1415	0.3117	3.6618	2.50E-04	0.0020
lpxD	164.8784	-0.7074	0.2294	-3.0837	0.0020	0.0111
lrhA	125.6188	1.4311	0.3974	3.6009	3.17E-04	0.0024
ltaE	37.0822	-1.3708	0.3387	-4.0476	5.17E-05	5.39E-04
lysA	14.5986	-2.0352	0.6224	-3.2701	0.0011	0.0067
lysC	139.8717	-1.6819	0.5035	-3.3404	8.37E-04	0.0055
lysP	223.6144	1.8299	0.4878	3.7511	1.76E-04	0.0015

lysT	365.7474	1.9143	0.4132	4.6324	3.62E-06	5.31E-05
lysY	70.1662	2.1251	0.7513	2.8287	0.0047	0.0220
lysZ	133.0509	2.3688	0.4667	5.0754	3.87E-07	7.87E-06
maK	11.7704	-1.6040	0.4947	-3.2420	0.0012	0.0073
malI	16.3347	2.0109	0.5006	4.0169	5.90E-05	5.98E-04
malP	16.9295	-3.0361	0.7139	-4.2530	2.11E-05	2.51E-04
marA	19.5891	2.1511	0.5061	4.2503	2.13E-05	2.53E-04
mdtK	60.6328	0.8988	0.3092	2.9062	0.0037	0.0180
metE	227.1578	-4.8494	0.4578	-10.5934	3.20E-26	9.05E-24
mfD	265.6321	1.5474	0.3330	4.6465	3.38E-06	5.03E-05
mgrB	76.3768	2.8408	0.6418	4.4263	9.59E-06	1.25E-04
mgrR	14.3310	2.1782	0.7566	2.8789	0.0040	0.0194
mgtA	2645.4046	4.2381	0.8771	4.8319	1.35E-06	2.31E-05
mgtL	469.5853	4.3498	0.7537	5.7713	7.87E-09	2.61E-07
miaA	1026.4875	2.8299	0.3933	7.1954	6.23E-13	4.31E-11
miaB	72.0458	1.1137	0.3523	3.1614	0.0016	0.0090
minE	28.3352	-1.3657	0.4796	-2.8475	0.0044	0.0210
mipA	165.7631	1.8143	0.4968	3.6521	2.60E-04	0.0021
mlaB	27.9371	1.3404	0.4684	2.8616	0.0042	0.0203
mlaF	108.2725	1.8601	0.4235	4.3921	1.12E-05	1.43E-04
mlC	82.6689	2.4606	0.2604	9.4478	3.46E-21	5.13E-19
mlrA	7.8020	-2.5221	0.6883	-3.6641	2.48E-04	0.0020
mltD	485.9148	1.4830	0.3515	4.2185	2.46E-05	2.87E-04
moaA	53.8765	-1.5360	0.4798	-3.2010	0.0014	0.0081
moaB	27.2209	-2.1775	0.4033	-5.3999	6.67E-08	1.70E-06
moaC	16.4231	-2.3501	0.4848	-4.8473	1.25E-06	2.16E-05
moaD	3.1475	-2.7278	0.9536	-2.8604	0.0042	0.0203
moaE	18.6211	-3.0040	0.5439	-5.5228	3.34E-08	9.44E-07
mobB	5.2185	-2.5523	0.8694	-2.9356	0.0033	0.0166
modF	27.9121	-1.7384	0.4683	-3.7119	2.06E-04	0.0017
mqsA	52.8469	2.4424	0.5373	4.5458	5.47E-06	7.68E-05
mqsR	62.2148	2.9500	0.4033	7.3155	2.56E-13	2.00E-11
mraY	15.9637	-1.9515	0.5329	-3.6622	2.50E-04	0.0020
mreB	224.6452	1.4428	0.5009	2.8806	0.0040	0.0194
mscK	88.1717	0.7853	0.2178	3.6059	3.11E-04	0.0024
mscL	59.2731	-2.2100	0.3442	-6.4200	1.36E-10	6.84E-09
mscS	211.0824	-2.0183	0.4319	-4.6731	2.97E-06	4.60E-05
msyB	26.0955	-3.1436	0.9130	-3.4432	5.75E-04	0.0040
mtlA	15.8921	-2.2172	0.5509	-4.0249	5.70E-05	5.82E-04
murC	56.6153	-0.7682	0.2546	-3.0173	0.0026	0.0133
murE	47.1332	-1.1750	0.3909	-3.0060	0.0026	0.0136
mutM	37.4293	3.4929	0.4959	7.0434	1.88E-12	1.19E-10
mzrA	29.7861	2.4176	0.5156	4.6889	2.75E-06	4.30E-05
nadR	28.4920	-1.7896	0.4703	-3.8051	1.42E-04	0.0012
nagZ	30.4986	-1.5747	0.4102	-3.8386	1.24E-04	0.0011
narP	49.8583	2.4102	0.4524	5.3271	9.98E-08	2.43E-06
nhaA	443.8046	3.6715	0.2750	13.3508	1.17E-40	6.08E-38
nhaR	80.6050	2.4520	0.2702	9.0735	1.15E-19	1.63E-17
nlpI	675.9969	2.1665	0.6326	3.4249	6.15E-04	0.0042
nnR	24.1333	-1.7328	0.3917	-4.4237	9.70E-06	1.26E-04
norR	22.9749	1.8286	0.5171	3.5365	4.05E-04	0.0030
nrdA	34.8821	-2.5675	0.5229	-4.9099	9.11E-07	1.65E-05
nrdE	87.8160	-2.0984	0.5767	-3.6389	2.74E-04	0.0022

nrdF	32.8012	-1.9609	0.5370	-3.6513	2.61E-04	0.0021
nudC	15.8070	-1.7655	0.5237	-3.3715	7.47E-04	0.0050
nudE	112.4928	1.5927	0.4969	3.2052	0.0013	0.0080
nudF	21.5778	-1.3994	0.4926	-2.8409	0.0045	0.0214
nuoC	32.9881	-2.1146	0.5807	-3.6412	2.71E-04	0.0021
nusB	40.1384	1.6313	0.3446	4.7342	2.20E-06	3.58E-05
ogT	7.3251	2.0431	0.6788	3.0099	0.0026	0.0135
ompF	876.5537	-1.6191	0.3393	-4.7717	1.83E-06	3.02E-05
opgB	110.2024	1.9179	0.3019	6.3524	2.12E-10	1.03E-08
opgD	101.9575	1.1770	0.3028	3.8874	1.01E-04	9.20E-04
opgG	62.5900	0.8558	0.2535	3.3758	7.36E-04	0.0049
osmB	562.2381	4.3879	0.6353	6.9067	4.96E-12	2.97E-10
osmE	71.8239	-3.0911	0.8130	-3.8021	1.43E-04	0.0013
osmF	9.1397	-3.9319	0.7850	-5.0087	5.48E-07	1.05E-05
osmY	82.3883	-3.2213	0.7414	-4.3448	1.39E-05	1.74E-04
otsA	28.8326	-3.1402	0.6036	-5.2028	1.96E-07	4.46E-06
patA	46.9852	-4.0316	0.8047	-5.0101	5.44E-07	1.05E-05
pcK	84.6685	2.2303	0.3510	6.3544	2.09E-10	1.03E-08
pdxH	33.2436	-1.9325	0.5291	-3.6524	2.60E-04	0.0021
pdxJ	33.1834	-1.1958	0.3398	-3.5195	4.32E-04	0.0031
pdxK	17.5108	-2.0454	0.5162	-3.9627	7.41E-05	7.14E-04
pdxY	18.9552	-1.6029	0.5109	-3.1372	0.0017	0.0096
pepN	93.5983	-0.8457	0.2567	-3.2941	9.88E-04	0.0063
pepT	61.9316	-0.8968	0.3039	-2.9507	0.0032	0.0159
pfkB	14.2034	-2.9482	0.5998	-4.9151	8.88E-07	1.63E-05
pflB	227.9401	-1.3238	0.2602	-5.0868	3.64E-07	7.46E-06
pfO	35.7367	-2.3288	0.5602	-4.1570	3.22E-05	3.67E-04
pgL	34.0496	-2.1611	0.5950	-3.6325	2.81E-04	0.0022
pheA	246.3539	-2.5685	0.5477	-4.6894	2.74E-06	4.30E-05
phoB	24.2674	2.1394	0.5495	3.8933	9.89E-05	9.02E-04
phoH	36.3689	-1.7746	0.5321	-3.3349	8.53E-04	0.0056
phoP	54.2082	1.1386	0.3511	3.2432	0.0012	0.0072
phR	8.9555	-2.2650	0.6377	-3.5519	3.83E-04	0.0028
plaP	66.7254	1.6327	0.3511	4.6498	3.32E-06	4.97E-05
pntB	129.0025	-1.6656	0.4851	-3.4335	5.96E-04	0.0041
poxB	31.5305	-4.6027	0.6253	-7.3603	1.84E-13	1.46E-11
ppC	156.2793	-0.9540	0.2502	-3.8127	1.37E-04	0.0012
ppiA	96.9611	2.0255	0.5377	3.7671	1.65E-04	0.0014
prC	172.6114	-0.8522	0.3016	-2.8254	0.0047	0.0222
prfA	30.2134	1.3177	0.4474	2.9450	0.0032	0.0162
prkB	22.3715	-2.1348	0.6884	-3.1013	0.0019	0.0106
prlC	163.4824	2.0165	0.4665	4.3223	1.54E-05	1.91E-04
proV	37.1041	-1.8918	0.6447	-2.9345	0.0033	0.0166
prpR	3.6931	-2.7809	0.8900	-3.1244	0.0018	0.0099
pspA	122.7713	3.5921	0.5767	6.2284	4.71E-10	2.10E-08
pspC	10.7286	2.2644	0.6197	3.6541	2.58E-04	0.0021
pspE	29.6213	2.5098	0.4975	5.0451	4.53E-07	8.93E-06
pspG	10.6075	2.1616	0.6152	3.5134	4.42E-04	0.0032
pssA	107.4887	-1.2744	0.3889	-3.2768	0.0010	0.0066
ptwF	4.2764	3.2774	0.9620	3.4070	6.57E-04	0.0044
purD	89.3002	1.4163	0.4956	2.8579	0.0043	0.0204
purF	166.8782	1.6001	0.3881	4.1233	3.73E-05	4.11E-04
purL	358.8707	1.3375	0.2960	4.5191	6.21E-06	8.59E-05

pykF	169.0487	-1.4460	0.3812	-3.7935	1.49E-04	0.0013
qorA	22.8718	-1.6176	0.4204	-3.8475	1.19E-04	0.0011
raiA	1468.4669	2.5685	0.4769	5.3856	7.22E-08	1.81E-06
rbsD	57.9053	2.3026	0.7193	3.2009	0.0014	0.0081
rclA	5.2196	-2.4387	0.7725	-3.1568	0.0016	0.0091
recD	58.5513	1.2521	0.3567	3.5105	4.47E-04	0.0032
recJ	78.2368	0.8049	0.2600	3.0954	0.0020	0.0108
relB	38.4067	2.5356	0.7163	3.5397	4.01E-04	0.0029
relE	49.1182	2.8857	0.6685	4.3169	1.58E-05	1.95E-04
rhlB	61.2700	-1.1227	0.3706	-3.0294	0.0025	0.0128
ribE	29.7205	1.3342	0.3980	3.3518	8.03E-04	0.0053
rimM	1278.5966	2.7883	0.7466	3.7347	1.88E-04	0.0016
rlmE	495.6980	3.2061	0.6368	5.0344	4.79E-07	9.38E-06
rlmL	76.1451	1.5509	0.3565	4.3501	1.36E-05	1.71E-04
rlmN	97.3410	1.7533	0.5747	3.0506	0.0023	0.0121
rluB	79.1984	1.4138	0.3674	3.8478	1.19E-04	0.0011
rluF	24.9508	-1.9531	0.6906	-2.8282	0.0047	0.0220
rnC	82.4497	1.0648	0.3604	2.9546	0.0031	0.0158
roxA	97.7697	0.7313	0.2386	3.0644	0.0022	0.0116
rpE	20.1052	-1.4710	0.4433	-3.3186	9.05E-04	0.0058
rplA	989.6979	2.0679	0.5136	4.0261	5.67E-05	5.81E-04
rplE	584.0206	2.0858	0.4469	4.6676	3.05E-06	4.67E-05
rplF	396.0214	1.2564	0.4025	3.1214	0.0018	0.0100
rplI	161.0359	1.5643	0.4338	3.6061	3.11E-04	0.0024
rplJ	1737.9112	2.5678	0.6458	3.9760	7.01E-05	6.84E-04
rplK	725.7552	1.7401	0.3432	5.0695	3.99E-07	8.06E-06
rplL	1328.8659	2.7204	0.7199	3.7790	1.57E-04	0.0014
rplM	812.9183	1.9255	0.5337	3.6078	3.09E-04	0.0024
rplN	948.1770	1.9001	0.5413	3.5101	4.48E-04	0.0032
rplO	460.2324	2.5446	0.4693	5.4226	5.88E-08	1.52E-06
rplP	188.1913	1.5169	0.4709	3.2209	0.0013	0.0077
rplQ	538.3331	1.9493	0.3106	6.2759	3.48E-10	1.59E-08
rplS	941.7046	2.9451	0.4418	6.6661	2.63E-11	1.41E-09
rplT	1854.3319	2.6876	0.6709	4.0059	6.18E-05	6.23E-04
rplU	694.1227	2.2987	0.6414	3.5838	3.39E-04	0.0026
rplV	124.5581	1.3898	0.3417	4.0676	4.75E-05	5.01E-04
rplX	279.3430	2.0490	0.4770	4.2953	1.74E-05	2.12E-04
rplY	238.6800	2.9035	0.5702	5.0925	3.53E-07	7.33E-06
rpmD	38.3253	2.0434	0.5350	3.8197	1.34E-04	0.0012
rpmE	1673.6222	3.7343	0.8051	4.6384	3.51E-06	5.18E-05
rpmH	319.6441	2.3571	0.6240	3.7773	1.59E-04	0.0014
rpmI	1269.4784	2.5878	0.6485	3.9906	6.59E-05	6.53E-04
rpmJ	216.9949	2.0539	0.3950	5.2005	1.99E-07	4.48E-06
rpoA	1268.0005	1.2469	0.3909	3.1901	0.0014	0.0084
rpoB	511.0932	0.7613	0.1956	3.8929	9.90E-05	9.02E-04
rpoC	1031.6640	0.9294	0.2498	3.7200	1.99E-04	0.0017
rpoD	382.7254	2.0175	0.3298	6.1176	9.50E-10	4.00E-08
rpoH	651.0465	2.5935	0.4875	5.3205	1.03E-07	2.50E-06
rpsA	1727.8655	1.3301	0.2708	4.9111	9.06E-07	1.65E-05
rpsB	2435.6991	3.1648	0.3123	10.1333	3.93E-24	8.16E-22
rpsC	353.6177	1.3418	0.3410	3.9353	8.31E-05	7.81E-04
rpsD	656.4737	1.3368	0.3238	4.1285	3.65E-05	4.05E-04
rpsE	360.4873	1.8128	0.4029	4.4994	6.81E-06	9.26E-05

rpsG	677.4636	1.8351	0.5702	3.2182	0.0013	0.0078
rpsH	222.7654	1.4507	0.3531	4.1082	3.99E-05	4.35E-04
rpsK	399.5320	1.5314	0.3144	4.8717	1.11E-06	1.95E-05
rpsL	896.0547	1.9014	0.5904	3.2208	0.0013	0.0077
rpsM	736.0815	1.6542	0.3229	5.1232	3.00E-07	6.41E-06
rpsN	280.7857	1.5347	0.3628	4.2305	2.33E-05	2.74E-04
rpsO	915.5335	2.1867	0.7093	3.0829	0.0020	0.0111
rpsP	680.3206	2.6697	0.7522	3.5490	3.87E-04	0.0029
rpsQ	222.7374	1.4088	0.3363	4.1886	2.81E-05	3.25E-04
rpsS	93.1708	1.0979	0.2754	3.9860	6.72E-05	6.64E-04
rpsT	735.5870	0.8740	0.2906	3.0076	0.0026	0.0136
rpsU	1120.4577	2.1241	0.6972	3.0467	0.0023	0.0122
rsmB	40.4076	-2.7902	0.7600	-3.6712	2.41E-04	0.0020
rssA	24.3061	-1.7080	0.3785	-4.5127	6.40E-06	8.78E-05
rssB	34.6812	-2.3941	0.5940	-4.0302	5.57E-05	5.73E-04
rstA	78.7238	1.8420	0.4014	4.5885	4.46E-06	6.37E-05
rstB	49.9957	1.1063	0.3410	3.2445	0.0012	0.0072
rsxA	29.9599	1.5346	0.5199	2.9516	0.0032	0.0159
satP	22.5486	2.3840	0.5077	4.6960	2.65E-06	4.21E-05
sbcD	38.8293	1.7241	0.4334	3.9782	6.95E-05	6.84E-04
sdaA	915.8868	5.6402	0.5113	11.0311	2.70E-28	9.35E-26
sdaB	36.4824	3.0461	0.5808	5.2442	1.57E-07	3.62E-06
sdaC	79.6355	3.7455	0.4809	7.7881	6.80E-15	6.42E-13
sdhA	163.4790	1.1632	0.2387	4.8727	1.10E-06	1.95E-05
sdhC	40.4426	1.4970	0.4039	3.7064	2.10E-04	0.0018
secA	268.0939	0.7997	0.1916	4.1729	3.01E-05	3.45E-04
secD	237.1383	0.9109	0.2970	3.0673	0.0022	0.0116
secF	147.6545	1.3387	0.2948	4.5403	5.62E-06	7.84E-05
secY	2531.8522	2.3508	0.4420	5.3186	1.05E-07	2.50E-06
serA	381.4620	-2.1852	0.6969	-3.1355	0.0017	0.0096
serC	341.2322	-1.9111	0.4034	-4.7378	2.16E-06	3.54E-05
skP	88.0796	-1.8151	0.3219	-5.6384	1.72E-08	5.14E-07
slyB	1218.0733	2.4912	0.8385	2.9711	0.0030	0.0151
solA	29.9008	-1.6947	0.4102	-4.1317	3.60E-05	4.00E-04
soxS	141.8499	3.3116	0.5964	5.5527	2.81E-08	8.11E-07
spY	192.9851	4.2392	0.6129	6.9171	4.61E-12	2.81E-10
srkA	172.5376	2.8439	0.6949	4.0927	4.26E-05	4.59E-04
stpA	34.3891	-3.3201	0.6162	-5.3881	7.12E-08	1.80E-06
sufC	40.3621	-2.4743	0.7186	-3.4433	5.75E-04	0.0040
sufD	46.5605	-1.7435	0.4510	-3.8662	1.11E-04	9.94E-04
sufS	54.9135	-1.4948	0.4650	-3.2146	0.0013	0.0078
talA	29.3545	-3.6082	0.6125	-5.8911	3.84E-09	1.37E-07
taS	30.8528	-1.3857	0.4235	-3.2720	0.0011	0.0067
tesA	129.9320	3.2702	0.5199	6.2899	3.18E-10	1.48E-08
tff	461.2490	2.6074	0.4786	5.4480	5.09E-08	1.34E-06
thiE	48.9052	-2.1479	0.5480	-3.9195	8.87E-05	8.25E-04
thiF	32.0364	-2.0705	0.5410	-3.8273	1.30E-04	0.0012
thiG	25.2136	-1.8708	0.5938	-3.1506	0.0016	0.0093
thiI	73.8781	1.2963	0.4357	2.9755	0.0029	0.0150
thrL	141.3907	-1.1765	0.2502	-4.7026	2.57E-06	4.10E-05
tiG	556.7160	0.9975	0.3340	2.9862	0.0028	0.0145
tisB	25.5485	1.7392	0.5099	3.4110	6.47E-04	0.0044
tktB	27.8268	-4.2004	0.7037	-5.9688	2.39E-09	8.86E-08

tmcA	23.8815	-1.5854	0.5149	-3.0789	0.0021	0.0112
tomB	155.9341	2.6979	0.4532	5.9531	2.63E-09	9.64E-08
topA	343.4325	1.3698	0.2204	6.2139	5.17E-10	2.27E-08
torR	15.8675	1.8367	0.5309	3.4600	5.40E-04	0.0038
tpiA	134.7403	-1.8591	0.4471	-4.1586	3.20E-05	3.66E-04
treA	5.4964	-2.0057	0.7005	-2.8635	0.0042	0.0202
treF	7.8897	-2.3517	0.6602	-3.5622	3.68E-04	0.0028
trkA	43.1615	-2.1038	0.5334	-3.9441	8.01E-05	7.60E-04
trmD	1521.8933	2.7006	0.7572	3.5664	3.62E-04	0.0027
trmJ	112.1810	2.1821	0.6139	3.5544	3.79E-04	0.0028
trpA	37.5440	-3.0680	0.5601	-5.4776	4.31E-08	1.15E-06
trpB	65.0196	-3.6516	0.4712	-7.7487	9.28E-15	8.50E-13
trpC	79.8260	-3.4244	0.3456	-9.9070	3.88E-23	7.11E-21
trpD	93.9514	-3.0497	0.5368	-5.6818	1.33E-08	4.15E-07
trpE	44.5957	-3.7115	0.6095	-6.0892	1.13E-09	4.65E-08
truA	71.5130	1.4601	0.4224	3.4566	5.47E-04	0.0038
truD	31.6042	-1.6333	0.4165	-3.9217	8.79E-05	8.19E-04
trxB	156.9451	-1.3606	0.4663	-2.9179	0.0035	0.0174
tsF	1040.8905	2.6901	0.3104	8.6655	4.49E-18	5.83E-16
tufA	1766.0578	1.3150	0.4203	3.1284	0.0018	0.0098
tusB	65.6765	2.5957	0.5560	4.6682	3.04E-06	4.67E-05
tyrA	233.6352	-3.7461	0.6268	-5.9765	2.28E-09	8.55E-08
tyrB	37.0635	-2.1593	0.5694	-3.7923	1.49E-04	0.0013
tyrU	95.3600	1.4520	0.5172	2.8077	0.0050	0.0232
ucpA	22.1889	1.4413	0.4851	2.9710	0.0030	0.0151
ugpA	4.2437	-4.2577	1.1218	-3.7954	1.47E-04	0.0013
ugpB	28.6655	-3.8230	0.7944	-4.8124	1.49E-06	2.51E-05
uoF	16.6709	1.8123	0.5710	3.1742	0.0015	0.0088
upP	154.6417	1.6942	0.5303	3.1948	0.0014	0.0083
uspC	10.3256	-2.3013	0.8167	-2.8180	0.0048	0.0226
uspG	39.7580	2.0974	0.5299	3.9580	7.56E-05	7.26E-04
uxaA	14.6327	2.3857	0.6422	3.7147	2.03E-04	0.0017
uxuA	45.2137	3.0069	0.8173	3.6791	2.34E-04	0.0019
uxuB	31.2835	2.8555	0.6268	4.5559	5.22E-06	7.38E-05
uxuR	41.8549	1.6598	0.4745	3.4979	4.69E-04	0.0034
valT	70.5103	1.6275	0.4493	3.6221	2.92E-04	0.0023
valU	31.4282	2.0489	0.6282	3.2614	0.0011	0.0069
valX	95.9470	2.1328	0.7355	2.8997	0.0037	0.0183
waaC	11.9663	-1.7327	0.5557	-3.1179	0.0018	0.0101
wecF	15.4887	-1.3888	0.4856	-2.8598	0.0042	0.0203
wrbA	44.8201	-4.2259	0.7762	-5.4443	5.20E-08	1.36E-06
wzyE	6.2299	-3.7859	0.9521	-3.9764	7.00E-05	6.84E-04
xerC	12.7019	-1.5038	0.5065	-2.9690	0.0030	0.0151
yabI	31.2726	1.1703	0.3800	3.0793	0.0021	0.0112
yaeH	38.1982	-1.4129	0.4750	-2.9742	0.0029	0.0150
yafE	22.9152	1.5080	0.4850	3.1091	0.0019	0.0104
yagI	58.1086	2.7931	0.4207	6.6396	3.15E-11	1.66E-09
yagP	5.3761	2.5045	0.8104	3.0905	0.0020	0.0109
yagU	20.4831	-3.9097	0.8813	-4.4363	9.15E-06	1.21E-04
yahK	13.5970	-3.1574	0.7366	-4.2864	1.82E-05	2.20E-04
yahO	29.1597	-4.3685	0.9805	-4.4556	8.37E-06	1.11E-04
yaiI	17.3492	-2.3313	0.7974	-2.9236	0.0035	0.0172
yajC	258.7349	2.2267	0.5424	4.1051	4.04E-05	4.40E-04

yajO	30.0130	-1.7110	0.3815	-4.4849	7.29E-06	9.80E-05
ybaL	102.3186	1.7039	0.3614	4.7144	2.42E-06	3.91E-05
ybaT	16.0154	-3.6106	0.6588	-5.4806	4.24E-08	1.14E-06
ybaY	45.0979	-2.9249	0.7364	-3.9718	7.13E-05	6.92E-04
ybbA	52.1729	2.9025	0.5532	5.2472	1.54E-07	3.59E-06
ybbN	319.6311	3.3804	0.3268	10.3449	4.42E-25	9.82E-23
ybbP	76.0252	2.4426	0.4567	5.3490	8.84E-08	2.18E-06
ybcF	7.2383	-2.7336	0.9659	-2.8300	0.0047	0.0220
ybdZ	8.4803	-1.5969	0.5666	-2.8184	0.0048	0.0226
ybeD	470.5137	4.1970	0.3332	12.5950	2.25E-36	1.00E-33
ybeY	50.7290	1.3494	0.4383	3.0790	0.0021	0.0112
ybeZ	251.9548	2.3720	0.2829	8.3857	5.04E-17	5.61E-15
ybfA	192.1723	2.9263	0.7976	3.6688	2.44E-04	0.0020
ybgA	4.7709	-3.3508	0.8921	-3.7559	1.73E-04	0.0015
ybgI	46.8884	-0.9982	0.3485	-2.8642	0.0042	0.0202
ybgK	28.0047	-1.1250	0.3910	-2.8770	0.0040	0.0195
ybhB	34.7242	-1.3555	0.4050	-3.3466	8.18E-04	0.0054
ybhP	5.2777	-3.8374	0.8820	-4.3510	1.36E-05	1.71E-04
ybiB	25.7281	-2.1659	0.5394	-4.0156	5.93E-05	5.99E-04
ybiC	74.6027	-2.5997	0.5872	-4.4273	9.54E-06	1.25E-04
ybiI	4.8606	-2.2160	0.7210	-3.0737	0.0021	0.0114
ybiU	15.2303	-2.2811	0.5699	-4.0024	6.27E-05	6.28E-04
ybiX	19.4367	-2.4449	0.7120	-3.4337	5.95E-04	0.0041
ybjG	109.4191	3.3966	0.6170	5.5048	3.70E-08	1.04E-06
ybjP	19.3429	-1.9029	0.5657	-3.3641	7.68E-04	0.0051
ybjT	16.8732	-2.1987	0.6383	-3.4445	5.72E-04	0.0040
ybjX	252.3540	3.2937	0.3179	10.3598	3.78E-25	9.05E-23
ycaC	17.7904	-5.3839	0.9510	-5.6615	1.50E-08	4.58E-07
ycaL	11.8087	-3.1418	0.9919	-3.1675	0.0015	0.0089
yccA	1014.4862	2.7689	0.7010	3.9500	7.81E-05	7.46E-04
yccJ	16.4828	-3.0087	0.6517	-4.6168	3.90E-06	5.67E-05
yceD	1019.2731	2.3451	0.5869	3.9955	6.46E-05	6.42E-04
yceI	63.7748	1.9254	0.6098	3.1576	0.0016	0.0091
yceK	8.8197	-3.3301	0.9746	-3.4169	6.33E-04	0.0043
ycfJ	245.2190	5.4992	0.6484	8.4813	2.23E-17	2.67E-15
ycfL	12.7111	-1.4655	0.4830	-3.0339	0.0024	0.0127
ycfP	23.0595	-1.6718	0.4561	-3.6655	2.47E-04	0.0020
ycgB	21.2682	-4.1021	0.5333	-7.6924	1.44E-14	1.28E-12
ycgX	3.5970	-3.9387	1.0971	-3.5902	3.30E-04	0.0025
ychF	94.1521	1.2556	0.3669	3.4222	6.21E-04	0.0042
ychH	40.7609	2.4679	0.6166	4.0026	6.26E-05	6.28E-04
yciB	50.9651	2.3697	0.4054	5.8447	5.07E-09	1.72E-07
yciC	85.1343	1.8768	0.2790	6.7272	1.73E-11	9.79E-10
yciE	6.7506	-3.4094	0.8346	-4.0850	4.41E-05	4.70E-04
yciF	6.2061	-4.5312	0.9593	-4.7234	2.32E-06	3.76E-05
yciG	6.5057	-5.9054	1.0265	-5.7528	8.78E-09	2.88E-07
yciM	155.8727	1.9426	0.2479	7.8374	4.60E-15	4.48E-13
yciQ	16.0020	-1.7678	0.6278	-2.8159	0.0049	0.0227
yciS	91.9568	2.2759	0.4719	4.8233	1.41E-06	2.40E-05
ycjX	259.0368	3.6566	0.4546	8.0436	8.72E-16	9.05E-14
ydaM	23.4328	-1.3690	0.3977	-3.4422	5.77E-04	0.0040
ydcJ	11.8684	-2.2829	0.7982	-2.8602	0.0042	0.0203
ydcK	9.4092	-4.1170	0.8030	-5.1269	2.95E-07	6.33E-06

ydcP	146.5753	2.4207	0.4128	5.8642	4.51E-09	1.56E-07
ydeP	28.8260	2.9396	0.4703	6.2511	4.08E-10	1.84E-08
ydeT	25.7932	2.6170	0.8679	3.0153	0.0026	0.0133
ydgJ	46.0393	-1.0884	0.3567	-3.0514	0.0023	0.0121
ydhL	4.6288	-2.5733	0.8409	-3.0601	0.0022	0.0118
ydhP	14.3599	-2.6194	0.8071	-3.2453	0.0012	0.0072
ydhS	9.8139	-2.2144	0.7315	-3.0272	0.0025	0.0129
ydhZ	10.4602	-2.3968	0.6851	-3.4987	4.67E-04	0.0034
ydiZ	9.2429	-2.9892	0.7606	-3.9300	8.49E-05	7.96E-04
ydjF	24.5052	2.6200	0.5615	4.6664	3.07E-06	4.68E-05
yeaG	33.5109	-3.5492	0.6245	-5.6831	1.32E-08	4.15E-07
yeaH	6.9906	-2.5603	0.8497	-3.0131	0.0026	0.0134
yeaQ	37.0583	-3.2642	0.8371	-3.8995	9.64E-05	8.85E-04
yeaY	22.6729	1.1382	0.4053	2.8083	0.0050	0.0232
yebE	453.8967	5.2453	0.5257	9.9784	1.89E-23	3.69E-21
yebF	28.1545	-1.8309	0.5783	-3.1659	0.0015	0.0089
yebO	136.0702	3.1350	0.6755	4.6413	3.46E-06	5.13E-05
yebT	44.6916	-2.5393	0.6493	-3.9107	9.20E-05	8.47E-04
yebV	44.8998	-4.8084	0.9680	-4.9674	6.79E-07	1.27E-05
yecH	4.3112	-2.7361	0.9506	-2.8784	0.0040	0.0194
yecS	7.8854	-2.5063	0.8728	-2.8715	0.0041	0.0198
yedI	12.8115	-1.6004	0.5148	-3.1088	0.0019	0.0104
yedP	9.4258	-2.7826	0.7701	-3.6132	3.02E-04	0.0023
yedQ	16.1157	-1.8957	0.4486	-4.2261	2.38E-05	2.78E-04
yeeD	42.7379	1.7421	0.6015	2.8965	0.0038	0.0185
yegE	23.3014	-1.1581	0.3829	-3.0243	0.0025	0.0130
yegH	18.6296	-1.8724	0.6010	-3.1153	0.0018	0.0102
yegP	20.7107	-3.5748	0.8739	-4.0905	4.31E-05	4.62E-04
yegS	11.6160	-2.2892	0.7531	-3.0397	0.0024	0.0125
yehE	8.5579	-2.9481	0.7285	-4.0466	5.20E-05	5.39E-04
yehW	4.0478	-3.1628	0.8698	-3.6364	2.76E-04	0.0022
yehX	6.5175	-3.5032	0.8819	-3.9724	7.12E-05	6.92E-04
yehY	4.6885	-2.8676	0.8284	-3.4617	5.37E-04	0.0038
yeiB	20.5481	-2.5546	0.7780	-3.2835	0.0010	0.0065
yejG	166.5280	2.5388	0.6438	3.9433	8.04E-05	7.61E-04
yejK	46.3410	1.0954	0.3319	3.3003	9.66E-04	0.0062
yfcF	9.1713	-2.3941	0.5901	-4.0573	4.96E-05	5.20E-04
yfcG	4.8794	-2.3380	0.7949	-2.9413	0.0033	0.0164
yfhM	99.3141	-0.7311	0.2346	-3.1157	0.0018	0.0102
ygaM	48.6382	-2.1677	0.5229	-4.1454	3.39E-05	3.80E-04
ygaY	11.9745	-3.4116	0.9738	-3.5033	4.60E-04	0.0033
ygdR	66.5415	2.3309	0.5473	4.2586	2.06E-05	2.46E-04
ygfZ	29.3429	-1.2546	0.3428	-3.6602	2.52E-04	0.0020
yghA	35.1465	-5.2458	0.9189	-5.7085	1.14E-08	3.70E-07
yghX	5.3086	-3.4130	0.8169	-4.1780	2.94E-05	3.39E-04
yghX	4.1335	-3.3684	0.9641	-3.4938	4.76E-04	0.0034
ygiC	129.2387	1.4031	0.2588	5.4219	5.90E-08	1.52E-06
ygiM	45.1855	1.3052	0.3813	3.4228	6.20E-04	0.0042
yhbO	7.3121	-4.7686	1.0826	-4.4047	1.06E-05	1.36E-04
yhbW	7.9043	-2.7746	0.6316	-4.3933	1.12E-05	1.42E-04
yheO	55.7899	-2.1035	0.6368	-3.3033	9.56E-04	0.0061
yheT	23.5891	-3.3506	0.8061	-4.1567	3.23E-05	3.67E-04
yheU	7.8253	-4.0480	1.0456	-3.8714	1.08E-04	9.77E-04

yhgF	26.7321	-1.1929	0.3884	-3.0716	0.0021	0.0114
yhgN	12.7215	2.0833	0.7136	2.9195	0.0035	0.0174
yhiD	10.0077	-6.1043	1.0769	-5.6683	1.44E-08	4.44E-07
yhiM	6.2320	-3.7309	0.8790	-4.2448	2.19E-05	2.58E-04
yhjD	13.2136	-2.0310	0.6456	-3.1460	0.0017	0.0094
yhjE	32.2871	-2.2039	0.6721	-3.2792	0.0010	0.0066
yhjG	9.5988	-3.0648	0.6233	-4.9172	8.78E-07	1.62E-05
yhjY	8.7726	-1.7811	0.6123	-2.9088	0.0036	0.0179
yiaG	24.7804	-3.5345	0.9764	-3.6200	2.95E-04	0.0023
yibH	4.2174	-2.9181	0.9055	-3.2226	0.0013	0.0077
yigA	10.0211	-1.7981	0.6409	-2.8056	0.0050	0.0233
yigB	10.9073	-1.8724	0.5785	-3.2367	0.0012	0.0074
yigM	22.0008	-2.0831	0.7001	-2.9755	0.0029	0.0150
yiiM	15.9205	-2.4467	0.6638	-3.6860	2.28E-04	0.0019
yiiX	29.1367	2.0037	0.5825	3.4397	5.82E-04	0.0040
yjcC	8.8232	-2.6180	0.8722	-3.0015	0.0027	0.0138
yjdC	15.1203	-2.1834	0.5327	-4.0990	4.15E-05	4.49E-04
yjdM	19.8612	1.7381	0.4652	3.7364	1.87E-04	0.0016
yjfN	68.1073	3.5167	0.7359	4.7790	1.76E-06	2.93E-05
yjgR	10.2843	-1.7245	0.5592	-3.0837	0.0020	0.0111
ylaB	11.9524	-1.8583	0.6039	-3.0772	0.0021	0.0113
yliI	11.3204	-3.5923	0.9573	-3.7527	1.75E-04	0.0015
ymgD	14.7525	2.1287	0.6450	3.3004	9.66E-04	0.0062
ymgG	6.0425	2.6624	0.7595	3.5056	4.56E-04	0.0033
yncJ	186.8641	5.7621	0.6568	8.7734	1.73E-18	2.35E-16
yncL	8.2749	-2.7139	0.7346	-3.6946	2.20E-04	0.0018
yneM	4197.2269	5.7796	0.9545	6.0549	1.40E-09	5.54E-08
ynfD	42.7537	3.0180	0.6997	4.3130	1.61E-05	1.97E-04
ynfK	13.3162	1.9118	0.5388	3.5480	3.88E-04	0.0029
yoaC	5.8583	-2.1607	0.7061	-3.0601	0.0022	0.0118
yobB	92.1889	2.7435	0.3356	8.1743	2.98E-16	3.20E-14
yodC	7.4247	-3.0442	0.8409	-3.6201	2.94E-04	0.0023
yodD	5.4371	-3.4545	0.9603	-3.5975	3.21E-04	0.0024
yohC	8.1015	-1.9983	0.6161	-3.2436	0.0012	0.0072
ypdA	10.6319	-2.0724	0.6405	-3.2357	0.0012	0.0074
ypdK	9.7202	2.6078	0.7191	3.6267	2.87E-04	0.0022
ypfG	53.6877	2.6651	0.5997	4.4437	8.84E-06	1.17E-04
yqaA	32.7406	-2.9349	0.7579	-3.8726	1.08E-04	9.75E-04
yqaE	80.4429	2.3608	0.8279	2.8514	0.0044	0.0208
yqeF	24.3647	1.3500	0.4754	2.8395	0.0045	0.0214
yqjG	10.8148	-2.8447	0.6990	-4.0699	4.70E-05	5.00E-04
yqjI	42.2741	2.7400	0.4097	6.6884	2.26E-11	1.23E-09
yrbN	15.3361	3.7485	0.6835	5.4840	4.16E-08	1.13E-06
yrdA	54.5800	1.0575	0.3552	2.9776	0.0029	0.0149
yrfG	93.6013	2.7963	0.4717	5.9288	3.05E-09	1.10E-07
ytfE	15.0410	2.4405	0.5643	4.3248	1.53E-05	1.89E-04
ytfK	276.7519	1.9998	0.6320	3.1644	0.0016	0.0089
ytjA	24.2736	-4.1606	0.8046	-5.1709	2.33E-07	5.14E-06
zapE	20.5061	-1.4108	0.4474	-3.1533	0.0016	0.0092

t=120 vs. t=0 (p<0.005)

Gene	BaseMean	log$_2$ Fold Change	lfcSE	stat	*p*-value	padj
aas	29.1386	-1.4144	0.3243	-4.3612	1.29E-05	1.62E-04
aceB	324.6456	-1.8250	0.3327	-5.4858	4.12E-08	1.06E-06
ackA	180.3401	1.6857	0.4954	3.4030	6.66E-04	0.0047
acnA	50.2069	-1.3576	0.3586	-3.7863	1.53E-04	0.0014
acuI	21.3695	-2.3587	0.6104	-3.8642	1.11E-04	0.0011
adhE	103.0873	-1.4759	0.3696	-3.9933	6.52E-05	6.55E-04
adhP	21.8856	-4.6907	0.6387	-7.3444	2.07E-13	1.40E-11
ahr	11.7657	-3.8941	0.6525	-5.9680	2.40E-09	8.21E-08
aidB	12.8906	-3.8308	0.6304	-6.0772	1.22E-09	4.70E-08
aldB	4.6081	-2.5598	0.7471	-3.4261	6.12E-04	0.0044
amiA	71.2954	2.0829	0.5706	3.6505	2.62E-04	0.0022
amn	38.1308	-1.5680	0.4714	-3.3262	8.80E-04	0.0060
amyA	20.9495	-2.3392	0.5064	-4.6194	3.85E-06	5.90E-05
ansP	20.1247	2.6438	0.5156	5.1277	2.93E-07	6.05E-06
araC	58.0605	1.4915	0.3427	4.3529	1.34E-05	1.66E-04
argA	573.4813	2.6781	0.5809	4.6106	4.01E-06	6.13E-05
argB	162.2474	2.7497	0.5567	4.9388	7.86E-07	1.49E-05
argC	544.7538	3.1524	0.5843	5.3951	6.85E-08	1.67E-06
argE	353.4858	1.8163	0.5441	3.3380	8.44E-04	0.0058
argF	224.6939	3.5300	0.5525	6.3887	1.67E-10	7.66E-09
argG	1067.2312	2.7144	0.8369	3.2434	0.0012	0.0075
argH	337.7552	2.7444	0.4573	6.0018	1.95E-09	6.90E-08
argI	190.4276	3.3605	0.5555	6.0491	1.46E-09	5.40E-08
argT	63.7453	-1.4327	0.4315	-3.3201	9.00E-04	0.0060
aroA	53.5643	-2.1935	0.5216	-4.2049	2.61E-05	2.97E-04
aroE	25.3601	-2.0158	0.6156	-3.2745	0.0011	0.0069
aroG	327.2786	-2.0167	0.5909	-3.4132	6.42E-04	0.0046
aroP	109.3223	-2.2725	0.4127	-5.5061	3.67E-08	9.68E-07
artJ	890.1429	3.1364	0.6478	4.8416	1.29E-06	2.25E-05
artM	35.3219	1.1124	0.3676	3.0262	0.0025	0.0137
asnA	115.8790	2.9795	0.5951	5.0070	5.53E-07	1.07E-05
asnS	451.7534	0.6936	0.2028	3.4202	6.26E-04	0.0045
aspV	26.4039	1.4141	0.4693	3.0134	0.0026	0.0141
astC	4.3344	-3.0224	0.9647	-3.1328	0.0017	0.0103
atoS	8.8000	1.7338	0.5816	2.9812	0.0029	0.0154
atpC	164.2234	1.0500	0.3015	3.4831	4.96E-04	0.0037
bcsE	26.5329	-1.8579	0.4460	-4.1661	3.10E-05	3.41E-04
bcsG	11.9896	-2.2681	0.4989	-4.5457	5.48E-06	7.96E-05
betA	31.8390	1.6757	0.3737	4.4844	7.31E-06	1.00E-04
betB	76.5106	2.2511	0.4599	4.8949	9.84E-07	1.81E-05
betI	65.5681	2.6294	0.4234	6.2100	5.30E-10	2.17E-08
betT	75.8656	1.9793	0.3792	5.2196	1.79E-07	3.93E-06
bhsA	45.7884	2.6306	0.6690	3.9323	8.41E-05	8.11E-04
bioB	76.1983	-0.9197	0.2583	-3.5610	3.70E-04	0.0029
bisC	27.1451	-1.9657	0.4441	-4.4266	9.57E-06	1.26E-04
bolA	69.1033	-2.3632	0.4176	-5.6587	1.52E-08	4.44E-07
borD	160.1467	2.7997	0.7303	3.8337	1.26E-04	0.0012
brnQ	57.9731	1.3779	0.3134	4.3967	1.10E-05	1.42E-04

bssS	249.8527	4.1691	0.5173	8.0587	7.71E-16	7.74E-14
btuE	26.0777	-3.4827	0.6611	-5.2684	1.38E-07	3.08E-06
can	233.1977	-2.3052	0.3529	-6.5314	6.52E-11	3.03E-09
cfa	92.6151	-2.3441	0.7074	-3.3139	9.20E-04	0.0061
chaA	1801.5463	4.1221	0.5483	7.5176	5.58E-14	4.24E-12
chaB	6.5901	-2.9790	0.7329	-4.0649	4.81E-05	5.05E-04
clpA	625.9362	0.6525	0.2327	2.8040	0.0050	0.0237
clpB	2232.3087	4.5397	0.4212	10.7781	4.37E-27	1.05E-24
clpP	171.4154	1.6362	0.2605	6.2821	3.34E-10	1.42E-08
clpS	79.8024	0.8906	0.2641	3.3722	7.46E-04	0.0052
clpX	374.5339	1.4759	0.2236	6.6021	4.05E-11	1.97E-09
clsB	5.2879	-4.2134	0.8637	-4.8782	1.07E-06	1.94E-05
cohE	49.8958	1.6830	0.4736	3.5534	3.80E-04	0.0030
cpxP	1421.5659	4.7297	0.5535	8.5448	1.29E-17	1.67E-15
crfC	12.7291	-3.8326	0.9584	-3.9990	6.36E-05	6.43E-04
csgE	3.8345	-5.2596	1.0495	-5.0115	5.40E-07	1.05E-05
csgG	9.4775	-1.7596	0.5376	-3.2733	0.0011	0.0069
csiD	6.9070	-3.0297	0.6827	-4.4377	9.09E-06	1.21E-04
cspA	248.2614	3.7275	0.6314	5.9035	3.56E-09	1.18E-07
cspD	171.4356	-0.8193	0.2601	-3.1500	0.0016	0.0099
curA	14.8910	-2.7767	0.5980	-4.6433	3.43E-06	5.31E-05
cusR	31.5167	-2.4859	0.8274	-3.0045	0.0027	0.0144
cusS	19.6410	-2.2878	0.6382	-3.5847	3.37E-04	0.0027
cutC	91.8922	1.6025	0.3817	4.1982	2.69E-05	3.05E-04
cvpA	162.2143	1.8758	0.5144	3.6464	2.66E-04	0.0022
cysS	103.5158	0.9784	0.3417	2.8632	0.0042	0.0208
damX	85.7220	-1.2460	0.3584	-3.4768	5.07E-04	0.0038
dapB	67.5693	-1.8083	0.4039	-4.4774	7.56E-06	1.03E-04
dapD	282.6125	-1.2899	0.3141	-4.1066	4.01E-05	4.29E-04
dcp	74.4693	-1.3228	0.3669	-3.6055	3.12E-04	0.0025
deaD	786.2489	2.4114	0.5425	4.4453	8.78E-06	1.17E-04
dedA	74.3600	1.9926	0.2941	6.7763	1.23E-11	6.74E-10
degP	955.0686	3.9038	0.4660	8.3768	5.44E-17	6.05E-15
deoA	17.4026	-2.2817	0.6380	-3.5766	3.48E-04	0.0027
dgcZ	377.3155	4.0247	0.6649	6.0533	1.42E-09	5.32E-08
dkgA	5.7852	-3.3792	0.7910	-4.2721	1.94E-05	2.27E-04
dmsA	6.3416	2.2879	0.6561	3.4870	4.88E-04	0.0037
dnaA	326.3602	1.1506	0.3349	3.4352	5.92E-04	0.0043
dnaG	131.8946	1.1322	0.2829	4.0020	6.28E-05	6.37E-04
dnaJ	361.8432	3.5162	0.3849	9.1361	6.48E-20	1.01E-17
dnaK	4429.9742	4.9053	0.2499	19.6327	8.12E-86	2.53E-82
dosC	11.2787	-2.9267	0.5469	-5.3510	8.75E-08	2.03E-06
dosP	9.2437	-2.1079	0.6769	-3.1141	0.0018	0.0109
dps	168.7634	-3.3087	0.8876	-3.7276	1.93E-04	0.0017
dsbA	263.4807	2.3539	0.5908	3.9845	6.76E-05	6.72E-04
dtpB	9.4400	-2.1295	0.7333	-2.9041	0.0037	0.0187
eamA	22.4494	-1.4382	0.3903	-3.6851	2.29E-04	0.0019
ecnB	46.9753	-4.6663	0.8816	-5.2930	1.20E-07	2.71E-06
efeB	23.8871	-2.8556	0.6105	-4.6772	2.91E-06	4.64E-05
efeO	28.2223	-3.4018	0.6237	-5.4541	4.92E-08	1.23E-06
efeU	17.9876	-3.3265	0.5339	-6.2311	4.63E-10	1.92E-08
efeU	4.8893	-2.8095	0.8376	-3.3542	7.96E-04	0.0055
elaB	65.6709	-4.3599	0.9660	-4.5134	6.38E-06	9.15E-05

entC	98.5741	-2.3211	0.6256	-3.7099	2.07E-04	0.0018
eptB	36.5605	1.5133	0.3957	3.8245	1.31E-04	0.0012
era	61.5226	0.8366	0.2938	2.8474	0.0044	0.0216
fabF	628.7953	2.5434	0.4524	5.6214	1.89E-08	5.31E-07
fbaB	58.4233	-2.4587	0.8279	-2.9699	0.0030	0.0159
fdhF	28.3324	2.4424	0.4834	5.0524	4.36E-07	8.65E-06
fdoG	78.0274	1.8499	0.2513	7.3609	1.83E-13	1.26E-11
fecA	47.1225	-2.4976	0.7598	-3.2873	0.0010	0.0066
fes	84.6999	-2.1981	0.7397	-2.9717	0.0030	0.0158
fhuE	89.9102	-1.9462	0.5286	-3.6818	2.32E-04	0.0020
fiu	98.2584	-2.3433	0.6467	-3.6234	2.91E-04	0.0023
fkpB	43.1394	1.4530	0.3370	4.3122	1.62E-05	1.93E-04
fliZ	3.3598	-2.7797	0.9879	-2.8137	0.0049	0.0233
folE	69.7526	-1.8001	0.4491	-4.0082	6.12E-05	6.23E-04
fruA	41.4352	1.6695	0.5894	2.8326	0.0046	0.0223
ftnB	71.9762	1.7790	0.5391	3.3001	9.67E-04	0.0064
ftsH	1021.4470	1.8325	0.2876	6.3722	1.86E-10	8.29E-09
fucR	13.2538	-1.6484	0.5135	-3.2099	0.0013	0.0083
fxsA	326.8943	2.6889	0.7311	3.6777	2.35E-04	0.0020
gabD	6.3291	-4.7859	0.9453	-5.0626	4.14E-07	8.31E-06
gabT	7.8461	-3.2299	0.6545	-4.9351	8.01E-07	1.50E-05
gadA	13.7680	-4.5507	0.9685	-4.6989	2.62E-06	4.26E-05
gadB	22.3374	-5.7689	0.9381	-6.1499	7.75E-10	3.06E-08
gadC	36.9329	-3.7854	0.5705	-6.6349	3.25E-11	1.63E-09
gadE	11.9782	-6.0255	1.0672	-5.6459	1.64E-08	4.74E-07
gadW	13.9756	-3.9572	0.8120	-4.8736	1.10E-06	1.97E-05
galM	78.6021	-1.3610	0.3123	-4.3580	1.31E-05	1.63E-04
galP	35.4977	1.9418	0.5801	3.3475	8.15E-04	0.0056
gatA	27.0150	-2.3421	0.8169	-2.8669	0.0041	0.0206
gatB	12.8033	-2.7357	0.9305	-2.9399	0.0033	0.0171
gcd	39.4542	-1.9807	0.4664	-4.2470	2.17E-05	2.53E-04
gcvB	106.5418	5.2740	0.5599	9.4202	4.50E-21	8.24E-19
gcvH	15.8421	1.6410	0.5376	3.0525	0.0023	0.0128
ggt	8.4322	-3.9139	0.7094	-5.5176	3.44E-08	9.22E-07
ghrB	48.7207	-2.7224	0.5079	-5.3601	8.32E-08	1.95E-06
glcB	12.4920	-1.5889	0.5089	-3.1225	0.0018	0.0106
glcC	20.7198	1.3966	0.4758	2.9354	0.0033	0.0173
glgA	37.2273	-2.3377	0.4084	-5.7243	1.04E-08	3.14E-07
glgB	100.2297	-2.7818	0.4043	-6.8808	5.95E-12	3.50E-10
glgC	34.1668	-2.1796	0.3192	-6.8273	8.65E-12	4.90E-10
glgP	78.4846	-1.6117	0.3329	-4.8417	1.29E-06	2.25E-05
glgX	64.0716	-2.0948	0.3534	-5.9271	3.08E-09	1.03E-07
glnE	32.4117	-1.4228	0.3382	-4.2068	2.59E-05	2.96E-04
glnQ	40.0977	1.3808	0.3808	3.6264	2.87E-04	0.0023
glsA	7.2168	-3.9200	0.7780	-5.0385	4.69E-07	9.24E-06
gltB	272.2884	-1.2256	0.4270	-2.8704	0.0041	0.0205
gltP	55.4565	1.2608	0.4221	2.9867	0.0028	0.0152
gltS	63.6972	1.0047	0.3520	2.8541	0.0043	0.0213
gltW	221.4872	0.9061	0.3182	2.8477	0.0044	0.0216
glyX	25.3220	2.1860	0.5957	3.6699	2.43E-04	0.0020
gmk	149.6654	1.3670	0.4871	2.8063	0.0050	0.0236
gmr	35.7604	-1.7090	0.5795	-2.9493	0.0032	0.0167
gntP	22.1217	3.5201	0.6408	5.4937	3.94E-08	1.03E-06

gntX	33.5307	1.9253	0.4233	4.5487	5.40E-06	7.89E-05
gph	21.1385	-1.6229	0.5494	-2.9538	0.0031	0.0165
gpr	15.5213	-2.0964	0.7041	-2.9773	0.0029	0.0156
gpsA	49.0238	-2.0678	0.3947	-5.2384	1.62E-07	3.60E-06
groL	3826.4466	4.2018	0.4595	9.1447	5.98E-20	9.80E-18
groS	1062.6779	4.0362	0.2820	14.3119	1.84E-46	1.43E-43
grpE	1019.9289	3.5492	0.7251	4.8947	9.85E-07	1.81E-05
gshA	89.2596	-1.4385	0.4672	-3.0792	0.0021	0.0120
gss	31.5094	-1.5290	0.3393	-4.5060	6.60E-06	9.35E-05
gstA	49.9369	-1.3938	0.3951	-3.5274	4.20E-04	0.0032
gstB	35.7960	-2.1538	0.4318	-4.9878	6.11E-07	1.17E-05
guaC	70.4250	-1.3164	0.3227	-4.0792	4.52E-05	4.78E-04
gyrA	360.5763	0.9134	0.3226	2.8313	0.0046	0.0223
gyrB	210.6058	1.3837	0.2023	6.8396	7.94E-12	4.58E-10
hchA	16.7830	-3.7858	0.6900	-5.4865	4.10E-08	1.06E-06
hdeA	137.1506	-6.5713	0.7819	-8.4047	4.29E-17	5.13E-15
hdeB	67.1532	-5.8812	0.9636	-6.1033	1.04E-09	4.04E-08
hdeD	27.6560	-6.6030	0.9839	-6.7110	1.93E-11	1.02E-09
hdhA	38.7263	-2.2384	0.7427	-3.0141	0.0026	0.0141
helD	37.5432	-1.3886	0.4728	-2.9367	0.0033	0.0173
hemA	65.7330	1.3223	0.3459	3.8223	1.32E-04	0.0012
hemC	28.4590	-1.3716	0.4336	-3.1637	0.0016	0.0094
hemD	17.2744	-2.1189	0.7015	-3.0203	0.0025	0.0139
hflC	195.3413	1.4450	0.2173	6.6490	2.95E-11	1.53E-09
hflX	463.6176	1.5055	0.4210	3.5765	3.48E-04	0.0027
hha	71.4556	2.0991	0.6350	3.3059	9.47E-04	0.0063
hicA	4.9648	2.3987	0.8086	2.9664	0.0030	0.0160
hinT	25.5826	-1.5653	0.4518	-3.4647	5.31E-04	0.0040
hisG	69.7516	1.6753	0.5750	2.9137	0.0036	0.0183
hisJ	231.7730	2.0008	0.5322	3.7596	1.70E-04	0.0015
hisS	81.8327	-0.6345	0.2146	-2.9561	0.0031	0.0164
hokD	66.6550	2.6116	0.6638	3.9345	8.34E-05	8.06E-04
hsdR	23.6117	-1.3702	0.4217	-3.2490	0.0012	0.0074
hslJ	68.2994	2.6202	0.5777	4.5358	5.74E-06	8.31E-05
hslO	118.2126	3.4460	0.5750	5.9927	2.06E-09	7.14E-08
hslR	45.4486	4.8760	0.6351	7.6770	1.63E-14	1.33E-12
hslU	204.1247	2.5429	0.4110	6.1864	6.15E-10	2.46E-08
hslV	195.3605	4.4250	0.3137	14.1073	3.42E-45	2.13E-42
hspQ	587.3926	4.0213	0.7253	5.5447	2.94E-08	8.18E-07
htpG	1246.1117	3.3027	0.5977	5.5261	3.27E-08	8.94E-07
htpX	1656.5956	4.5219	0.4000	11.3057	1.23E-29	4.26E-27
iap	27.5401	2.5075	0.4591	5.4612	4.73E-08	1.19E-06
ibpA	2628.8038	7.2687	0.4005	18.1480	1.33E-73	1.38E-70
ibpB	2288.1887	8.1213	0.4452	18.2410	2.44E-74	3.80E-71
ileS	330.9931	0.8568	0.2057	4.1660	3.10E-05	3.41E-04
ilvB	68.9162	-1.8118	0.6200	-2.9221	0.0035	0.0179
ilvC	148.0484	-3.9426	0.9137	-4.3153	1.59E-05	1.92E-04
ilvH	18.7467	-2.6852	0.5182	-5.1814	2.20E-07	4.73E-06
ilvI	40.9462	-1.8809	0.5168	-3.6395	2.73E-04	0.0022
ilvN	19.4295	-3.4940	0.7180	-4.8661	1.14E-06	2.02E-05
infC	1722.1083	2.1924	0.5467	4.0103	6.06E-05	6.19E-04
insL1	52.1856	3.1379	0.3977	7.8900	3.02E-15	2.85E-13
insL1	24.6771	2.4030	0.5258	4.5704	4.87E-06	7.28E-05

intF	88.1297	1.7937	0.4329	4.1436	3.42E-05	3.73E-04
iraP	8.7132	-2.9276	0.8922	-3.2813	0.0010	0.0068
ispH	69.3410	1.3251	0.2848	4.6535	3.26E-06	5.08E-05
katE	16.2156	-3.0999	0.5762	-5.3801	7.44E-08	1.77E-06
kch	21.9150	-3.2373	0.7690	-4.2098	2.56E-05	2.94E-04
kefC	7.2674	-1.7031	0.5689	-2.9940	0.0028	0.0149
kup	14.6701	-1.5169	0.4116	-3.6854	2.28E-04	0.0019
ldhA	198.6914	2.6933	0.5676	4.7452	2.08E-06	3.49E-05
ldtB	249.3909	2.1714	0.3919	5.5401	3.02E-08	8.33E-07
ldtC	180.0621	3.6527	0.6413	5.6959	1.23E-08	3.64E-07
ldtE	37.5237	-1.5275	0.4797	-3.1844	0.0015	0.0089
leuC	54.9912	-1.4567	0.4431	-3.2875	0.0010	0.0066
leuD	100.6599	-1.6901	0.4233	-3.9930	6.53E-05	6.55E-04
leuL	67.3598	-1.6095	0.3390	-4.7477	2.06E-06	3.46E-05
leuQ	13.1400	2.0038	0.5948	3.3687	7.55E-04	0.0053
lexA	70.2417	1.2317	0.4381	2.8117	0.0049	0.0234
lhgO	4.8458	-3.2153	0.7991	-4.0238	5.73E-05	5.88E-04
ligA	46.0839	-1.7815	0.6266	-2.8431	0.0045	0.0219
lipA	166.1518	1.8010	0.4306	4.1829	2.88E-05	3.21E-04
livF	35.0614	-1.1238	0.3954	-2.8422	0.0045	0.0219
livJ	91.8910	-3.8393	0.5340	-7.1901	6.47E-13	4.07E-11
livK	103.1145	-1.7065	0.5139	-3.3207	8.98E-04	0.0060
livM	46.8520	-1.5594	0.5343	-2.9186	0.0035	0.0180
lldD	22.2430	-2.3680	0.7099	-3.3358	8.51E-04	0.0058
lnt	57.2332	1.3045	0.3314	3.9362	8.28E-05	8.03E-04
lolA	62.2637	1.5446	0.3900	3.9602	7.49E-05	7.33E-04
lon	1368.7973	2.2004	0.5054	4.3542	1.34E-05	1.66E-04
lpoA	31.4509	-1.6252	0.4345	-3.7401	1.84E-04	0.0016
lpoB	19.5541	-1.3076	0.4314	-3.0309	0.0024	0.0135
lptD	152.8850	-1.0080	0.1978	-5.0973	3.44E-07	7.06E-06
lpxC	721.1082	1.2865	0.3111	4.1353	3.55E-05	3.85E-04
lpxD	164.8784	-0.6670	0.2250	-2.9652	0.0030	0.0161
lrhA	125.6188	1.7758	0.3938	4.5090	6.51E-06	9.30E-05
lspA	67.6595	1.8689	0.4099	4.5598	5.12E-06	7.59E-05
ltaE	37.0822	-1.4076	0.3253	-4.3264	1.52E-05	1.83E-04
lysC	139.8717	-2.6356	0.5073	-5.1959	2.04E-07	4.40E-06
lysT	365.7474	1.3316	0.4133	3.2219	0.0013	0.0080
lysZ	133.0509	1.7819	0.4669	3.8167	1.35E-04	0.0012
maeA	135.0750	-1.5954	0.5674	-2.8120	0.0049	0.0234
malP	16.9295	-4.0323	0.7404	-5.4460	5.15E-08	1.27E-06
marA	19.5891	2.2347	0.4971	4.4953	6.95E-06	9.62E-05
marB	6.7128	2.1402	0.7009	3.0535	0.0023	0.0128
marR	12.2012	2.6726	0.6390	4.1827	2.88E-05	3.21E-04
mazE	11.5974	1.2572	0.4454	2.8228	0.0048	0.0228
mcbR	4.9313	-2.4909	0.7718	-3.2276	0.0012	0.0079
mdtK	60.6328	0.9627	0.3030	3.1775	0.0015	0.0091
metE	227.1578	-4.8759	0.4481	-10.8801	1.43E-27	3.72E-25
metH	105.7695	-2.0691	0.6133	-3.3735	7.42E-04	0.0052
mfd	265.6321	1.7026	0.3315	5.1368	2.79E-07	5.83E-06
mgrB	76.3768	2.1033	0.6427	3.2728	0.0011	0.0069
mgtA	2645.4046	2.6093	0.8772	2.9746	0.0029	0.0157
mgtL	469.5853	2.7699	0.7542	3.6724	2.40E-04	0.0020
miaA	1026.4875	2.4945	0.3932	6.3443	2.23E-10	9.66E-09

miaB	72.0458	1.0774	0.3485	3.0916	0.0020	0.0115
minE	28.3352	-1.7834	0.4775	-3.7347	1.88E-04	0.0016
mlaB	27.9371	1.3163	0.4613	2.8535	0.0043	0.0213
mlaC	66.5422	1.4709	0.4634	3.1744	0.0015	0.0092
mlaF	108.2725	1.1984	0.4242	2.8254	0.0047	0.0227
mlc	82.6689	2.4564	0.2562	9.5885	8.94E-22	1.86E-19
mlrA	7.8020	-3.2307	0.7094	-4.5543	5.25E-06	7.72E-05
moaA	53.8765	-1.7319	0.4754	-3.6431	2.69E-04	0.0022
moaB	27.2209	-2.5385	0.3988	-6.3656	1.95E-10	8.53E-09
moaC	16.4231	-1.7174	0.4265	-4.0269	5.65E-05	5.84E-04
moaE	18.6211	-2.5388	0.4914	-5.1660	2.39E-07	5.06E-06
modF	27.9121	-1.7598	0.4553	-3.8652	1.11E-04	0.0011
mqsA	52.8469	2.4876	0.5340	4.6584	3.19E-06	5.04E-05
mqsR	62.2148	3.7377	0.3941	9.4840	2.45E-21	4.76E-19
mscK	88.1717	1.0815	0.2090	5.1743	2.29E-07	4.88E-06
mscL	59.2731	-2.5071	0.3394	-7.3864	1.51E-13	1.07E-11
mscS	211.0824	-1.8379	0.4285	-4.2888	1.80E-05	2.13E-04
msyB	26.0955	-3.4480	0.9092	-3.7924	1.49E-04	0.0013
mtlA	15.8921	-2.5572	0.5445	-4.6969	2.64E-06	4.28E-05
murC	56.6153	-0.7084	0.2436	-2.9074	0.0036	0.0186
murE	47.1332	-1.1263	0.3807	-2.9585	0.0031	0.0163
mutM	37.4293	4.1121	0.4866	8.4501	2.91E-17	3.62E-15
mzrA	29.7861	2.5383	0.5083	4.9932	5.94E-07	1.14E-05
nadR	28.4920	-1.3939	0.4463	-3.1232	0.0018	0.0106
nagZ	30.4986	-1.1564	0.3845	-3.0077	0.0026	0.0143
napC	7.0656	2.1905	0.6697	3.2708	0.0011	0.0069
narP	49.8583	2.9383	0.4447	6.6074	3.91E-11	1.93E-09
narQ	15.9819	1.5819	0.4522	3.4981	4.69E-04	0.0036
nhaA	443.8046	3.0680	0.2751	11.1512	7.06E-29	2.20E-26
nhaR	80.6050	2.0592	0.2693	7.6477	2.05E-14	1.63E-12
nlpI	675.9969	2.0286	0.6324	3.2076	0.0013	0.0083
nnr	24.1333	-2.2981	0.3968	-5.7912	6.99E-09	2.18E-07
norR	22.9749	2.5891	0.4977	5.2020	1.97E-07	4.29E-06
nrdA	34.8821	-2.1629	0.4996	-4.3293	1.50E-05	1.81E-04
nrdE	87.8160	-2.2114	0.5732	-3.8582	1.14E-04	0.0011
nrdF	32.8012	-2.8054	0.5462	-5.1358	2.81E-07	5.83E-06
nudC	15.8070	-2.2299	0.5232	-4.2617	2.03E-05	2.37E-04
nudE	112.4928	1.5051	0.4953	3.0386	0.0024	0.0132
nusB	40.1384	1.9989	0.3332	5.9986	1.99E-09	6.96E-08
ompF	876.5537	-1.2302	0.3382	-3.6374	2.75E-04	0.0022
opgB	110.2024	1.6188	0.3004	5.3886	7.10E-08	1.71E-06
opgD	101.9575	1.1665	0.2990	3.9009	9.58E-05	9.18E-04
orn	28.6490	-1.2080	0.3654	-3.3056	9.48E-04	0.0063
osmB	562.2381	4.8819	0.6349	7.6886	1.49E-14	1.25E-12
osmE	71.8239	-2.7528	0.8062	-3.4147	6.39E-04	0.0046
osmF	9.1397	-2.8884	0.6621	-4.3627	1.28E-05	1.62E-04
osmY	82.3883	-2.8438	0.7336	-3.8763	1.06E-04	0.0010
otsA	28.8326	-2.6863	0.5727	-4.6907	2.72E-06	4.39E-05
otsB	14.5063	-3.2644	1.0173	-3.2090	0.0013	0.0083
panC	53.2524	-0.9296	0.2800	-3.3203	8.99E-04	0.0060
panD	70.7031	-1.0771	0.3745	-2.8761	0.0040	0.0201
panM	11.7626	-2.4705	0.8625	-2.8643	0.0042	0.0208
patA	46.9852	-3.7710	0.7883	-4.7835	1.72E-06	2.96E-05

pck	84.6685	1.4240	0.3532	4.0313	5.55E-05	5.76E-04
pdxJ	33.1834	-0.9801	0.3203	-3.0601	0.0022	0.0126
pdxK	17.5108	-2.2899	0.5063	-4.5228	6.10E-06	8.79E-05
pepN	93.5983	-0.9556	0.2512	-3.8043	1.42E-04	0.0013
pfkB	14.2034	-2.4971	0.5461	-4.5730	4.81E-06	7.23E-05
pflB	227.9401	-1.1205	0.2559	-4.3787	1.19E-05	1.52E-04
pfo	35.7367	-2.0464	0.5447	-3.7566	1.72E-04	0.0015
pgl	34.0496	-1.8373	0.5796	-3.1698	0.0015	0.0093
pgpC	40.8343	1.6973	0.5324	3.1879	0.0014	0.0089
pheA	246.3539	-2.2501	0.5446	-4.1318	3.60E-05	3.89E-04
phoB	24.2674	3.4981	0.5263	6.6462	3.01E-11	1.54E-09
phoH	36.3689	-1.4631	0.5163	-2.8338	0.0046	0.0222
phoR	34.6735	2.7626	0.5208	5.3043	1.13E-07	2.59E-06
phoU	48.6648	3.2010	0.7148	4.4784	7.52E-06	1.03E-04
phr	8.9555	-1.6111	0.5709	-2.8223	0.0048	0.0228
plaP	66.7254	1.3852	0.3490	3.9696	7.20E-05	7.11E-04
pldA	32.4124	1.2441	0.3957	3.1442	0.0017	0.0100
pntB	129.0025	-1.4645	0.4809	-3.0454	0.0023	0.0130
potG	11.7113	-1.2599	0.4377	-2.8780	0.0040	0.0201
poxB	31.5305	-4.7469	0.6034	-7.8672	3.63E-15	3.32E-13
ppc	156.2793	-1.1455	0.2474	-4.6309	3.64E-06	5.61E-05
ppsR	17.1323	-1.9393	0.6636	-2.9224	0.0035	0.0179
prc	172.6114	-0.8467	0.2985	-2.8365	0.0046	0.0221
prfA	30.2134	1.6238	0.4367	3.7186	2.00E-04	0.0017
prkB	22.3715	-1.9559	0.6734	-2.9045	0.0037	0.0187
prlC	163.4824	2.2763	0.4648	4.8970	9.73E-07	1.81E-05
proV	37.1041	-3.0640	0.6581	-4.6559	3.23E-06	5.05E-05
proX	27.0756	-2.0797	0.6248	-3.3288	8.72E-04	0.0059
pspA	122.7713	2.7621	0.5776	4.7822	1.73E-06	2.97E-05
pspE	29.6213	1.8317	0.5000	3.6637	2.49E-04	0.0021
pssA	107.4887	-1.3265	0.3851	-3.4447	5.72E-04	0.0042
pstA	23.1447	2.6996	0.6937	3.8918	9.95E-05	9.47E-04
pstB	50.2584	3.6182	0.7122	5.0803	3.77E-07	7.67E-06
pstC	43.8657	2.1816	0.7464	2.9230	0.0035	0.0179
pstS	102.9160	3.4417	0.8147	4.2246	2.39E-05	2.76E-04
ptsH	193.6968	-1.2787	0.3878	-3.2970	9.77E-04	0.0064
ptwF	4.2764	3.7742	0.9381	4.0232	5.74E-05	5.88E-04
purF	166.8782	1.1856	0.3877	3.0583	0.0022	0.0126
purL	358.8707	0.9007	0.2957	3.0458	0.0023	0.0130
putP	33.7593	-1.8444	0.5896	-3.1280	0.0018	0.0105
qorA	22.8718	-2.0438	0.4187	-4.8813	1.05E-06	1.93E-05
raiA	1468.4669	2.2207	0.4769	4.6569	3.21E-06	5.05E-05
rapA	46.9319	1.6881	0.2871	5.8790	4.13E-09	1.34E-07
ravA	12.7800	-1.6571	0.4931	-3.3606	7.78E-04	0.0054
rbsD	57.9053	2.0733	0.7181	2.8872	0.0039	0.0196
rclA	5.2196	-3.6382	0.8382	-4.3406	1.42E-05	1.73E-04
rcsC	74.5572	1.2455	0.3040	4.0966	4.19E-05	4.45E-04
recD	58.5513	1.0854	0.3529	3.0757	0.0021	0.0121
recJ	78.2368	0.9044	0.2535	3.5675	3.60E-04	0.0028
relB	38.4067	2.6757	0.7130	3.7528	1.75E-04	0.0015
relE	49.1182	2.5174	0.6677	3.7700	1.63E-04	0.0014
rhlB	61.2700	-1.2976	0.3656	-3.5496	3.86E-04	0.0030
rho	153.4762	1.1809	0.3895	3.0319	0.0024	0.0135

ribE	29.7205	1.6562	0.3850	4.3018	1.69E-05	2.01E-04
rimM	1278.5966	2.3245	0.7466	3.1135	0.0018	0.0109
rlmE	495.6980	2.9008	0.6367	4.5558	5.22E-06	7.70E-05
rlmN	97.3410	1.6109	0.5735	2.8090	0.0050	0.0235
rluA	15.7130	1.3079	0.4209	3.1074	0.0019	0.0111
rluB	79.1984	1.5360	0.3630	4.2310	2.33E-05	2.69E-04
rnlA	79.6855	1.8578	0.6352	2.9245	0.0034	0.0178
rplA	989.6979	1.7389	0.5136	3.3860	7.09E-04	0.0050
rplE	584.0206	1.6288	0.4468	3.6454	2.67E-04	0.0022
rplJ	1737.9112	1.9456	0.6458	3.0126	0.0026	0.0141
rplK	725.7552	1.4193	0.3431	4.1372	3.52E-05	3.83E-04
rplL	1328.8659	2.0600	0.7199	2.8615	0.0042	0.0208
rplO	460.2324	2.1516	0.4691	4.5863	4.51E-06	6.82E-05
rplP	188.1913	1.6225	0.4696	3.4548	5.51E-04	0.0041
rplQ	538.3331	1.8095	0.3101	5.8347	5.39E-09	1.71E-07
rplS	941.7046	2.4175	0.4418	5.4718	4.46E-08	1.13E-06
rplT	1854.3319	2.4314	0.6709	3.6243	2.90E-04	0.0023
rplV	124.5581	1.1926	0.3401	3.5064	4.54E-04	0.0035
rplX	279.3430	1.3729	0.4772	2.8768	0.0040	0.0201
rplY	238.6800	2.5192	0.5700	4.4198	9.88E-06	1.29E-04
rpmD	38.3253	1.5184	0.5350	2.8384	0.0045	0.0221
rpmE	1673.6222	3.2991	0.8051	4.0979	4.17E-05	4.45E-04
rpmI	1269.4784	2.4297	0.6484	3.7474	1.79E-04	0.0016
rpmJ	216.9949	1.5687	0.3948	3.9731	7.10E-05	7.03E-04
rpoA	1268.0005	1.1244	0.3907	2.8779	0.0040	0.0201
rpoB	511.0932	0.6264	0.1946	3.2185	0.0013	0.0081
rpoC	1031.6640	0.9374	0.2493	3.7595	1.70E-04	0.0015
rpoD	382.7254	2.3618	0.3285	7.1889	6.53E-13	4.07E-11
rpoH	651.0465	2.6454	0.4871	5.4307	5.61E-08	1.38E-06
rpsA	1727.8655	1.2650	0.2706	4.6742	2.95E-06	4.69E-05
rpsB	2435.6991	2.4372	0.3124	7.8023	6.08E-15	5.26E-13
rpsC	353.6177	1.3689	0.3400	4.0258	5.68E-05	5.85E-04
rpsD	656.4737	1.1658	0.3235	3.6043	3.13E-04	0.0025
rpsE	360.4873	1.2978	0.4029	3.2215	0.0013	0.0080
rpsH	222.7654	0.9922	0.3529	2.8113	0.0049	0.0234
rpsK	399.5320	1.2719	0.3139	4.0519	5.08E-05	5.32E-04
rpsM	736.0815	1.3786	0.3227	4.2726	1.93E-05	2.27E-04
rpsN	280.7857	1.1414	0.3625	3.1490	0.0016	0.0099
rpsP	680.3206	2.1993	0.7522	2.9238	0.0035	0.0179
rpsQ	222.7374	1.4806	0.3347	4.4242	9.68E-06	1.27E-04
rpsS	93.1708	1.0494	0.2717	3.8627	1.12E-04	0.0011
rsd	44.1092	-1.2817	0.4527	-2.8311	0.0046	0.0223
rseC	24.3229	-2.7158	0.9024	-3.0095	0.0026	0.0142
rsmB	40.4076	-2.3254	0.7475	-3.1110	0.0019	0.0110
rssA	24.3061	-0.9831	0.3324	-2.9578	0.0031	0.0163
rssB	34.6812	-2.0001	0.5766	-3.4685	5.23E-04	0.0039
satP	22.5486	2.3493	0.5014	4.6854	2.79E-06	4.48E-05
sbcD	38.8293	1.8788	0.4264	4.4061	1.05E-05	1.37E-04
sdaA	915.8868	5.6416	0.5111	11.0379	2.51E-28	7.10E-26
sdaB	36.4824	4.1018	0.5693	7.2051	5.80E-13	3.76E-11
sdaC	79.6355	4.0062	0.4777	8.3866	5.00E-17	5.77E-15
secA	268.0939	0.6319	0.1899	3.3271	8.78E-04	0.0060
secD	237.1383	0.8464	0.2954	2.8651	0.0042	0.0207

secF	147.6545	1.3923	0.2920	4.7685	1.86E-06	3.16E-05
secY	2531.8522	1.8513	0.4420	4.1886	2.81E-05	3.16E-04
serC	341.2322	-1.8901	0.4016	-4.7067	2.52E-06	4.15E-05
shoB	15.9392	2.1715	0.4856	4.4714	7.77E-06	1.05E-04
skp	88.0796	-2.2718	0.3212	-7.0734	1.51E-12	9.23E-11
slmA	18.0984	-1.4602	0.4629	-3.1545	0.0016	0.0097
smg	26.7631	-1.3314	0.4304	-3.0934	0.0020	0.0115
sodB	66.4134	2.5626	0.7887	3.2492	0.0012	0.0074
solA	29.9008	-1.3480	0.3851	-3.5005	4.64E-04	0.0035
soxS	141.8499	2.1084	0.5989	3.5206	4.31E-04	0.0033
speD	110.6286	1.2410	0.3621	3.4275	6.09E-04	0.0044
spy	192.9851	4.5526	0.6117	7.4430	9.84E-14	7.29E-12
sra	83.6513	-3.1248	0.9102	-3.4332	5.96E-04	0.0044
srkA	172.5376	2.8233	0.6942	4.0670	4.76E-05	5.03E-04
stpA	34.3891	-3.8790	0.6188	-6.2691	3.63E-10	1.53E-08
sufC	40.3621	-2.9564	0.7180	-4.1178	3.83E-05	4.12E-04
sufD	46.5605	-3.1118	0.4736	-6.5712	4.99E-11	2.39E-09
sufE	15.5097	-1.8411	0.6433	-2.8621	0.0042	0.0208
sufS	54.9135	-2.2738	0.4695	-4.8430	1.28E-06	2.25E-05
surA	90.1149	-0.8461	0.2135	-3.9634	7.39E-05	7.28E-04
talA	29.3545	-3.9780	0.6075	-6.5487	5.80E-11	2.74E-09
talB	322.1046	-0.7736	0.2057	-3.7611	1.69E-04	0.0015
tas	30.8528	-1.4256	0.4118	-3.4617	5.37E-04	0.0040
tehA	20.2298	-2.0673	0.7285	-2.8379	0.0045	0.0221
tesA	129.9320	3.5707	0.5177	6.8976	5.29E-12	3.17E-10
tff	461.2490	2.4045	0.4783	5.0268	4.99E-07	9.76E-06
thiE	48.9052	-2.2240	0.5409	-4.1120	3.92E-05	4.21E-04
thiF	32.0364	-2.3214	0.5345	-4.3429	1.41E-05	1.72E-04
thiG	25.2136	-2.6231	0.6013	-4.3622	1.29E-05	1.62E-04
thiH	66.7324	-1.4555	0.4957	-2.9364	0.0033	0.0173
thrL	141.3907	-1.0836	0.2437	-4.4472	8.70E-06	1.17E-04
tktB	27.8268	-3.6138	0.6554	-5.5137	3.51E-08	9.35E-07
tomB	155.9341	2.5716	0.4519	5.6906	1.27E-08	3.72E-07
topA	343.4325	1.7110	0.2182	7.8420	4.43E-15	3.94E-13
torC	3.0394	2.9022	1.0029	2.8938	0.0038	0.0193
torR	15.8675	2.1441	0.5143	4.1689	3.06E-05	3.39E-04
tpiA	134.7403	-1.9943	0.4442	-4.4894	7.14E-06	9.84E-05
treF	7.8897	-1.9552	0.6016	-3.2501	0.0012	0.0074
trkA	43.1615	-1.9837	0.5225	-3.7967	1.47E-04	0.0013
trmD	1521.8933	2.3255	0.7572	3.0711	0.0021	0.0122
trmJ	112.1810	1.8649	0.6134	3.0405	0.0024	0.0132
trpA	37.5440	-3.4455	0.5562	-6.1941	5.86E-10	2.37E-08
trpB	65.0196	-4.0069	0.4669	-8.5824	9.29E-18	1.26E-15
trpC	79.8260	-3.9747	0.3488	-11.3957	4.40E-30	1.71E-27
trpD	93.9514	-3.6518	0.5381	-6.7864	1.15E-11	6.39E-10
trpE	44.5957	-3.0703	0.5772	-5.3195	1.04E-07	2.40E-06
truA	71.5130	2.3718	0.4136	5.7341	9.81E-09	2.99E-07
trxB	156.9451	-1.5779	0.4648	-3.3949	6.87E-04	0.0049
tsaE	5.6977	-2.1354	0.6944	-3.0753	0.0021	0.0121
tsf	1040.8905	1.7847	0.3107	5.7440	9.24E-09	2.85E-07
tusB	65.6765	2.3051	0.5550	4.1533	3.28E-05	3.59E-04
tyrA	233.6352	-2.2679	0.6179	-3.6703	2.42E-04	0.0020
tyrB	37.0635	-1.9660	0.5561	-3.5353	4.07E-04	0.0031

ucpA	22.1889	1.8141	0.4707	3.8539	1.16E-04	0.0011
ugpA	4.2437	-3.3860	1.0914	-3.1024	0.0019	0.0112
ugpB	28.6655	-2.5611	0.7510	-3.4101	6.49E-04	0.0046
upp	154.6417	1.7434	0.5291	3.2952	9.83E-04	0.0065
ushA	21.5007	-1.8317	0.4979	-3.6790	2.34E-04	0.0020
uspB	17.1986	-2.0627	0.6420	-3.2130	0.0013	0.0082
uspC	10.3256	-2.4513	0.8043	-3.0477	0.0023	0.0130
uspG	39.7580	2.0278	0.5259	3.8555	1.15E-04	0.0011
uxaA	14.6327	2.1160	0.6385	3.3139	9.20E-04	0.0061
uxuA	45.2137	3.6294	0.8140	4.4587	8.25E-06	1.11E-04
uxuB	31.2835	3.6120	0.6175	5.8491	4.94E-09	1.59E-07
uxuR	41.8549	1.6854	0.4692	3.5924	3.28E-04	0.0026
valT	70.5103	1.3691	0.4476	3.0588	0.0022	0.0126
waaF	20.6549	-1.2186	0.3632	-3.3553	7.93E-04	0.0055
waaU	7.9991	-2.3682	0.7904	-2.9962	0.0027	0.0148
waaY	8.1255	-1.8881	0.5864	-3.2199	0.0013	0.0080
wrbA	44.8201	-3.8088	0.7526	-5.0609	4.17E-07	8.33E-06
yaaX	14.5625	1.8351	0.5065	3.6230	2.91E-04	0.0023
yaeH	38.1982	-2.1009	0.4789	-4.3869	1.15E-05	1.48E-04
yaeP	21.3329	-1.2168	0.3940	-3.0880	0.0020	0.0116
yafD	129.3895	1.3249	0.3357	3.9467	7.92E-05	7.71E-04
yafE	22.9152	2.7729	0.4570	6.0682	1.29E-09	4.91E-08
yagI	58.1086	2.8155	0.4165	6.7605	1.37E-11	7.38E-10
yagP	5.3761	2.4885	0.7975	3.1204	0.0018	0.0107
yagU	20.4831	-4.1037	0.8702	-4.7158	2.41E-06	3.99E-05
yahK	13.5970	-3.1548	0.7128	-4.4261	9.60E-06	1.26E-04
yahO	29.1597	-5.2580	0.9928	-5.2963	1.18E-07	2.69E-06
yaiT	18.7462	1.3882	0.4255	3.2626	0.0011	0.0071
yajC	258.7349	1.7515	0.5423	3.2297	0.0012	0.0078
yajO	30.0130	-1.0931	0.3483	-3.1379	0.0017	0.0102
ybaL	102.3186	1.5636	0.3592	4.3525	1.35E-05	1.66E-04
ybaT	16.0154	-3.8765	0.6455	-6.0051	1.91E-09	6.84E-08
ybbA	52.1729	3.3035	0.5474	6.0344	1.60E-09	5.84E-08
ybbN	319.6311	3.7468	0.3253	11.5192	1.06E-30	5.48E-28
ybbP	76.0252	2.3438	0.4542	5.1607	2.46E-07	5.18E-06
ybdZ	8.4803	-2.3374	0.5917	-3.9506	7.80E-05	7.61E-04
ybeD	470.5137	3.8276	0.3330	11.4935	1.42E-30	6.32E-28
ybeX	107.2678	1.2359	0.4090	3.0220	0.0025	0.0138
ybeY	50.7290	1.3176	0.4337	3.0379	0.0024	0.0132
ybeZ	251.9548	2.0469	0.2822	7.2521	4.10E-13	2.72E-11
ybfA	192.1723	3.4935	0.7968	4.3845	1.16E-05	1.49E-04
ybgA	4.7709	-2.8710	0.8166	-3.5160	4.38E-04	0.0034
ybgI	46.8884	-0.9953	0.3386	-2.9392	0.0033	0.0172
ybgJ	18.7554	-1.3426	0.4408	-3.0460	0.0023	0.0130
ybhN	3.0369	-3.3888	0.9847	-3.4413	5.79E-04	0.0043
ybhP	5.2777	-2.9779	0.7630	-3.9027	9.51E-05	9.14E-04
ybiB	25.7281	-1.8553	0.5171	-3.5882	3.33E-04	0.0026
ybiC	74.6027	-2.4370	0.5793	-4.2066	2.59E-05	2.96E-04
ybiI	4.8606	-2.1659	0.6793	-3.1883	0.0014	0.0089
ybiJ	7.0377	-1.8077	0.5950	-3.0381	0.0024	0.0132
ybiU	15.2303	-1.6012	0.5205	-3.0762	0.0021	0.0121
ybiX	19.4367	-2.5954	0.7020	-3.6972	2.18E-04	0.0019
ybjG	109.4191	2.2715	0.6187	3.6715	2.41E-04	0.0020

ybjI	19.0226	1.3844	0.4694	2.9493	0.0032	0.0167
ybjJ	15.8258	2.2219	0.5098	4.3585	1.31E-05	1.63E-04
ybjT	16.8732	-1.7397	0.6056	-2.8724	0.0041	0.0204
ybjX	252.3540	2.5431	0.3185	7.9840	1.42E-15	1.38E-13
ycaC	17.7904	-3.8751	0.8411	-4.6069	4.09E-06	6.21E-05
ycaL	11.8087	-2.9149	0.9745	-2.9912	0.0028	0.0150
yccA	1014.4862	2.3679	0.7010	3.3781	7.30E-04	0.0051
yccJ	16.4828	-4.0852	0.6884	-5.9348	2.94E-09	9.96E-08
yccU	19.0161	-1.1628	0.3695	-3.1473	0.0016	0.0099
yceD	1019.2731	1.7395	0.5870	2.9635	0.0030	0.0161
yceK	8.8197	-3.1555	0.9505	-3.3198	9.01E-04	0.0060
ycfJ	245.2190	6.3135	0.6473	9.7537	1.78E-22	3.95E-20
ycfL	12.7111	-1.4085	0.4559	-3.0895	0.0020	0.0116
ycfP	23.0595	-1.3644	0.4305	-3.1691	0.0015	0.0093
ycgB	21.2682	-4.1325	0.4961	-8.3296	8.11E-17	8.71E-15
ychF	94.1521	1.3062	0.3635	3.5939	3.26E-04	0.0026
ychH	40.7609	2.6425	0.6127	4.3129	1.61E-05	1.93E-04
yciB	50.9651	1.8253	0.4057	4.4990	6.83E-06	9.53E-05
yciC	85.1343	1.3614	0.2791	4.8785	1.07E-06	1.94E-05
yciE	6.7506	-2.9055	0.7605	-3.8207	1.33E-04	0.0012
yciF	6.2061	-4.3641	0.9069	-4.8120	1.49E-06	2.60E-05
yciG	6.5057	-6.1097	1.0140	-6.0255	1.69E-09	6.10E-08
yciM	155.8727	2.1805	0.2441	8.9327	4.16E-19	6.16E-17
yciS	91.9568	2.5855	0.4684	5.5196	3.40E-08	9.20E-07
ycjX	259.0368	3.6633	0.4538	8.0727	6.87E-16	7.13E-14
ydbA	71.6218	0.9660	0.2858	3.3802	7.24E-04	0.0051
ydbH	40.2679	1.4909	0.3310	4.5045	6.65E-06	9.37E-05
ydcK	9.4092	-3.3080	0.6939	-4.7674	1.87E-06	3.16E-05
ydcP	146.5753	2.3146	0.4114	5.6267	1.84E-08	5.20E-07
yddB	13.7528	-1.9050	0.5253	-3.6263	2.87E-04	0.0023
ydeP	28.8260	3.4054	0.4591	7.4180	1.19E-13	8.61E-12
ydgJ	46.0393	-1.3601	0.3522	-3.8618	1.13E-04	0.0011
ydhL	4.6288	-2.6504	0.8129	-3.2604	0.0011	0.0072
ydhP	14.3599	-2.2690	0.7833	-2.8967	0.0038	0.0191
ydhS	9.8139	-2.9508	0.7447	-3.9622	7.43E-05	7.29E-04
ydhZ	10.4602	-2.3723	0.6591	-3.5994	3.19E-04	0.0025
ydiZ	9.2429	-3.9298	0.7962	-4.9359	7.98E-07	1.50E-05
ydjF	24.5052	1.9728	0.5631	3.5032	4.60E-04	0.0035
yeaG	33.5109	-2.9976	0.5912	-5.0708	3.96E-07	8.01E-06
yeaH	6.9906	-3.2908	0.8640	-3.8087	1.40E-04	0.0013
yeaQ	37.0583	-2.4037	0.8187	-2.9358	0.0033	0.0173
yebE	453.8967	4.8729	0.5255	9.2730	1.81E-20	3.13E-18
yebF	28.1545	-1.7557	0.5657	-3.1034	0.0019	0.0112
yebO	136.0702	2.5706	0.6755	3.8055	1.42E-04	0.0013
yebT	44.6916	-1.9134	0.6341	-3.0176	0.0025	0.0140
yebV	44.8998	-4.1245	0.9447	-4.3661	1.27E-05	1.61E-04
yecM	12.8734	-1.2974	0.4575	-2.8358	0.0046	0.0221
yecS	7.8854	-3.0132	0.8739	-3.4481	5.65E-04	0.0042
yedE	23.5953	1.4672	0.4790	3.0629	0.0022	0.0125
yedI	12.8115	-1.6379	0.4930	-3.3224	8.92E-04	0.0060
yedP	9.4258	-2.4083	0.7255	-3.3195	9.02E-04	0.0060
yedQ	16.1157	-1.2767	0.3903	-3.2713	0.0011	0.0069
yeeD	42.7379	1.9345	0.5969	3.2411	0.0012	0.0075

yeeE	83.6663	1.5939	0.5033	3.1667	0.0015	0.0094
yefM	8.9094	1.6697	0.5928	2.8165	0.0049	0.0232
yegE	23.3014	-1.3200	0.3720	-3.5489	3.87E-04	0.0030
yegH	18.6296	-1.6524	0.5810	-2.8439	0.0045	0.0218
yegP	20.7107	-3.9736	0.8707	-4.5638	5.02E-06	7.48E-05
yegQ	42.6372	1.7013	0.4408	3.8600	1.13E-04	0.0011
yehE	8.5579	-2.2461	0.6545	-3.4319	5.99E-04	0.0044
yehW	4.0478	-2.3650	0.7558	-3.1291	0.0018	0.0104
yehX	6.5175	-2.7336	0.7998	-3.4180	6.31E-04	0.0046
yehY	4.6885	-3.3849	0.8357	-4.0504	5.11E-05	5.34E-04
yeiB	20.5481	-3.0251	0.7770	-3.8930	9.90E-05	9.45E-04
yejG	166.5280	1.8562	0.6441	2.8819	0.0040	0.0199
yfcD	27.5242	-1.3090	0.4652	-2.8138	0.0049	0.0233
yfcF	9.1713	-1.9599	0.5291	-3.7040	2.12E-04	0.0018
yfcG	4.8794	-2.7379	0.7912	-3.4605	5.39E-04	0.0040
yfdC	8.2723	-2.2907	0.7696	-2.9763	0.0029	0.0156
yfhM	99.3141	-0.6438	0.2270	-2.8367	0.0046	0.0221
ygaM	48.6382	-2.1778	0.5146	-4.2320	2.32E-05	2.69E-04
ygdR	66.5415	2.4502	0.5445	4.4997	6.80E-06	9.53E-05
ygfZ	29.3429	-0.9343	0.3167	-2.9505	0.0032	0.0167
yghA	35.1465	-5.2096	0.8963	-5.8121	6.17E-09	1.94E-07
yghX	5.3086	-4.1269	0.8479	-4.8673	1.13E-06	2.02E-05
yghX	4.1335	-3.2095	0.9216	-3.4826	4.97E-04	0.0037
ygiC	129.2387	1.2118	0.2564	4.7256	2.29E-06	3.82E-05
yhbO	7.3121	-3.4568	1.0156	-3.4036	6.65E-04	0.0047
yhbW	7.9043	-2.5974	0.5778	-4.4951	6.95E-06	9.62E-05
yhcO	3.1886	-2.9718	1.0595	-2.8048	0.0050	0.0237
yheO	55.7899	-2.1230	0.6314	-3.3624	7.73E-04	0.0054
yheT	23.5891	-2.9661	0.7822	-3.7919	1.50E-04	0.0013
yheU	7.8253	-2.9914	0.9899	-3.0220	0.0025	0.0138
yhiD	10.0077	-6.2961	1.0678	-5.8964	3.71E-09	1.22E-07
yhjD	13.2136	-2.7387	0.6560	-4.1752	2.98E-05	3.31E-04
yhjG	9.5988	-3.2116	0.5975	-5.3749	7.66E-08	1.81E-06
yhjY	8.7726	-1.8823	0.5923	-3.1782	0.0015	0.0091
yiaG	24.7804	-4.7686	0.9946	-4.7946	1.63E-06	2.82E-05
yidA	18.9811	-1.9627	0.6731	-2.9161	0.0035	0.0181
yidB	9.4343	-1.7746	0.5330	-3.3292	8.71E-04	0.0059
yigZ	9.4520	-1.8251	0.5885	-3.1011	0.0019	0.0112
yiiM	15.9205	-2.0950	0.6325	-3.3122	9.26E-04	0.0062
yiiX	29.1367	2.6844	0.5710	4.7009	2.59E-06	4.24E-05
yijO	5.4646	-2.6931	0.8459	-3.1838	0.0015	0.0089
yjbD	14.2634	-1.8237	0.5883	-3.0998	0.0019	0.0113
yjcC	8.8232	-2.9879	0.8672	-3.4453	5.70E-04	0.0042
yjdC	15.1203	-2.1182	0.5057	-4.1884	2.81E-05	3.16E-04
yjdM	19.8612	1.3169	0.4637	2.8398	0.0045	0.0220
yjdN	3.4825	-3.4439	1.0041	-3.4300	6.04E-04	0.0044
yjdP	14.0922	2.1260	0.6299	3.3750	7.38E-04	0.0052
yjfN	68.1073	3.3110	0.7347	4.5069	6.58E-06	9.35E-05
yjgH	4.4487	-2.9902	0.8174	-3.6583	2.54E-04	0.0021
yjgR	10.2843	-2.2476	0.5630	-3.9920	6.55E-05	6.56E-04
yjiN	7.8251	-2.1422	0.6766	-3.1661	0.0015	0.0094
yliI	11.3204	-3.1386	0.9241	-3.3963	6.83E-04	0.0048
ymdB	10.4492	-1.6657	0.5505	-3.0259	0.0025	0.0137

ymdF	6.9368	-2.6452	0.9422	-2.8076	0.0050	0.0236
ymgD	14.7525	2.3988	0.6343	3.7817	1.56E-04	0.0014
ymgG	6.0425	2.5603	0.7501	3.4134	6.42E-04	0.0046
yncJ	186.8641	5.6911	0.6561	8.6747	4.15E-18	5.87E-16
yncL	8.2749	-1.9049	0.6612	-2.8808	0.0040	0.0200
yneM	4197.2269	4.9841	0.9545	5.2216	1.77E-07	3.92E-06
ynfD	42.7537	2.7844	0.6982	3.9879	6.67E-05	6.65E-04
ynfK	13.3162	2.1164	0.5245	4.0349	5.46E-05	5.69E-04
yoaC	5.8583	-2.1016	0.6688	-3.1422	0.0017	0.0100
yobB	92.1889	2.5264	0.3333	7.5792	3.48E-14	2.71E-12
yodD	5.4371	-3.0452	0.9088	-3.3508	8.06E-04	0.0055
yohC	8.1015	-1.6721	0.5640	-2.9644	0.0030	0.0161
yohF	5.4090	-1.9511	0.6958	-2.8042	0.0050	0.0237
ypdK	9.7202	2.3135	0.7151	3.2353	0.0012	0.0077
ypeC	88.8115	1.8801	0.4341	4.3306	1.49E-05	1.81E-04
ypfG	53.6877	3.3884	0.5944	5.7009	1.19E-08	3.57E-07
ypfJ	32.9984	-1.8348	0.6461	-2.8397	0.0045	0.0220
yqaA	32.7406	-2.2564	0.7377	-3.0586	0.0022	0.0126
yqcA	26.0379	-2.9713	0.8000	-3.7142	2.04E-04	0.0018
yqjG	10.8148	-2.3684	0.6447	-3.6739	2.39E-04	0.0020
yqjI	42.2741	2.2058	0.4100	5.3804	7.43E-08	1.77E-06
yraR	11.1909	-1.9538	0.6007	-3.2527	0.0011	0.0073
yrbN	15.3361	3.8125	0.6767	5.6343	1.76E-08	5.02E-07
yrdA	54.5800	1.1364	0.3492	3.2540	0.0011	0.0073
yrfF	60.9368	1.0952	0.2859	3.8302	1.28E-04	0.0012
yrfG	93.6013	2.9893	0.4690	6.3739	1.84E-10	8.29E-09
ysgA	20.8748	-2.3950	0.7376	-3.2472	0.0012	0.0074
ytfE	15.0410	2.9854	0.5456	5.4719	4.45E-08	1.13E-06
ytfK	276.7519	1.8356	0.6316	2.9065	0.0037	0.0186
ytjA	24.2736	-3.3511	0.7567	-4.4283	9.50E-06	1.26E-04
zapA	95.5201	-1.7007	0.4991	-3.4075	6.56E-04	0.0047
zapE	20.5061	-1.2985	0.4261	-3.0473	0.0023	0.0130

t=60 vs. t=30 (p<0.05)

Gene	BaseMean	log$_2$ Fold Change	lfcSE	stat	*p*-value	padj
acs	38.9100	-1.7426	0.3299	-5.2826	1.27E-07	2.12E-04
argT	63.7453	-1.1220	0.4190	-2.6777	0.0074	0.4680
clpP	171.4154	0.6797	0.2542	2.6742	0.0075	0.4680
clpX	374.5339	0.5407	0.2221	2.4352	0.0149	0.5904
cpxR	112.4011	-0.5367	0.2681	-2.0022	0.0453	0.9991
cspD	171.4356	-0.8287	0.2565	-3.2311	0.0012	0.2116
cstA	76.0891	-0.5133	0.2593	-1.9796	0.0478	0.9991
dapB	67.5693	-1.0873	0.4028	-2.6995	0.0069	0.4680
dapD	282.6125	-0.7078	0.3151	-2.2464	0.0247	0.9039
dedA	74.3600	0.6817	0.2776	2.4561	0.0140	0.5849
dhaK	26.0554	-1.1884	0.4838	-2.4567	0.0140	0.5849
dhaM	26.9616	-1.1085	0.5082	-2.1813	0.0292	0.9991
dnaG	131.8946	0.7560	0.2765	2.7347	0.0062	0.4680
ftnB	71.9762	-1.1230	0.5096	-2.2038	0.0275	0.9762
galP	35.4977	1.8263	0.5881	3.1053	0.0019	0.2639
gcvB	106.5418	1.3223	0.4928	2.6833	0.0073	0.4680

glgP	78.4846	-0.7308	0.3427	-2.1327	0.0329	0.9991
glgX	64.0716	-0.9505	0.3563	-2.6677	0.0076	0.4680
hslJ	68.2994	1.3626	0.5714	2.3846	0.0171	0.6624
iap	27.5401	1.2759	0.4618	2.7630	0.0057	0.4680
insL1	52.1856	0.6676	0.3074	2.1715	0.0299	0.9991
ispH	69.3410	0.6006	0.2966	2.0252	0.0428	0.9991
ldtB	249.3909	0.9068	0.3890	2.3310	0.0198	0.7478
leuL	67.3598	-1.3618	0.3526	-3.8626	1.12E-04	0.0620
ltaE	37.0822	-0.7231	0.3428	-2.1091	0.0349	0.9991
lysC	139.8717	-1.6214	0.5032	-3.2223	0.0013	0.2116
malT	136.2267	-1.0274	0.3749	-2.7405	0.0061	0.4680
manZ	85.8188	-0.8695	0.4326	-2.0099	0.0444	0.9991
marA	19.5891	1.3044	0.4610	2.8294	0.0047	0.4680
metE	227.1578	-1.6581	0.4633	-3.5790	3.45E-04	0.0951
mlc	82.6689	0.5655	0.2128	2.6578	0.0079	0.4680
mrcB	56.5209	0.6870	0.2764	2.4855	0.0129	0.5849
mutM	37.4293	1.1328	0.3756	3.0163	0.0026	0.3045
nmpC	69.5198	-1.3303	0.3624	-3.6705	2.42E-04	0.0807
nusB	40.1384	0.6783	0.3126	2.1703	0.0300	0.9991
osmB	562.2381	1.9053	0.6266	3.0406	0.0024	0.3025
pepN	93.5983	-0.5246	0.2570	-2.0412	0.0412	0.9991
pepQ	51.1668	-0.6873	0.3421	-2.0090	0.0445	0.9991
phoR	34.6735	1.0695	0.5315	2.0122	0.0442	0.9991
plaP	66.7254	0.8223	0.3365	2.4433	0.0146	0.5904
polB	25.5378	0.9055	0.3685	2.4570	0.0140	0.5849
prlC	163.4824	0.9799	0.4599	2.1309	0.0331	0.9991
rapA	46.9319	0.5867	0.2983	1.9669	0.0492	0.9991
rpoD	382.7254	0.8372	0.3249	2.5764	0.0100	0.5544
rpsS	93.1708	0.5268	0.2663	1.9782	0.0479	0.9991
satP	22.5486	1.2534	0.4565	2.7457	0.0060	0.4680
sdaC	79.6355	0.9341	0.4166	2.2421	0.0250	0.9039
sdhA	163.4790	-1.0084	0.2237	-4.5086	6.53E-06	0.0054
sdhC	40.4426	-0.9980	0.3611	-2.7640	0.0057	0.4680
sfsA	59.9863	0.8501	0.4196	2.0261	0.0428	0.9991
soxS	141.8499	-1.1584	0.5679	-2.0396	0.0414	0.9991
sucA	145.3545	-0.8757	0.3326	-2.6333	0.0085	0.4858
sucC	101.5568	-0.6853	0.2402	-2.8534	0.0043	0.4680
thrL	141.3907	-0.8101	0.2505	-3.2335	0.0012	0.2116
topA	343.4325	0.7660	0.2164	3.5404	3.99E-04	0.0951
trpC	79.8260	-0.9194	0.3590	-2.5611	0.0104	0.5608
wzzB	256.5802	0.8460	0.3986	2.1225	0.0338	0.9991
ybbN	319.6311	0.7543	0.3065	2.4613	0.0138	0.5849
ycdZ	22.4526	0.8385	0.3406	2.4615	0.0138	0.5849
ycfJ	245.2190	2.2652	0.5972	3.7930	1.49E-04	0.0620
yciM	155.8727	0.5860	0.2309	2.5376	0.0112	0.5811
ydbH	40.2679	1.0935	0.3422	3.1953	0.0014	0.2116
ydeP	28.8260	0.9197	0.3653	2.5179	0.0118	0.5849
yobB	92.1889	-0.5695	0.2790	-2.0415	0.0412	0.9991
ypfG	53.6877	1.5728	0.5753	2.7339	0.0063	0.4680
yqeF	24.3647	-0.8533	0.4285	-1.9911	0.0465	0.9991
yrfF	60.9368	0.7150	0.2893	2.4713	0.0135	0.5849
znuA	31.7726	-0.7598	0.3704	-2.0515	0.0402	0.9991

t=120 vs. t=60 (p<0.05)

Gene	BaseMean	log$_2$ Fold Change	lfcSE	stat	*p*-value	padj
acs	38.9100	-1.1255	0.3879	-2.9014	0.0037	0.8243
ahpF	105.5387	0.7222	0.2789	2.5897	0.0096	1
ansP	20.1247	0.9184	0.4673	1.9654	0.0494	1
argT	63.7453	-1.0051	0.4405	-2.2817	0.0225	1
argZ	51.3680	-0.9398	0.4178	-2.2492	0.0245	1
atoS	8.8000	1.1346	0.5756	1.9711	0.0487	1
atpG	107.6051	-0.4944	0.2265	-2.1830	0.0290	1
chaA	1801.5463	-1.1879	0.5411	-2.1955	0.0281	1
cho	13.1777	-1.0253	0.4815	-2.1292	0.0332	1
cspD	171.4356	-0.5743	0.2649	-2.1684	0.0301	1
cstA	76.0891	-0.9046	0.2780	-3.2536	0.0011	0.6834
ecpA	6.3501	-1.3741	0.6922	-1.9852	0.0471	1
fkpB	43.1394	0.7294	0.3322	2.1959	0.0281	1
fucR	13.2538	-1.1453	0.5413	-2.1159	0.0344	1
gcl	2.1098	2.3775	1.0481	2.2683	0.0233	1
gcvB	106.5418	0.9742	0.4856	2.0063	0.0448	1
gcvH	15.8421	1.1127	0.5367	2.0733	0.0381	1
glnQ	40.0977	0.9782	0.3831	2.5531	0.0107	1
glpR	9.5305	1.4577	0.6793	2.1461	0.0319	1
gstB	35.7960	-0.9444	0.4537	-2.0817	0.0374	1
gyrB	210.6058	0.4976	0.1994	2.4949	0.0126	1
iap	27.5401	1.0045	0.4293	2.3399	0.0193	1
ibpA	2628.8038	-0.8137	0.3473	-2.3430	0.0191	1
ispH	69.3410	0.8599	0.2855	3.0120	0.0026	0.7529
katE	16.2156	1.7222	0.7934	2.1706	0.0300	1
kdgK	29.8456	-0.7013	0.3511	-1.9977	0.0457	1
kefC	7.2674	2.0345	0.8263	2.4621	0.0138	1
lolB	16.8211	0.9694	0.4901	1.9780	0.0479	1
malT	136.2267	-0.8087	0.3833	-2.1096	0.0349	1
map	139.0325	-0.7627	0.2756	-2.7680	0.0056	1
mazE	11.5974	0.9856	0.4560	2.1615	0.0307	1
mazF	8.8992	1.1305	0.5547	2.0380	0.0416	1
mcrC	1.9313	2.4882	1.0611	2.3450	0.0190	1
mdtA	4.1001	1.6530	0.7821	2.1137	0.0345	1
mdtC	10.4204	1.1091	0.4966	2.2333	0.0255	1
mgtL	469.5853	-1.5799	0.7476	-2.1133	0.0346	1
mqsR	62.2148	0.7877	0.3213	2.4516	0.0142	1
nadA	61.1093	0.6703	0.3066	2.1863	0.0288	1
narQ	15.9819	1.1058	0.4527	2.4429	0.0146	1
nhaA	443.8046	-0.6035	0.2547	-2.3698	0.0178	1
nmpC	69.5198	-1.3100	0.3910	-3.3504	0.0008	0.6834
pck	84.6685	-0.8063	0.3296	-2.4464	0.0144	1
pdxH	33.2436	1.0588	0.5357	1.9763	0.0481	1
phnF	0.5433	-2.2544	1.1460	-1.9673	0.0492	1
phoA	16.4182	2.7074	0.7562	3.5802	0.0003	0.6834
phoB	24.2674	1.3587	0.4557	2.9814	0.0029	0.7529
phoR	34.6735	1.5836	0.5055	3.1326	0.0017	0.7529
phoU	48.6648	2.1880	0.7087	3.0872	0.0020	0.7529

pstA	23.1447	2.0887	0.6916	3.0200	0.0025	0.7529
pstB	50.2584	2.3072	0.7008	3.2924	0.0010	0.6834
pstC	43.8657	2.1570	0.7512	2.8713	0.0041	0.8580
pstS	102.9160	2.4283	0.8122	2.9898	0.0028	0.7529
ptsH	193.6968	-0.8158	0.3910	-2.0862	0.0370	1
rapA	46.9319	0.9590	0.2813	3.4091	0.0007	0.6834
rcsC	74.5572	0.8382	0.3056	2.7432	0.0061	1
rffG	20.2316	0.9352	0.4595	2.0352	0.0418	1
rlpA	35.8923	0.8892	0.3809	2.3342	0.0196	1
rpsB	2435.6991	-0.7276	0.3105	-2.3437	0.0191	1
rseP	115.2467	-0.5017	0.2217	-2.2626	0.0237	1
rsmJ	13.6255	1.1592	0.5077	2.2830	0.0224	1
sdaB	36.4824	1.0557	0.4834	2.1838	0.0290	1
sdhA	163.4790	-1.0781	0.2378	-4.5326	5.83E-06	0.0245
sdhC	40.4426	-1.3351	0.3994	-3.3424	0.0008	0.6834
shoB	15.9392	0.9339	0.4497	2.0767	0.0378	1
sodB	66.4134	2.3887	0.7911	3.0193	0.0025	0.7529
soxS	141.8499	-1.2031	0.5740	-2.0961	0.0361	1
sucA	145.3545	-0.7573	0.3403	-2.2252	0.0261	1
sucB	64.9190	-0.8976	0.3311	-2.7112	0.0067	1
sucC	101.5568	-0.6714	0.2536	-2.6478	0.0081	1
sufD	46.5605	-1.3683	0.4948	-2.7656	0.0057	1
surA	90.1149	-0.5673	0.2228	-2.5470	0.0109	1
talB	322.1046	-0.4592	0.2090	-2.1976	0.0280	1
tdk	28.3118	-1.0795	0.5451	-1.9805	0.0476	1
tfaP	0.3977	2.2020	1.0996	2.0024	0.0452	1
tolC	313.8664	-0.6457	0.2900	-2.2263	0.0260	1
torS	7.2913	1.2540	0.5833	2.1500	0.0316	1
truA	71.5130	0.9116	0.4008	2.2744	0.0229	1
truD	31.6042	0.9993	0.4241	2.3563	0.0185	1
tsf	1040.8905	-0.9054	0.3076	-2.9436	0.0032	0.8010
tyrA	233.6352	1.4782	0.6291	2.3496	0.0188	1
wbbJ	20.7452	-0.9307	0.4065	-2.2896	0.0220	1
wecB	27.0646	0.8502	0.3729	2.2800	0.0226	1
wecF	15.4887	1.0865	0.4918	2.2090	0.0272	1
wzyE	6.2299	2.5527	0.9670	2.6397	0.0083	1
yafD	129.3895	0.9237	0.3367	2.7438	0.0061	1
yafE	22.9152	1.2650	0.4145	3.0519	0.0023	0.7529
yafO	1.2090	2.3712	1.0992	2.1572	0.0310	1
yahG	1.8620	2.3211	1.1210	2.0706	0.0384	1
ybhG	9.2138	1.2593	0.5709	2.2058	0.0274	1
ybjJ	15.8258	0.9828	0.4743	2.0720	0.0383	1
ybjM	4.3830	2.4391	0.8410	2.9001	0.0037	0.8243
ybjX	252.3540	-0.7506	0.2968	-2.5286	0.0115	1
ycbU	1.6210	2.5231	1.0778	2.3410	0.0192	1
yceJ	9.7658	-1.8323	0.8009	-2.2878	0.0222	1
ycgR	1.8347	2.2729	1.1333	2.0056	0.0449	1
yciC	85.1343	-0.5154	0.2565	-2.0091	0.0445	1
ydhQ	51.2436	0.6622	0.2820	2.3482	0.0189	1
yeeR	5.7264	-1.3264	0.6699	-1.9801	0.0477	1
yfcL	8.8183	1.3247	0.6351	2.0857	0.0370	1
yfgM	25.5923	-0.8663	0.3767	-2.3000	0.0214	1
ygiM	45.1855	-0.8100	0.3721	-2.1767	0.0295	1

yhjJ	37.1835	-0.7177	0.3330	-2.1551	0.0312	1
ykgH	1.3185	2.8072	1.1217	2.5027	0.0123	1
ylaB	11.9524	1.2058	0.6149	1.9610	0.0499	1
yneO	10.0660	1.1538	0.5537	2.0840	0.0372	1
yoaI	1.0332	-2.3120	1.1379	-2.0318	0.0422	1
yoeG	2.2636	2.9037	1.1346	2.5593	0.0105	1
yqeF	24.3647	-1.4805	0.4811	-3.0774	0.0021	0.7529
zntA	32.5651	1.9509	0.7490	2.6048	0.0092	1